Monitoring mitochondrial oxygen levels via protoporphyrin-IX triplet state lifetime technique: assessment of factors reducing measurement accuracy

M.A. Schoenmakers

Supervisors:
E.G. Mik, PhD
Dr. Ir. W. Olthuis
Drs. A. Lovink
Prof. dr. ir. P.H. Veltink

August 16, 2022

Contents

List of abbreviations

ALA = 5-aminolevulinic acid
BGS = background signal
BSA = bovine serum albumin
COMET = cellular oxygen metabolism monitor
DF = delayed fluorescence
DMF = dimethylformamide
DMSO = dimethylsulfoxide
E^{630} = intensity integral of the 630nm signal
E^{670} = intensity integral of the 670nm signal
I_0 = maximum intensity amplitude Hb = Hemoglobin I_0^{630} = maximum intensity amplitude of the 630nm signal
I_0^{670} = maximum intensity amplitude of the 670nm signal
LL = lab laser
LP = laser power
mitoPO_2 = mitochondrial partial oxygen pressure
ML = main laser
MS/s = mega samples per second
N_2 = nitrogen
O_2 = oxygen
PO_2 = partial oxygen pressure
SO_2 = oxygen saturation
OR = operating room
PBS = phosphate buffered saline
PdP = Palladium porphyrin
PF = prompt fluorescence
PpIX = protoporphyrin IX
PpIX-TSLT = protoporphyrin IX-triplet state lifetime technique
PtF_4 = platinum tetrafluoride
RISC = reverse intersystem crossing
SO_2 = oxygen saturation
SQP = self-quenching phenomenon
τ_0 = lifetime at zero oxygen level
τ = lifetime
τ_{BGS} = lifetime of the background signal
τ_{PpIX} = lifetime of the delayed fluorescence signal originating from excited PpIX molecules

Abstract

Rationale – With maintaining oxygen homeostasis as fundamental target in patient care, accurate monitoring at tissue level is essential. Accordingly, the protoporphyrin-IX triplet state lifetime technique (PpIX-TSLT) measures oxygen pressure levels in mitochondria (mitoPO$_2$) via porphyrin excitation which produce 630nm delayed fluorescence (DF). This DF's lifetime is oxygen-dependent. However, unexplained results let to hypotheses that background signal (BGS) and a self-quenching phenomenon (SQP) affect the PpIX-TSLT measurement accuracy. BGS is DF signal originating from different factors than the fluorescent porphyrins. The SQP theory proclaims that at high PpIX concentration, collision of excited porphyrins produce 670nm signal and alter the relation between DF lifetime and mitoPO$_2$ values. We aim to identify prominent causes of BGS which disturb the measurement accuracy, and whether SQP occurs within physiological setting.

Methods – The COMET (clinical application) and the laboratory laser (LL) (for cellular experiments) are assessed for BGS causes and their contribution to the DF signal (BGS-DF-ratio). The main laser is used to assess individual COMET parts' BGS and in vivo experiments including BGS-DF-ratios over increasing 5-aminulovulinic (ALA, required for the formation of PpIX) patch application time. The occurrence of SQP is examined via in vitro experiments concerning increasing PpIX concentrations in physiological samples (i.e., mainly containing phosphate buffered saline with albumin) and evaluating - at zero oxygen level - the lifetime and the 670nm to 630nm signal intensity ratio (670nm/630nm-ratio). Additionally, this is examined in the in vivo experiment.

Results – The COMET shows prominent BGS from skin measurement and its measurement fiber. The LL presents no replaceable contributor. With low porphyrin concentrations, the BGS-DF-ratio can be >50% for the COMET and LL. This decreases with increasing concentration; i.e., longer ALA application for clinical application. The COMET skin-BGS results in mitoPO$_2$ underestimation considering normoxia and overestimation with critically low values.

The SQP in vitro experiments confirm increasing PpIX concentration increases 670/630nm-ratios, which decreases the lifetimes. Longer ALA application did not increase 670/630nm-ratios, but an anticorrelation with the lifetime suggest the possibility of SQP in vivo.

Conclusions and recommendations – Regarding BGS, improving mitoPO$_2$ measurement accuracy could be achieved by boosting DF signal intensity through concentration increase – clinically, measure between 8-19hours after ALA application -; remove the measurement fiber of the COMET; and integrate a BGS correction method using average skin BGS.

SQP occurrence in physiological samples disturbs the lifetime measurement, at least at zero oxygen level. The effect on (in vivo) mitoPO$_2$ should be assessed.

1 Introduction

Oxygen is vital for our human existence, since it is indispensable for energy production and other biochemical processes [1]. Since oxygen homeostasis is a fundamental target in patient care, insight into oxygen balance between supply and demand is critical, especially at tissue level [1]. While oxygen demand exceeding its supply may result in hypoxia and cellular metabolic adaption [2], oxygen supply surpassing oxygen demand may cause tissue hyperoxia and therefore the risk of oxidative stress inducing a cellular adaptive response [3].

In clinical setting, the most commonly used parameter is the oxygen saturation (SO_2); which is expressed as the percentage of hemoglobin (Hb) bound to O_2. A different way to determine the amount of oxygen is use the partial oxygen pressure (PO_2) expressed in mmHg. PO_2 refers to the pressure that a given volume with the same temperature would have, if merely oxygen is present.[4] At 1 bar the air contains 160 mmHg O_2, which travels to our arterial blood getting it at a PO_2 of 100 mmHg and after cycling through our body the PO_2 ends at 40 mmHg in venous blood [5, 6, 7, 8].
Many techniques have been developed to measure oxygen in vivo as indicator of tissue oxygen supply [9, 5, 10]. Since hemodynamic targets - e.g. cardiac output, blood pressure and central venous oxygen saturation - merely modestly predict tissue perfusion and oxygen supply at microcirculatory or cellular level, complementary targets are investigated over the years [11]. This led to a set of perfusion targets, such as pulse-oximetry, oxygen electrodes, near-infrared spectroscopy and visible light spectroscopy. However, each method has its

disadvantageous; e.g., where pulse-oximetry measures the microcirculation arteriorly [12], NIR and visible light spectroscopy are inclined to focus on the venous part [13, 14], and the invasive oxygen electrodes, although considered the golden standard for tissue oximetry, are cumbersome and tissue destructive [1, 5, 10]. Recently, a device capable of measuring oxygen at mitochondrial level was introduced: the Cellular Oxygen METabolism monitor (COMET) [10, 15]. It enables quantitative oxygen pressure measurement at mitochondrial level (mitoPO$_2$). Since mitochondria, i.e. the powerhouses of the cell, consume approximately 98% of the total body oxygen consumption, it can be regarded as a direct indicator of the oxygen demand-supply-balance [1, 16, 17]. Due to this high consumption rate, mitochondria occupy the lowest end of the blood-to-tissue oxygen gradient and are considered the oxygen sink [1, 15]. Evaluating the end of the oxygen cascade provides the possibility to assess (pathological) shunting in the microcirculation or tissue edema, which can lead to cellular hypoxia [18, 10]. Therefore, being able to accurately determine the mitochondrial PO$_2$ (mitoPO$_2$) could be of great use. The COMET measures the mitoPO$_2$ via the protoporphyrin IX-triplet state lifetime technique (PpIX-TSLT) using the lifetime of long-lived red emission light, which is oxygen-dependent. The first detailed description of PpIX-TSLT was published in 2006 [19], and has evolved to not only measuring in living cells, but also in vivo [20].

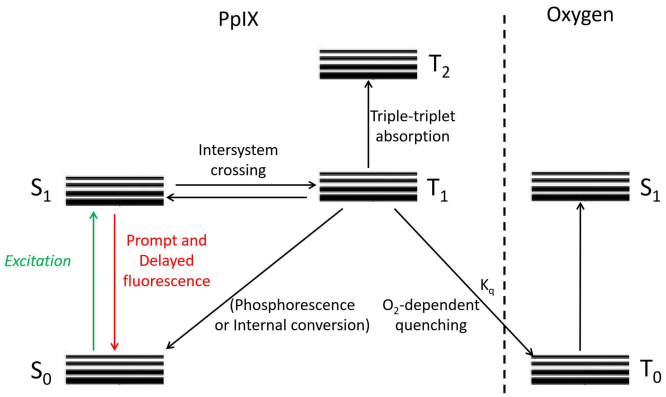

Figure 1: The principle of PpIX-TSLT in a Jablonski diagram: S_0 represents the PpIX molecule in ground state, S_1 in singlet excited state and T_1 triplet state. Collision of two T_1 state molecules results in T_2 state. Oxygen molecules have a T_0 ground state and get excited to S_1 via energy transfer from PpIX T_1 state molecules. Based on figure from [19] and [21]

1.1 Technical background PpIX-TSLT

PpIX-TSLT uses protoporphyrin IX (PpIX) to determine mitoPO$_2$, which is the final precursor of heme and is synthesized via the heme biosynthetic pathway in the mitochondria [22, 23]. In the heme biosynthetic pathway, PpIX is preceded by 5-aminolevulinic acid (ALA). Therefore, ALA is administrated to stimulate PpIX production [19]. Since the conversion of PpIX to heme is the rate-limiting step, this procedure results in increased PpIX concentration and ensures its mitochondrial origin [24, 25, 26, 27].
When illuminating PpIX with green light, it produces red prompt fluorescence (PF); but interesting is the production of a more long lived red emission, which is a fundamental aspect of PpIX-TSLT [19, 16]. This long lived emission is referred to as delayed fluorescence (DF). While the intensity (i.e., a power, an energy per unit time) of PF decays with a lifetime of nanoseconds, DF lifetimes are in the order of microseconds to milliseconds [16]. The DF lifetime decay is oxygen-dependent; i.e., with an increased oxygen concentration, the lifetime is shortened [16]. Accordingly, the mitoPO$_2$ relates quantitatively to the DF lifetime, which can be measured via PpIX considering it functions as a intramitochondrial oxygensensitive dye [1]. PpIX-TSLT is non-invasive and can be used safely in humans [1].

The Jablonski diagram of Figure 1 illustrates the principle of DF. The process starts with excitation of a molecule - PpIX in the case of PpIX-TSLT - from the ground state S_0, via absorbance of a photon, to the first excited singlet state S_1 [4]. Next, the excited molecule can return to its ground state with optional expression of PF, or change to the triplet state T_1 - called intersystem crossing - by adjustment of the spin orientation of the electron. Direct transfer from T_1 to S_0 with luminescence is called phosphorescence, and without photon emission internal conversion. Alternatively, the molecule can return to its ground state via S_1, therefore first undergoing reverse intersystem crossing (RISC), followed by radiant desexcitation - with the same spectrum as PF - to S_0; this process is referred to as delayed fluorescence. Due to its delay, DF can be distinguished from PF. RISC requires external energy, which can come from multiple sources, therefore, indicating a different type of DF: [1, 4]

(1) When thermal activation causes the molecule to transfers from T_1 to S_1, it is called *E-type DF* [28]. Accordingly, the temperature of the substance is of great importance [29]. E-type DF is a first order reaction

due to the requirement of merely one T_1 molecule, resulting in a linear relation of excitation intensity and DF intensity [4, 29]. This can be expressed as: $I(t) = I_0 exp(-t/\tau)$, with τ the lifetime and I_0 the initial DF intensity [21]. Correspondingly, the DF intensity is not affected by concentration or excitation light intensity [30]. Whether thermal energy is sufficient depends on the separation between S_1 and T_1. When this gap is too large for thermal activation, P-type DF can still be present [28].

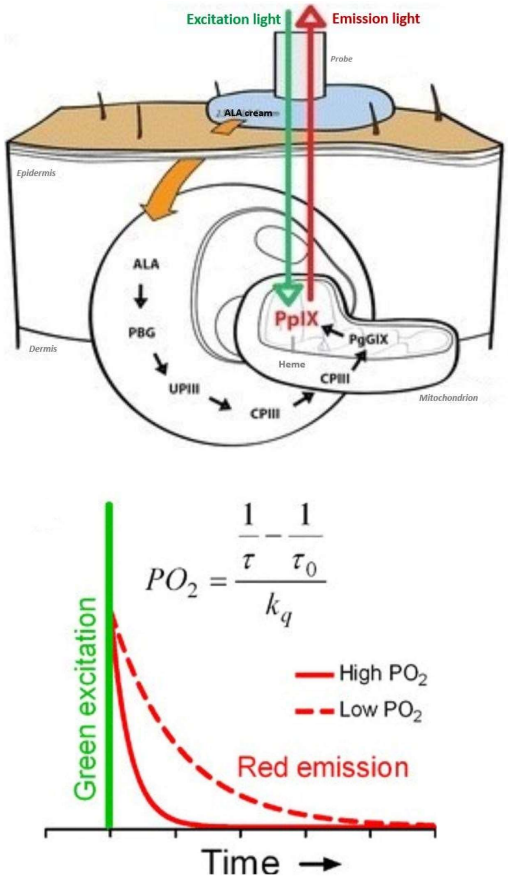

Figure 2: Schematic representation of PpIX-TSLT, used in the COMET; (A) shows ALA application to the skin which transfers into the cell, which starts the heme synthesis cycle, resulting in increased PpIX concentration in the depicted mitochondrion. With green excitation light PpIX molecules get excited which is followed by red (delayed) emission light. The graph in (B) displays the effect of oxygen on the lifetime (τ) of this emission light; i.e., with a high PO_2 the lifetime is shorter - seen as a steeper decreasing curve - compared to the low PO_2. With the formula on top of (B) the PO_2 can be calculated based on this τ. [15]

(2) With *P-type DF* two triplet state molecules collide, therefore transferring energy from one to the other, resulting in one molecule in S_1 state and another in S_0 [28, 29]. This reaction may result in formation of an excited dimer; also called excimer [31, 32]. P-type DF, also referred to as triplet-triplet annihilation, is a second order reaction since it requires two T1 state molecules. Therefore, the DF emission intensity corresponds to the square of the T_1 state molecule concentration [4, 29]. This can be expressed as $I = I_0 exp(-2t/\tau)$ [21].

(3) Singlet Oxygen Feedback Delayed Fluorescence (*SOFDF*) is the third DF method, observed in in vitro [4, 29, 33, 34]. This mechanism creates RISC via use of two T_1 state molecules and oxygen, producing a S_1 state molecule. Note, this is not the PpIX-TSLT used in the COMET where oxygen functions as quencher. Since SOFDF requires two T_1 state molecules, the DF intensity depends on the square of the T_1 concentration [29]. Whether SOFDF is also observed in human tissue is doubted based on the required excitation intensity and and PO_2 level [4, 29].

The PpIX-TSLT is considered to be E-type DF, and assumes P-type DF and SOFDF to have an insignificant effect on the measured DF [19]. This is based on experiments of Mik et al. [19], showing an approximately constant lifetime at zero oxygen levels with PpIX concentrations ranging from 0.1-10.0 µM, and linear reduction in emission intensity when neutral density filters were placed in the excitation path. With merely E-type DF, the measured lifetimes would be independent of PpIX concentration and excitation light intensity [35].

$$MitoPO_2 = \frac{\frac{1}{\tau} - \frac{1}{\tau_0}}{k_q} \quad (1)$$

with τ the measured DF lifetime, τ_0 the DF lifetime of spontaneous relaxtion - i.e., in absence of oxygen - and k_q the reaction rate constant of the quencing reaction, referred to as the quencing constant; in this case the quencing constant of oxygen [4, 10]. This calculation assumes the oxygen to be homogeneously distributed [10].

A schematic representation of PpIX-TSLT is shown in Figure 2A. The ALA is applied to the skin - in case of the current clinical COMET studies via a patch, but ALA cream can be used too [36]- where it is absorbed and transferred to PpIX which accumulates in the mitochondria.

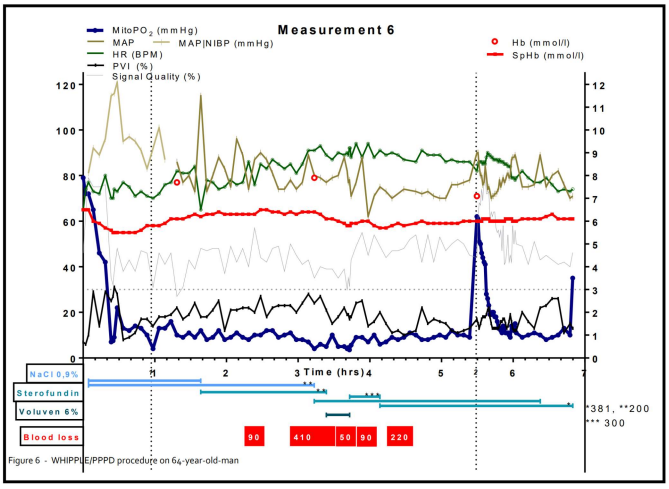

Figure 3: Physiologically unexplained mitoPO$_2$ results with assumed unphysiologically low values; during a WHIPPLE procedure in 59 year old patient, who's vital functions - i.e., heart rate (HR), mean arterial pressure (MAP) remain rather stable compared to the mitoPO$_2$ decrease. At 5.5 hours a consumption measurement - measure with a frequency of 1 pulse/sec when applying pressure on the probe to cutoff local blood transport - is performed resulting in a temporary mitoPO$_2$ increase. Below the graph the amount of blood loss and intravascular volume replenishment is shown. *PVI = pulse variation index, Hb = hemoglobin, SpHb = total hemoglobin, signal quality is represented for the COMET signal.* [37]

Several studies have shown it produces sufficient PpIX required for accurate determination of mitoPO$_2$ in skin and other organs of rats as well as human skin [15, 26, 27, 38]. Accordingly the PpIX-TSLT, as used in the COMET, started as a technical principle and evolved into a measurement tool for cells and in vivo application. Several studies are conducted ranging from organs such as animal heart and liver, to multiple clinical studies [16, 19, 20, 22, 26, 39, 40, 41, 42, 43]. Measuring mitoPO$_2$ in the skin is presumed to be able to function as the canary of the body, i.e. be an early indicator of oxygen shortage [44, 45]. Römers et al. showed the cutaneous mitoPO$_2$ can on an individual level sensitively indicate the physiologic limit of hemodilution in pigs [45]. Clinical relevance and interpretability is currently being assessed in multiple clinical trials.

1.2 Problem

The PpIX-TSLT could provide a remarkable and important measurement technique for both patient care and (cellular) research; and in many cases PpIX-TSLT, as incorporated in the COMET, seems to work appropriately. However, a share of the clinical measurement results cannot be explained (yet) in terms of erroneous technique or measurement method, nor physiologically. For example unphysiologically low mitoPO$_2$ values in patients, where all measurement parameters - such as blood pressure, saturation, et cetera - could not provide an explanation, see Figure 3; or cell experiments which show no detection of changing the PO$_2$ from 8%, to 5% and to 0% measured by the PpIX-TSLT measurement system. See Appendix A.1 Figure 29. Moreover, inconsistent values for τ_0 are observed in healthy subjects measured over time, see Figure 4, which should be stable according to the PpIX-TSLT theory.

These inexplicable results and inconsistencies imply there is more to PpIX-TSLT then currently known.

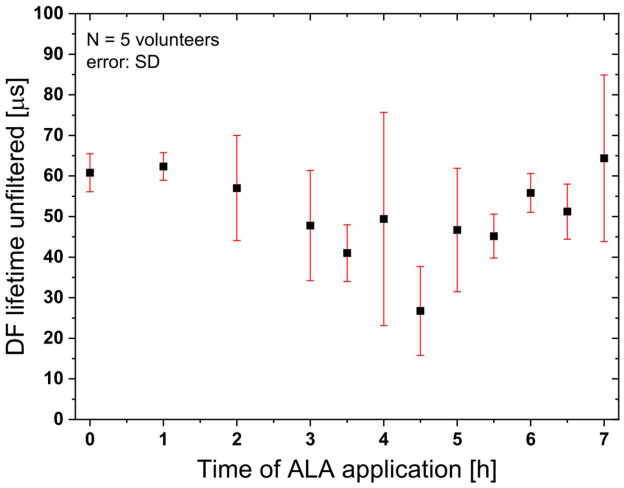

Figure 4: Inconsistent delayed fluorescence (DF) lifetime in healthy subjects with presumably an oxygen level of 0mmHg, with different 5-aminolevulinic acid (ALA) - the precursor of PpIX - application time. [4]

Background signal

We speculate there are two possible principles contributing to these inexplicable results. The first one is interfering DF from other contributors than PpIX. We define the signal caused by this extra and disturbing DF - with its lifetime - as **'background signal'** (BGS). Note, this is not the same as noise - without a lifetime - e.g., the electrical noise from the detector and continual ambient light. This speculations are based on preliminary studies in our department, which measured signals with lifetimes

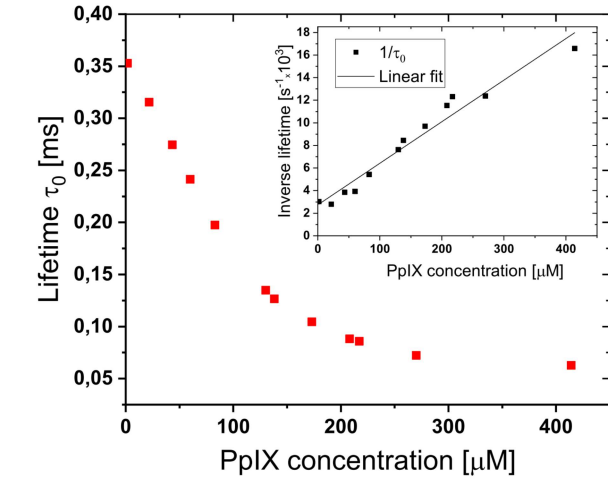

(a)

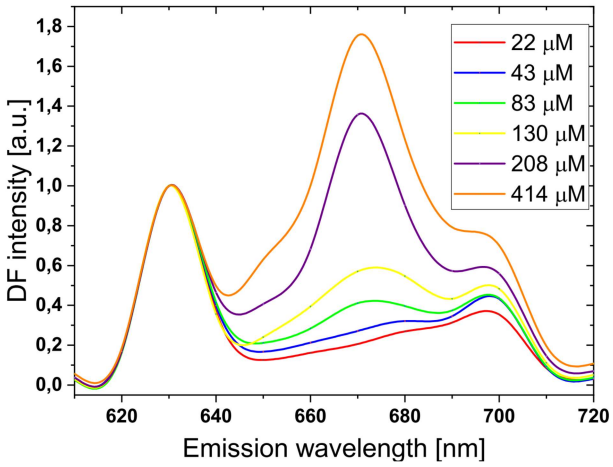

(b)

Figure 5: Inconsistencies within the current PpIX-TSLT, with (a) lifetime measured in absence of oxygen at increasing PpIX concentration; and (b) showing the emitted wavelengths at increasingPpIX concentration.[4]

in absence of PpIX. If BGS contributes significantly to the measured signal, this could affect the lifetime and therefore disrupt the determined PO_2. What factors contribute to the BGS and the extent of its effect on the PO_2 measurement is yet unknown. Other methods incorporating fluorescence are hardly troubled by the occurrence of BGS since they commonly use PF which is measured in orders of nanoseconds. The lifetime of BGS may be in the order of the PpIX-TSLT, i.e., tens to hunderds of nanoseconds. The current COMET device incorporates a form of BGS correction based on fitting the curve of measurements on aluminium to the measured curve. Based on how well it fits, a certain part of the curve is removed. It is questioned whether this is the most suitable method.

Self-quenching phenomenon

The second contributor to the inexplicable results, is the speculation that a **self-quenching phenomenon** (SQP) occurs at high PpIX concentrations. A self-quenching phenomenon would disturb the assumed linear relation between mitoPO_2 and the lifetime of the DF signal, based on solo contribution of E-type DF. The theory states that on collision of two excited PpIX molecules, they can form an excimer [21, 46].

The first identification of PpIX excimers is reported by Croizat et al. [21]. Excimers are aggregates of singlet and/or triplet state molecules and they can produce both PF as well as DF theoretically [31, 47]. The formation of excimers has been studies for several aromatic molecules, among other for pyrene [31, 32, 28, 35, 48, 46]. The formation of excimers can cause radiation of 670 nm light, which can be detected. Thus, SQP theory states that at certain PpIX concentrations, not merely oxygen performs as a quencher, but excited PpIX molecules collide and form excimers, therefore being a self-quencher [21]. This SQP could be (part of the) answer to the unexplained and inconsistent PpIX-TSLT results.

The inconsistencies regarding τ_0 and variable lifetimes within healthy subjects, could be explained by self-quenching of PpIX at high concentrations; i.e., the τ_0 was determined at different PpIX concentrations, and over time the PpIX concentration peaks followed be decrease therefore explaining the DF dip as seen in figure 4. Contrary to the expectations of a constant τ_0, Croizat et al. showed a decrease in lifetime with increasing in PpIX concentration when measuring in absence of oxygen, as shown in figure 5a. Furthermore, formation of this excimer appears to produce DF at 670 nm. With increasing PpIX concentration the amount of emitted DF at 670 nm increased gradually, see 5b [4]. However, the experiments of Croizat et al. show preliminary results obtained with a measurement setup different from the currently used set up for PpIX-TSLT, as used in the COMET. Moreover, the used laser produced a rather unstable output, which may have affected the result quality. Therefore, the results and speculations should be interpreted with care. To gain a better understanding of the occurring phenomena and its applicability in clinical patient setting, some experiments are repeated with better controlled equipment, e.g., a more accurate tunable laser, and additional experiments are performed.

All in order to assess the roll of the self-quenching phenomenon in PpIX-TSLT to either confirm of reject the assumption of the linear relation between mitoPO$_2$ and $1/\tau$.

1.3 Research goal

The aim of this study is in twofold. First, identify the most prominent causes of BGS and examine to what extent they could alter the mitoPO$_2$ measurement accuracy. Second, assess whether self-quenching of PpIX occurs in physiological solutions and in vivo.

Subsequently, with a better understanding of the PpIX-TSLT we hope this gained knowledge may lead to improvements leading towards more accurate mitoPO$_2$ determination as well as improved interpretability of the clinical results of PpIX-TSLT and the COMET; leading to a future with better patient care.

2 Methods

Based on the twofold research goal, the method section starts with the BGS which covers identification of prominent causes of BGS and assessment of their effect on the mitoPO$_2$ measurement accuracy. Followed by the SQP section regarding occurrence of SQP in a controlled – i.e., laboratory – environment. The (extensive) in vivo measurements of the BGS as well as the occurrence of SQP are combined within one experiment: the in vivo experiment. This is covered in the third section of the methods.

2.1 Background signal methods

The PpIX-TSLT is used in two research settings: with patients in the clinic and with cellular experiments in the laboratory. The COMET is used for patient studies, whereas a laser setup in the laboratory (LL) is used for the cell experiments. With a large difference in setup, we assume different BGS disturb the mitoPO$_2$ measurement accuracy. Since both patient and cellular studies are important for expansion of the PpIX-TSLT towards application in patient care, both setups are assessed regarding the presence and the effect of BGS on the mitoPO$_2$ measurement accuracy. Accordingly, we measure multiple measurement situations for evaluation of the presence of BGS and the difference between these situations; examined via the maximum amplitude and the lifetime of the signal. For the extent of the influence of BGS, we examine the ratio of BGS versus DF signal as well as the BGS lifetime. With use of a computer simulation we gain insight in the possible effect of BGS to the measurement accuracy.

2.1.1 BGS research goal

The effect of the BGS on the accuracy of the mitoPO$_2$ depends on several items:

- The ratio of the maximum intensity amplitude (I_0) of BGS (I_0^{BGS}) and of DF signal from the fluorescent porphyrin ($I_0^{Porphyrin}$); e.g., when the $I_0^{Porphyrin}$ predominates the measured signal, the impact of BGS on mitoPO$_2$ measurements is limited, when compared to a situation where I_0^{BGS} contributes more.
- Whether the lifetime of the BGS (τ_{BGS}) is longer or shorter than $\tau_{Porphyrin}$ (i.e., the lifetime of the DF signal originating from excited porphyrin molecules) – including oxygen quenching –; e.g., with a τ_{BGS} larger than $\tau_{Porphyrin}$, the mitoPO$_2$ would be underestimated, and vice versa with a smaller τ_{BGS}, i.e., an overestimation of mitoPO$_2$.
- How large the difference between τ_{BGS} and $\tau_{Porphyrin}$ is; e.g., a larger difference could result in a bigger deviation in determining mitoPO$_2$.

Therefore, it is important to gain understanding of the BGS. During development of the COMET and the PpIX-TSLT a thorough research of the BGS was never performed. This results in uncertainties regarding the impact of BGS. With the BGS assessment of this research we try to improve our knowledge regarding the BGS, its origin and its effect on mitoPO$_2$ measurements.

Accordingly, the end product of this BGS assessment is gaining understanding of the origin of BGS as well as the impact it could have on the accuracy of mitoPO$_2$ determinations. Moreover, the solution (direction) depends on the consistency of the BGS; e.g., if the BGS are comparable in the divers measurement situations, one could perhaps integrate one general BGS into the mitoPO$_2$ calculation for correction, but when the BGS differs significantly, one may for example consider introducing a calibration measurement before each measurement.

To summarize, the following subquestions will be answered in the BGS assessment:

- BGS-sq1: To what extent is BGS present in multiple measurement situations and how comparable are these BGS curves?
- BGS-sq2: To what extent does BGS interfere with the mitoPO$_2$ measurement results?

In answering BGS-sq1 we measure situations appropriate to the COMET as well as the LL, therefore gaining understanding of the origin of BGS for both setups. Furthermore, a third laser setup - build from scratch during this research and referred to as the main laser setup (ML) - enables us to measure separate components of the COMET laser system; in order to research whether certain components cause more BGS than others, and may therefore be more prone for replacement in the future generation COMET. The LL lacks this possibility to measure separate components due to one system not suited to dismantle.

For BGS-sq2, we compare these BGS to the signal from fluorescent phorphyrins - i.e., the signal of interest - to gain information regarding ratios of BGS compared to DF signal of interest. This presents the contribution BGS can have to the measured DF signal used for mitoPO$_2$ calculations. With an increasing concentration of a fluorescent substance, we expect to observe an decreasing ratio of BGS compared to the DF signal.

Additionally, we perform computer simulations for estimating mitoPO$_2$ with addition of measured BGS, to consider the influence of BGS of the mitoPO$_2$ determination and answer BGS-sq2.

2.1.2 BGS experiments

COMET BGS experiments

COMET setup Within the BGS COMET experiment, the BGS of multiple measurement situations are assessed using the COMET (Photonics Healthcare BV, Utrecht, The Netherlands); a class IIa medical device, according to the Medical Device Directive 93/42/EEC, and consists of a sensor and a monitor as shown in Figure 6. The sensor is made of biocompatible housing, holds one excitation and one emission fiber, which are protected by a flexible metal tube. For eyesight safety reasons, the emitted light is diverged via a diffusor. Light is detected approximately at a right angle from the sensor cable and follows a path of a reflecting mirror, two lenses and a filter, before following the emission fiber. The monitor contains a multi-touch screen with integrated user interface for controlling the system, light source, detection system and processing units. The light source is a 515nm pulsed laser, with pulse durations of 60ns and a 10Hz repetition rate. The detection system incorporates a gated red-sensitive photomultiplier tube [10, 22]. The COMET enables single, interval and dynamic measurements for both experimental as clinical setup.[10] The current COMET system incorporates a BGS correction mechanism based on a BGS measurement with aluminium, as it resembles complete reflection, which is fitted to the data and then subtracted to a certain extent.

Figure 6: The COMET monitor and skin sensor [10]

COMET measurements We start with assessing several measurement situations, for production of BGS and mutual comparison, which are described next. Since the COMET system itself may produce BGS, we measure into 2.5m of free air, called mid-air measurements. Human skin is measured as this is where the COMET is used for patient measurements. Moreover, we measure with physiological mitoPO$_2$ levels as well as mitoPO$_2$ levels brought to approximately 0mmHg, in order to evaluate the effect of oxygen on the BGS. Aluminium is measured for comparison of the current incorporated correction mechanism. Lastly, we examine the effect of bending the COMET fiber by measuring in bent and straight position, see Figure 7.

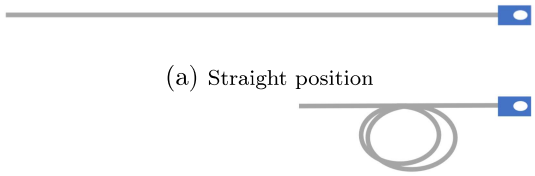

(a) Straight position

(b) Bent position

Figure 7: Schematic fiber position of the COMET for the BGS experiment, with (a) straight and (b) bent position.

Next, we examine the effect of pigmentation by measuring subjects with different skin types based on the Fitzpatrick scale. We include healthy volunteers who participate in the healthy volunteer study of our department (mec 2021-0160). The skin measurements are performed without ALA application in order to obtain a BGS of the skin of multiple subjects. We measure 30 light pulses of 515nm at a rate of 0.1 Hz.

In order to obtain ratios of DF signal of interest (including BGS) and BGS, we perform additional measurements with ALA applied to the skin; see paragraph 2.3 for details.

Each measurement situation is measured with at least thirty light pulses, performed in the dark room By performing each experiment in a dark, closed room without windows and shutting off or covering laptop and monitor screens, the amount of ambient light affecting the results in minimized.

Lab laser BGS experiments

Lab laser setup The lab laser setup (LL) consists of a computer-controlled tunable laser (Opolette 355-I, Opotek, Carlsbad, CA) which has alaser pulse width of 7ns, an energy output maximum at 6.5 mJ and typically 2-4 mJ/pulse, and a output range of 410 to 680nm and 740 to 2400nm. Excitation light levels at output of the excitation branch are for 524nm and 620nm [μJ/pulse]: 34 and 21 for laser power (LP) 60, 50 and 28 for LP80 and 66 and 42 for LP100.

The detection signal is caught in a gated microchannel plate photomultiplier tube (MCP-PMT R5916U series, Hamamatsu Photonics, Hamamatsu, Japan). The emission light is filtered using either a 590nm long pass filter (OG590, Newport, Irvine, CA) and a 675±25nm bandpass, 590 high pass filter (Omega Optical, Brattleboro, VT); or a 665 high pass filter(Omega Optical, Brattleboro, VT).

An amplifier (C6438-01, Hamamatsu Photonics, Iwata City, Japan) is used for amplification of the output current of the PMT. Data acquisition is performed at 10 mega samples per second (MS/s), by a system containing a 10 MS/s simultaneous sampling data acquisition board (NI-PCI-6115, National Instruments, Austin, TX).

The LL is predominantly used for experiments using cells in laboratorial setup. Therefore, the laser setup connected to a cabinet with an automatic pointer guider; guiding the fiber tip under each well of the well plate filled with cells. This cabinet bans all ambient light.

Lab laser measurements Usually in laboratory experiments, one uses well plates filled with different substances which may produce BGS. Therefore, we asses well plates filled with the following generally used substances: phosphate buffered saline (PBS), medium (William's E Medium, GibcoTM, ThermoFisher, 22551-022) used with cellular experiments, different concentrations of Palladium porphyrin (PdP), and different concentration of Platinum tetrafluoride (PtF_4) which binds to beads. Accordingly, the beads without PtF_4 bound to it (blanco beads) are assessed as well. The setup of the well plates are shown in Table 1 and 2. Additionally, to gain knowledge regarding the effect of the excitation intensity, i.e. LP, the experiments includes measurement at different LP levels.

Table 1: Well plate content with decreasing palladium porphyrin (Pdp) concentration in well 1 to 6 in row A and a duplicate in B; row C contains wells filled with PBS, medium or nothing; and the other rows display the tuned photomultiplier tube (PMT) setting to the Pdp concentration for each laser power (LP).

	1	**2**	**3**	**4**	**5**	**6**
A	270 μM	90 μM	30 μM	10 μM	3.3 μM	1.1 μM
B	270 μM	90 μM	30 μM	10 μM	3.3 μM	1.1 μM
C	PBS	PBS	Medium	Medium	Empty	Empty
PMT at LP60	*476*	*420*	*352*	*260*	*180*	*80*
PMT at LP80	*500*	*440*	*370*	*280*	*194*	*126*
PMT at LP100	*516*	*456*	*380*	*290*	*204*	*130*

Table 2: Well plate content with well 1 to 5 and for each row - A, B and C - the used photon multiplier tube (PMT) setting for each applied laser power (LP) tuned to the corresponding Pft4 beads concentration

	1 PtF_4 beads	**3** blanco beads	**3**	**4**	**5**		***PMT LP60***	***PMT LP80***	***PMT LP100***
A	0.6 mg/ml	0.6 mg/ml	Medium	PBS	Empty		*420*	*450*	*430*
B	0.4 mg/ml	0.4 mg/ml	Medium	PBS	Empty		*380*	*410*	*400*
C	0.2 mg/ml	0.2 mg/ml	Medium	PBS	Empty		*320*	*350*	*350*

The PdP measurements are performed in duplo, while PtF_4 beads are measured once. This was due to practicality of the experimental setup. Each well is measured three consecutive times with approximately 10-12 seconds between each measurement. Each porphyrin concentration requires its own PMT setting in order to amplify the signal for a clear view of the curve, and prevent saturation. As the excitation intensity, i.e. LP, affects the emission signal, the PMT setting is shown in the tables for each LP setting. Note, a higher PMT number means less signal amplification. Since each porphyrin concentration and LP have a particular tuned PTM setting, the wells with 'BGS-substances'- i.e., medium, PBS, blanco beads and empty wells – are measured simultaneously with each porphyrin concentration. For PtF_4 we use excitation light with a wavelength of 620nm and for Pdp 524nm, therefore suiting their absorption spectrum.

To determine the ratio between BGS and the DF signal of interest - i.e., coming from the PpIX in the mitochondria or other substances emitting DF with oxygen dependence -, different experiments require different substances. In most cellular and other experiments in the laboratory – where the LL is employed for – are not performed with PpIX, but with another porphyrin. PdP and PtF_4 are commonly used and therefore assessed within this research

Main laser BGS experiments

Main laser setup The main laser set up (ML) of this research consists of a compact computer-controlled tunable laser (Opolette 355-LD, Opotek, Carlsbad, CA) which provides pulses with a duration of 5 to 7ns in the tunable range of 410-2200nm. The maximum pulse peak energy is 9mJ at 450nm, with approximately 6mJ at 515nm [Opotek site]. The detection system contains two paths, each filtered at different wavelengths. In both paths, the detected light passes a filter, an amplifier (C6438-01, Hamamatsu Photonics, Iwata City, Japan) and photonsensor module (H11526-20, Hamamatsu Photonics, Iwata City, Japan). The used filters are focus around 631 ± 21nm and 676 ± 29nm. For data acquisition and system control, the NI USB-6366 Multifunction I/O Device is used (National Instruments, USB-6366 X Series DAQ, Austin, TX, USA), which has a sampling frequency of 2 MS/s per channel. We manually set the sampling frequency to 1 MS/s to ensure accurate sampling.

Main laser measurements As many separate parts of the COMET as possible were measured to obtain insight in the production of BGS from these parts. Accordingly, we measured the excitation fiber, emission fiber, diffusor, glue (on a glass slide) and the blue cover of the COMET sensor. Moreover, the BGS of a short emission fiber of 28cm is compared to a long emission fiber of 63cm. Each part is examined using 10 pulses of 515nm and 101 μJ/pulse.

The ML experiments concerning skin measurements are discussed in section 2.3, which includes assessment of the ratio between BGS and the DF signal of interest - i.e., coming from the PpIX in the mitochondria -. With measurement of subjects' skin with both the COMET and the ML, we can compare the effect of the laser setups.

Computer simulations of BGS effect on measurement accuracy

In order to get a sense of the effect BGS has on PO_2 determination, we simulated this effect within a computer simulation using MATLAB (R2022a, The MathWroks Inc., Natick, Massachusetts). The basis of the simulation is a series of 'ideal PO_2 measurements'; i.e., ascending from 0 to 180 mmHg in steps of 10 mmHg, transferred using the Stern-Volmer equation – see equation 1 – with τ_0 = 200 µs and k_q = 398e-6 $mmHg^{-1}s^{-1}$ [19], to a series of τ_1 values – i.e., lifetimes –. These lifetimes are combined with a BGS from multiple measured situations in experiments with the COMET, LL and ML; we call this the 'combined signal'. The proportion of BGS in this combined signal is adjusted to a contribution of 10%, 20%, 30%, 40% and 50%. Next, we fit a function to the combined signal and perform the reversed steps during obtainment of the ideal PO_2 signal. As such, we retrieve the τ_1 via the fitted function; which is the transferred to a PO_2 via the Stern-Volmer equation. Accordingly, this gives us the possibility to compare input PO_2 with the output PO_2, i.e., the generated ideal PO_2 with the determined PO_2. For the fit function we use two versions: a mono-exponential fit and a rectangular fit. The mono-exponential fit is used as the basic simulation, since the basic principle of PpIX-TSLT would (theoretically) produce a mono-exponential decaying curve if the PpIX is homogeneously distributed and free from other (DF) contributors. Therefore, the following function is used to fit the data: a*exp(-t/τ_1) with t the samples, to obtain a τ_1. In contrast to the theoretical situation,

oxygen is not distributed homogeneously in vivo and the data won't present a mono-exponential curve. The heterogeneous spread of oxygen results in a distribution of lifetimes. A mono-exponential fit does not accurately fit this distribution; it has a tendency to bias toward low mitoPO$_2$ values [49]. The rectangular fit lacks this bias and shows better results compared to the mono-exponential fit, by considering the sum of the rectangular distributions [50, 51]. Therefore, the COMET operates via the rectangular fit [10]:

$$Y(t) = exp(-(\frac{1}{\tau_0} + k_q < mitoPO_2 >)t\frac{sinh(k_q\delta t)}{k_q\delta t} \quad (2)$$

with Y(t) the normalized delayed fluorescence data, <mitoPO$_2$> the mean mitoPO$_2$ and t the samples.

By performing simulation with both fit function, we aim to obtain insight into the deviation BGS could produce when determining mitoPO$_2$.

2.2 Self-quenching phenomenon methods

2.2.1 SQP research goals

Although ambiguous, the results of Croizat et al. suggest there is more to the PpIX-TSLT than yet known [4, 21]. The current experiments were performed in non-physiological samples. Whether similar results are obtained in physiological setting is unknown. Therefore, the main research goal is assessing whether the self-quenching phenomenon, presumable caused by P-type DF, are apparent in physiological setting. Accordingly, experiments are performed to evaluate the repeatability of the SQP results presented by Croizat et al. [4, 21]; followed by assessment of possible SQP in physiological setting, with measurements in laboratory setup as well as in vivo. The in vivo measurements are covered in the in vivo experiment paragraph, see 2.3.

The SQP experiments aim to answer the following subquestions:

- SQP-sq1: Is τ_0 dependent on the PpIX concentration?
- SQP-sq2: Does an increase in PpIX concentration result in an increase in 670 nm DF intensity?
- SQP-sq3: Is the DF intensity ratio of 670 nm signal compared to 630 nm signal affected by the PpIX concentration?

All subquestions are assessed for dimythylformamide (DMF) solutions as well as more physiological solution, which mainly contain PBS with 2% bovine serum albumin (BSA). With SQP-sq1 we choose to focus on τ_0 rather than k_q due to practical reasons. Controlling the exact quencher - i.e, oxygen in our case - concentration requires specific equipment, which was not available for our measurement setup. Furthermore, regarding changes in τ_0 provides a first insight in the occurrence of SQP (in physiological setting).

2.2.2 SQP experiments

The measurements are performed with the ML which is connected to a holder placed on a hot plate put to its maximum of 42°C, resulting in a temperature of the aluminium holder of 36°C. The excitation and emission fiber are connected to the holder in a 90° angle. This optimized the collection of DF signal while minimizing leakage of excitation intensity to the PMT. [52]

The laser excitation intensity is tuned with neutral density filter (Edmund Optics, York, UK) to a value of 37.5 μJ/pulse, to obtain sufficient light and prevent bleaching and detector saturation.

Experiment 1 - Repeat literature
To evaluate the repeatability of the results of Croizat et al., we followed their protocol in assessment of multiple PpIX concentrations. This includes PpIX (Fluka, >99.5%) solutions in DMF (Sigma Aldrich D4551, >99%) of 414 μM, 208 μM and 22 μ; measured with a 410 nm excitation pulse. The PO$_2$ of the samples is reduced to approximately 0 mmHg by bubbling N$_2$ gas through the samples; while simultaneously, warming the samples a hot water bath of 32°C. Some differences between our approach and theirs are the result of practical restrictions. 410 nm is our laser's wavelength limit, therefore we do not measure at 405 nm as their protocol proscribes. We performed measurements not in the hot water bath while bubbling N$_2$ gas, but place the sample - after bubbling and heating in the bath - in the 32°C holder during the measurement. Furthermore, combining continuous stirring with simultaneous N$_2$ gas bubbling and heating the samples was not feasible. Therefore, we manually stirred the sample every eight minutes. Subsequently, we expected it to take longer to bring the samples to a PO$_2$ of 0mmHg. We expect a hour to be sufficient.

Experiment 2 - DMF solutions
Experiment 2 allows assessment of similar settings with PpIX as experiment 1; i.e., measuring PpIX DMF solutions, decreasing the PO_2 level by bubbling N_2 gas through the samples, heating in the hot water bath and measuring in the holder.

We change the excitation wavelength to 515 nm, therefore resembling the one used in the COMET. The temperature is increased from 32°C to 37°C for more comparability to the human body. Furthermore, we enhance the assessed range of PpIX concentrations with more concentrations - especially in the lower concentration range - to assess occurrence of SQP within this range; we created the following sample series: 200, 150, 100, 75, 50, 25, 9.4, 4.7, 2.3 and 1.2 μM.

The samples are exposed to bubbling with N_2 gas for approximately one to two hours to establish a PO_2 of approximately 0mmHg.

Experiment 3 - Physiological solutions
The same sample range as used in experiment 2 is used, but with a different solution. The physiological samples are created following the following protocol [53, 54, 55]:

1. Create a 7.5 μM PpIX stock by:
   (a) dissolving 8.4 mg PpIX in 1 ml 0.1M Trizma base (Sigma >99.9%, T1503) PBS solution;
   (b) followed by adding DMF in a 1:1 ratio - i.e., 1 ml - to the PpIX sample.
2. When a clear solution is obtained, the stock is combined with a solution of PBS with 2% BSA (Sigma, 98%, A7030). Creating samples of 2.5 ml with the same PpIX concentrations as used in experiment 2.

These solutions consist of mainly PBS 2% BSA and are therefore called the physiological solutions. The pH of samples was 7.33 and the samples are heated to a temperature of 37 °C in a hot water bath, followed by transferring to the sample holder of 36 °C (the maximum temperature of the holder).

The PO_2 level of the physiological samples was reduced using sodium-ascorbate (Sigma, PHR1279) and ascorbate oxidase (Sigma, from Curcubita sp., A0157), therefore following the approach of Lo et al. [52]:
the purchased ascorbate oxidase (Sigma, from Curcubita sp., A0157) was diluted in sodium phosphate monobasic dihydrate (NaH_2PO_4*$2H_2O$, Sigma, 71500) resulting in a solution with 1 unit ascorbate oxidase per μl. We added 2 units to each sample. Followed by adding 300 μl of 8 mM sodium-ascorbate; which was (more than) sufficient to reduce the PO_2 to approximately 0 mmHg.

2.3 In vivo experiment

The in vivo experiments concern the exploration of the potential BGS as well as SQP within the human skin. Therefore, ALA patches are applied to subjects' skin prior to the measurements. As Fauteck et al. showed, the DF intensity differs per ALA application time - i.e., the time the ALA patch is applied to the skin - which potentially affects the BGS-DF-ratio. With an improved - i.e., decreased - BGS-DF-ratio, the mitoPO_2 calculation accuracy could improve since it is less disturbed by BGS. Accordingly, the effect of ALA application time on the DF and on the BGS is evaluated as well.[36]

These measurements of the DF signal at different ALA application time suit the in vivo SQP research, since the PpIX concentration is essential for the occurrence of SQP [21].

Additionally, measuring with multiple ALA patches provides the opportunity to assess the behavior of the DF signal after removal of an ALA patch on healthy subjects. This knowledge can be essential for clinical application; e.g., within the OR we measure for more than eight hours on the same spot, lacking the knowledge whether the DF signal remains stable for this amount of time.

2.3.1 In vivo experiment research goals

With this in vivo research we aim to answer the following subquestions:

- ALA-sq1: What is the ratio of in vivo measured BGS compared to DF originating from PpIX in the mitochondria in the skin and how is this ratio affected by ALA application time?
- ALA-sq2: What happens with the DF signal intensity after removal of a patch?
- ALA-sq3: Does the ratio of DF signal intensity of 630 nm and 670 nm change with longer ALA application time?

Based on results of the ALA patches presented by Fauteck et al., we hypothesize to observe an increase of DF to at least 4 hours after application [36]. Whether

the DF signal remains stable afterwards, decreases of keeps increasing is to be seen. This, combined with the simultaneously measured BGS during the day, provides answers for ALA-sq1.

To get answers for ALA-sq2, an ALA-patch applied for 11 hours is used. Since this is longer than the DF intensity peak after 4 hours of application observed by Fauteck et al., we would expect to observe a decreasing trend in DF intensity after removal.

For ALA-sq3, we hypothesize that longer application time results in more PpIX (at least for 4 hours), therefore increasing the possibility for SQP to occur. This would be shown via an increased 670nm/630nm signal intensity ratio. Based on the knowledge that oxygen is a strong quencher we perform the measurements at mitoPO$_2$ of approximately 0mmHg as well, besides physiological mitoPO$_2$ values. Moreover, we expect this ratio to anticorrelate with the lifetime based on results of Croizat et al. [4], as Figure 32 in Appendix A.2 shows. This anticorrelation could indicate the occurrence of SQP, as the lifetime changes may be ascribed to the increase of 670 nm and decrease of 630 nm signal intensity following SQP.

2.3.2 In vivo experiment methods

We aim to include six to eight subjects. Each subject puts twelve half ALA patches (PD P 506 A) on their upper arms on, with every patch approximately 3cm apart. An intact patch (i.e., not yet cut in half) are 4cm^2 and contain 2 mg of ALA per 2cm^2 [36]. A designated spot on the arm is marked for the BGS measurements. Since blemished skin, such as birthmarks, can potentially affect the DF signal, these spots are avoided. The schedule for the timing of patch application by the subject as well as the measurements timing is presented in Table 3. Note that after a measurement, some patches are re-applied and measured again to obtain more data for different application times. A measurement consists of 5 pulses with an interval of 10s, to limit the effect of possible persisting excited PpIX molecules and (DF) light. The ML is used for the in vivo experiment, firing pulses of 515nm, with 101μJ/pulse. Additionally, the first two subjects are measured with the COMET as well. For the other subjects the measurement protocol is extended with measurements after reducing the mitoPO$_2$ to approximately 0mmHg. The method consists of pressing the measurement probe firmly to the skin, therefore obtaining microvascular occlusion. This method is commonly used for mitoVO$_2$ measurements [22, 20, 15]. Since the ML has no real time assessment of the mitoPO$_2$, the probe is pressed for more than 20seconds; which should, after consultation with experts, be more than sufficient to decrease the mitoPO$_2$ to a value <5mmHg.

Table 3: In vivo experiment application and measurement protocol; with measurement times after 1st application and re-application of ALA patches and the corresponding hours of application for each of the 12 ALA stickers.

Sticker number	Approx. time of application	Approx. time of measurement after 1st application	Approx. hours after application during 1st measurement	Approx. time of measurements after re-application	Approx. hours after application during 2nd-4th measurements
#1	21:40	08:40	11	-	-
#2	21:40	09:40	12	10:40	13
#3	21:40	10:40	13	11:40, 13:40, 15:40	14, 16, 18
#4	21:40	11:40	14	12:40, 14:40, 16:40	15, 17, 19
#5	06:40	09:40	3	10:40	4
#6	06:40	10:40	4	11:40	5
#7	06:40	11:40	5	12:40	6
#8	06:40	12:40	6	13:40	7
#9	06:40	13:40	7	14:40	8
#10	06:40	14:40	8	15:40	9
#11	06:40	15:40	9	16:40	10
#12	06:40	16:40	10	-	-

2.4 Analyses

The analysis of all experiments is performed with MATLAB (R2022a, The MathWroks Inc., Natick, Massachusetts). We average the measurements of each setting to reduce the effect of noise and artefacts. Per setting 5 to 50 measurements are obtained. No signal filtering is applied - except the hardware filters - unless specified within the results section, because filtering can affect the signal; especially the start and end, which is of great importance for our analyses. We did visually inspect each measured signal for outliers and deviating measurements. The continuous noise present on the measurement channel is removed; i.e, the value at the flat signal curve ending is subtracted from the entire signal, to ensure the ending of the curve ends at 0. We call this the corrected data. For comparison of the BGS curves in multiple measurement situations, we normalize the data. The maximum intensity amplitude (I_0) of each signal is obtained and used for the BGS-ratios as well as the I_0-ratios of the SQP experiments. The lifetimes are calculated using the rectangular fit function; with a k_q of 4.77*10$^-$4 and τ_0 of 800μs for COMET and ML measurement for PpIX [19, 38, 56], and for LL measurements using a k_q of 4.22*10$^-$4 mmHg$^-$1s$^-$1 and

τ_0 of 504μs for PdP [30] and for PtF_4 a k_q of 4.7*10$^-$4 and τ_0 of 46.6μs - based on in-house calibrations-. The function fit starts at the maximum amplitude value. The BGS-DF-ratio calculations are performed as: $\frac{I_0^{BGS}}{I_0^{DF}}$.

After several experiments, we were introduced to the fact that the COMET automatically tunes its excitation intensity according to the measured substance with a filter wheel, which takes approximately 2-5 measurements. Therefore, if sufficient data was obtained - i.e., at least 10 measurements -, we average the measurements minus the first five.

3 Results and discussion

3.1 Background signal results

3.1.1 Presence of background signal

This subsection contains the results to answer BGS-sq1 regarding the presence of BGS in multiple measurement situations and the comparability of this BGS between these situations.

Results of COMET experiments

Multiple COMET measurement situations

For each measurement situation, we obtained 50 measurements which are averaged minus the first five. The skin measurements are performed in two subjects with skin type I on the Fitzpatrick scale. Figure 8 shows the corrected data - i.e., the data after averaging the measurements and subtracting the ending of the curve to ensure its ending at 0 - as well as the normalized data of the measurement situations measured with the COMET. The corrected data shows a segregation into two groups regarding maximum intensity amplitude: the aluminium and skin measurements have a much higher intensity than the mid-air and fiber bent and straight.
The curves of the normalized data show a slight difference, with the aluminium measurement most deviating. The corresponding lifetimes are: 44μs for mid-air, 83μs for aluminium, 47μs for both the bent and straight fiber, for 55μs for the skin with physiological PO_2 and 56μs for the skin with PO_2 0mmHg. These lifetimes translate to 'PO_2' values of 26, 13, 24, 20 and 20 mmHg, respectively.

The increased BGS signal intensity for skin and aluminium measurements is expected, due to the reflecting capacity of the material, resulting in more rebounding light. The similar results of the two skin BGS values indicate that the mitoPO$_2$ seems to have no significant effect on the BGS. Moreover, whether the determined mitoPO$_2$ is over or underestimated - if the BGS contributes significantly to the measured signal and without correction for the BGS - depends on the subjects mitoPO$_2$ value. Commonly, the mitoPO$_2$ is in the range of 40 - 90mmHg for healthy subjects [22, 57]. In critical clinical situation - i.e., with a mitoPO$_2$ below 20 mmHg - the estimated mitoPO$_2$ can be higher as a result of the BGS with it's lifetime corresponding to 20 mmHg.
To bent or straighten the fiber appears to have a negligible effect.

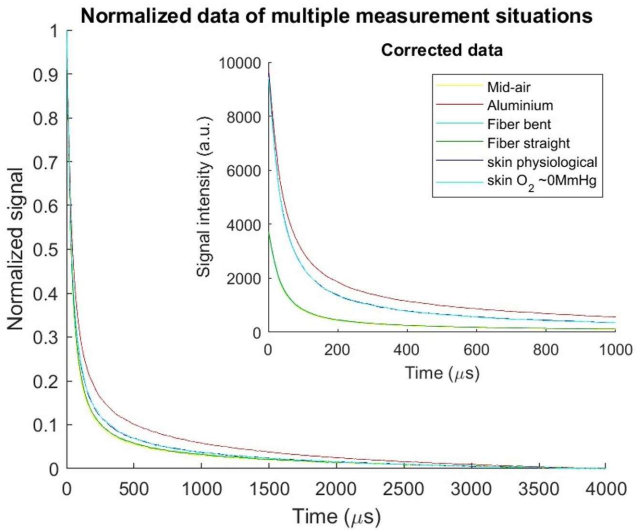

Figure 8: The normalized data of multiple measurement situations, measured with the COMET.

Whereas large intersubject BGS differences are not expected apart from pigmentation, we included merely two subject for this experiment, as a result of practical reasons. This assessment does give a first indication regarding the lack of influence mitoPO$_2$ has on the BGS. Moreover, the pigmentation experiment provides insight regarding the effect of pigmentation on the BGS. Note that the concentration of PpIX under normal - i.e., non-sensitized - conditions is very low and not detectable by the COMET [10].
We expect the temperature to remain rather stable during the measurements, therefore not affecting the result. However, full temperature stability cannot be

guaranteed. Whether temperature has effect on the BGS could be assessed in the future for full disclosure.
Known causes of disturbance, like ambient light, were eliminated by performing the experiments in the dark room. Moreover, the filter wheel within the COMET did indeed stabilize after five measurements, therefore ensuring equal excitation light intensity. Internal laser fluctuations may influence the excitation light intensity, however, with the number of measurements this effect is minimized, resulting in a reliable signal.

Based on these results we conclude that the COMET device itself produces BGS; which is significantly increased when measuring on material, such as human skin. The similarity of the BGS lifetimes of both fiber positions as well as skin measurements indicates for clinical practice that both the fiber position and mitoPO_2 value can be neglected.
Currently, the COMET includes the correction mechanism based on an aluminium measurement. The shown difference in BGS lifetime of aluminium and skin could therefore result in wrongful corrections. Accordingly, a BGS correction using skin BGS could be more appropriate.

Effect of pigmentation

Measurements regarding different pigmentation levels are performed for four subjects with for subjects with skin type I, V and VI on the Fitzpatrick scale.

The signal results of the effect of pigmentation on the BGS, displayed in Figure 9, show similar curves for the different subjects. The lifetime of subject A – D are, 55, 60, 54 and 52μs, respectively.

With the difference in lifetimes between skin type I (subject A and B) and the higher pigmentation levels (subject C and D) showing merely a few microseconds, we conclude the level of pigmentation does not affect the BGS.

The minimal difference between the low and high pigmentation levels, could be the result of measurement set up. Since subject C and D are measured not in the dark COMET room, but in rooms with more ambient light.

These four subject give a first indication of the effect of pigmentation on the BGS. To conclude whether or not to determine a BGS for each individual due to different pigmentation levels, a more extensive study should be performed. However, these results suggest no large discrepancies will show.

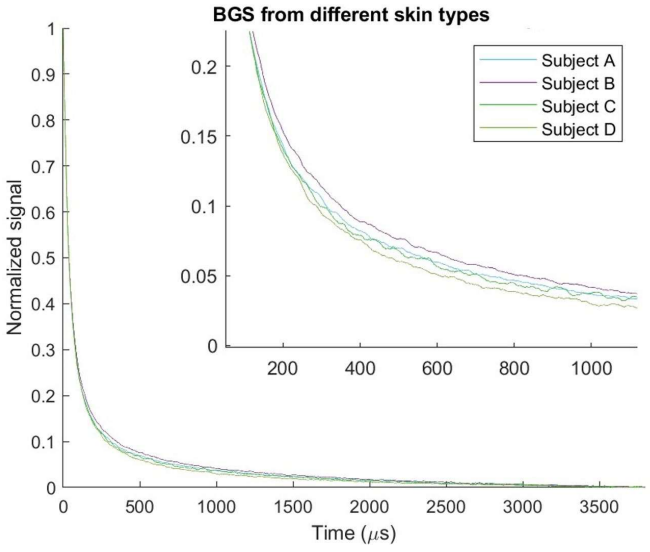

Figure 9: COMET measurement results of the BGS from subjects with different skin types based on the Fitzpatrick scale; subject A and B are type I, subject C type V and subject D type VI.

Results of lab laser experiments

When combining the signals of the measured wells within the LL experiment, one obtains figures such as Figure 10; both for PdP as well as PtF_4 beads experiments. The figure for each concentration combined with the simultaneously measured BGS can be found in Appendix B.1.1. Figure 10 shows the different signals from the PdP experiment, measured with the LL, for the 10μM sample; i.e., the signal from the PdP sample with simultaneously measured wells with medium, PBS and empty wells. All BGS measurements are comparable and the PdP signal overpowers these signals. Examples of these overlapping BGS are found in the same Appendix section.

Curves with similar shapes imply similar lifetimes. When assessing the lifetimes of the PdP BGS measurements, we observe high values in the range of 147 to 257μs, with on average 209μs. The lifetimes results of the medium measurements are visible in Table 4; for the results for PBS and empty wells we refer to Appendix B.1.1, Table 8 and 9, respectively.

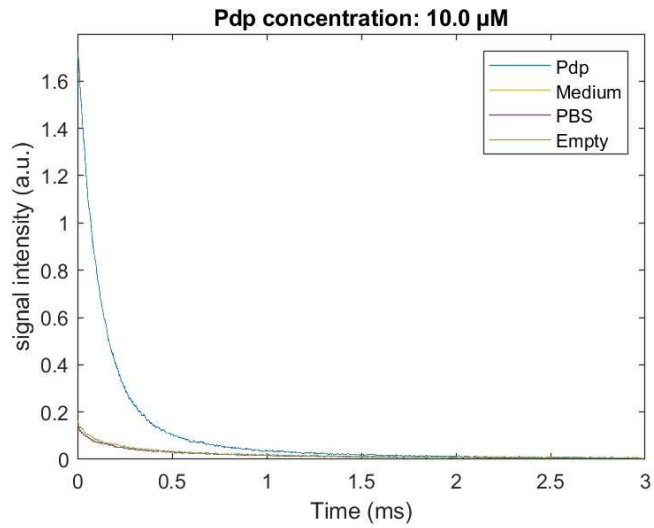

Figure 10: Curves of palladium porphyrin (10 μM), measured simultaneously with wells filled with medium, phosphate buffered saline (PBS) and empty wells.

When regarding the lifetime results of the PtF_4 beads measurements, we observe for the BGS of the average lifetime of 119μs (minimal 76μs and maximal 143μs). The different BGS substances present similar lifetimes per beads concentration and the complementary PMT setting. As example and since these wells contain 'all' BGS contributors, the lifetimes of the blanco beads measurement are found in Table 5, while the other lifetimes are found in Appendix B.1.1. Both the laser power as well as the PMT strength, which differs per PdP/PtF_4 beads concentration, seem to have a moderate effect on the determined lifetime.
Since the medium BGS measurements differ for the PdP and PtF_4 measurements, we conclude that the excitation light wavelength affects the BGS as well.

The effect of these BGS measurements would for these experiments be the following: The lifetime of the samples with increasing PdP concentrations range between 100 to 140 μs for these experiments, see Table 7 in Appendix B.1.1, which corresponds to a PO_2 of 18.9 to 12.2mmHg. Subsequently, the higher lifetime of BGS than the PdP samples would decrease the calculated PO_2 compared to the real value in this case. The average lifetime of the PtF4 beads samples is 105μs, which is close to the BGS lifetime. This would therefore lead to a smaller deviation in calculated PO_2 than the deviation within the PdP experiments, assuming the ratio of BGS to DF signal is constant.

Table 4: Lifetimes of the BGS from wells filled with medium, ranked per pdp concentration, therefore, corresponding to the accessory PMT setting.

Lifetime of BGS from medium, ranked per pdp concentration (μM)	**270**	**90**	**30**	**10**	**3.3**	**1.1**
LP60	178	185	184	222	226	220
LP80	257	187	205	222	219	215
LP100	180	199	215	215	223	214

Table 5: Lifetimes of the wells with blanco beads for multiple concentrations; presented for each laser power (LP) measurement.

Lifetime for blanco beads concentration (mg/ml)	**0.6**	**0.4**	**0.2**
LP60	76	119	136
LP80	106	126	137
LP100	110	132	144

Note that air-saturated samples were closed and placed in the climate box, therefore the PO_2 was at the start conform the PO_2 of the room (which depends on the atmospheric pressure and humidity et cetera). The light pulses on the fluorescent materials might result in oxygen consumption. Therefore, the PO_2 value of the samples is uncertain. Although unexpected and not shown in the COMET skin BGS experiments (see Figure 8), the BGS could be affected by PO_2 in this setting. Assessment is required to obtain confirmation regarding this concept.

Because of the research regarding hypoxia, the low PO_2 values are of most interest; i.e., long lifetimes. Therefore, the relatively short lifetimes of the BGS measurements imply that if the BGS is a significant component in the received DF signal, this would cause the determined PO_2 to be higher than the true value, when not accurately compensated. The example mentioned in the introduction and shown in Appendix A.1 corresponds with this idea; i.e., the measured oxygen levels was higher than the applied levels of 5% and 0%.

The contribution of the measured BGS to the DF signal is examined in section 3.1.2.

Based on these results with the varying BGS lifetimes as a result of LP, PMT setting as well as excitation light wavelength, we consider using BGS compensation measures adapted to individual experimental set ups most appropriate.

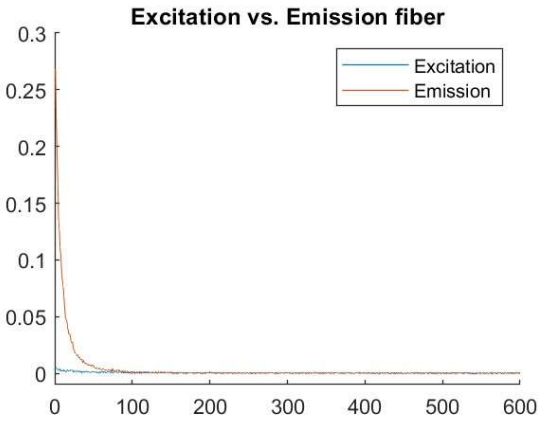

(a) Excitation vs. emission fiber

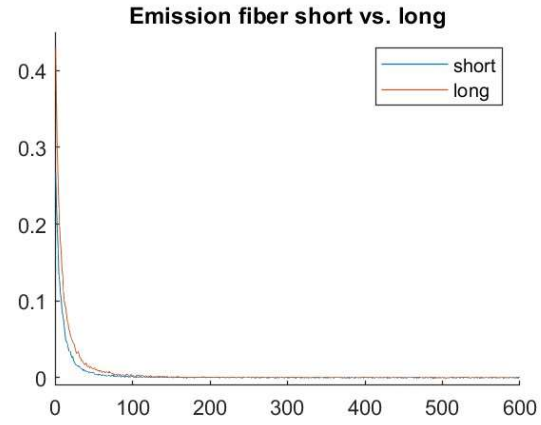

(b) Long and short emission fiber

Figure 11: BGS measurements of separate COMET parts with (a) the excitation and emission fibers and (b) the comparison of a long and short emission fiber.

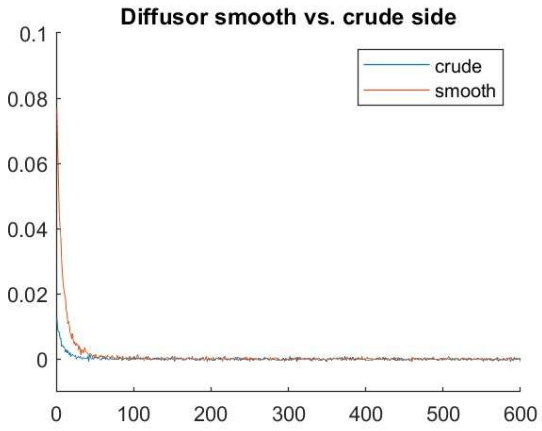

(a) Diffusor sides

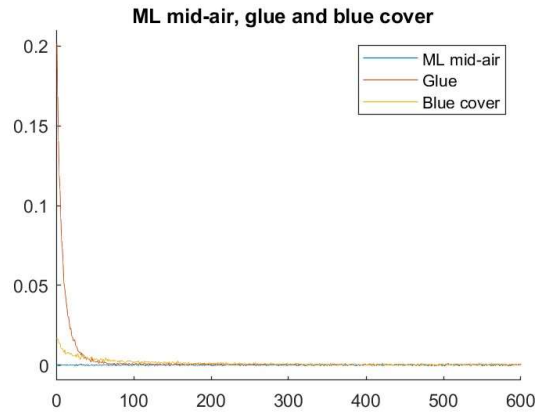

(b) BGS ML mid-air, glue and blue sensor head cover

Figure 12: BGS measurements of separate COMET parts with (a) the two side of the diffusor and (b) the internal BGS of the ML, glue and blue sensor cover.

Results of main laser experiments

COMET parts

The results of the BGS measurement of the COMET parts shown in Figure 11 and 12. As shown, the signal intensities differ per part. The ML itself seems to show no BGS production as it merely fluctuates around 0, see Figure 12b. The emission fiber and glue have the larges BGS in regard of intensity (i.e., maximum amplitude) and lifetime. The emission fiber produces more BGS signal when compared to the excitation fiber. A longer fiber may increase the BGS intensity. Finally, the smooth side of the diffusor seems to increase back-scattering of the signal.

These results imply that a short emission fiber is preferred and minimal use of the glue in creating the COMET sensor head. If the light doses could be reduced to ensure users safety without a diffusor this would decrease the BGS as well. Possibly the wavelength of 405 nm could be used instead of 515 nm; the PpIX absorbance spectrum shows significantly more absorbance at 405 nm than 515 nm. However, 405 nm penetrates significantly less than 515 nm. Whether this may still provide sufficient measurement volume in vivo should be examined.

The COMET contains more components than the ones examined. However, the evaluated parts are considered the most important component regarding possible BGS production. The glue was stuck on a glass slide (as used for microscopic purposes), which possibly affects the measured BGS.

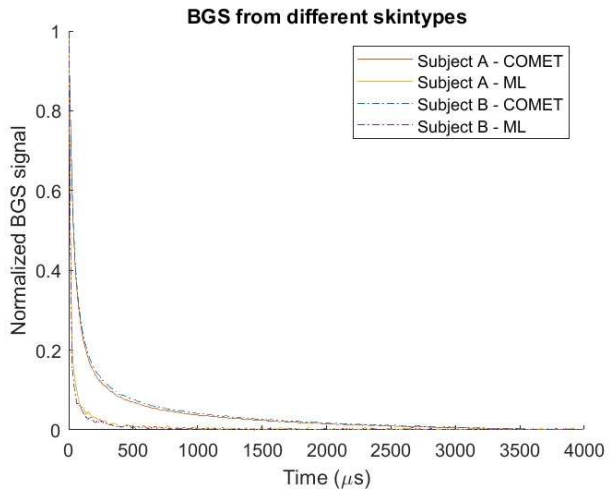

Figure 13: Two subjects, A en B, measured with two laser set ups; i.e., the COMET and the main laser set up (ML). The BGS are measured on the subjects skin - without ALA - and normalized.

Comparison of BGS in main laser and COMET

Two subjects are measured with the COMET as well as the ML. These results are displayed in Figure 13, and show a large difference between the laser setups and limited difference within one setup intersubjectively. The lifetime corresponding to the signals of Figure 13 are for subject A 55μs in the COMET and 11.9μs in the ML, and for subject B 60μs and 10.5μs, respectively.

A large difference between laser is shown, implying comparison of measurements between laser should be done with great care. Moreover, a compensation mechanism for the BGS should be specific to each laser type. The ML has different hardware than the COMET, for future studies it might be interesting to asses whether a difference between COMETs exists as well.

3.1.2 Influence of BGS

This section concerns the results regarding the influence BGS may have on the mitoPO_2 calculation accuracy, i.e. BGS-sq2 as well as ALA-sq1. The computer simulation indicates this potential effect for different BGS with multiple BGS to DF proportions. The signal intensity comparison of BGS to DF provide insight into the contribution of BGS within the measured DF signal with the shown ratios. For human skin we measured with both the COMET and the ML, while for the LL the ratios are determined for PtF_4 beads and PdP.

Computer simulation of BGS effect

In Figure 14, three examples of the simulation of the possible effect BGS could have on the determined PO_2 are shown: the rectangular fit simulation with COMET skin BGS and with LL medium BGS, and a mono-exponential fit simulation of the ML skin BGS. The other simulation results are found in Appendix B.2.

With an increasing percentage of BGS in the combined signal, the output PO_2 deviates progressively. When regarding the RMSE of the simulations in Figure 15, even a small contribution of 10% or 20% of BGS to the signal, could result in a deviation of 9.7-36.7 mmHg on average. However, the largest discrepancies are in the higher PO_2 range with these BGS. This coincides with the low lifetimes at high PO_2's and the high(er) BGS lifetimes; i.e., the larger the difference between the BGS lifetime and the true lifetime, the more the BGS affects the calculated PO_2.

Within the simulation with the mono-exponential fit and the ML skin BGS, the relatively small deviation in PO_2 indicate this BGS is closely related to the mono-exponential input; the lifetime of this BGS lies around 150 mmHg.

Where the rectangular fit has no trouble fitting the combined signal, the mono-exponential fit fits poorly when the combined signal differs from the input mono-exponent; an example of this poor fit is shown in Appendix B.2 Figure 40b. Moreover, the results of the simulation with a mono-exponential fit with COMET mid-air BGS and LL medium BGS show a constant underestimation of the PO_2, caused by the inability of the mono-exponential fit to accurately fit the combined signal, as well as the longer lifetime of the added BGS. This indicates that the rectangular fit is better suitable for application in the PpIX-TSLT.

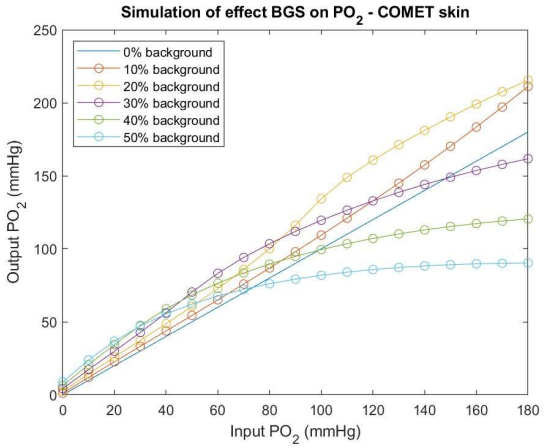

(a) COMET - rectangular fit

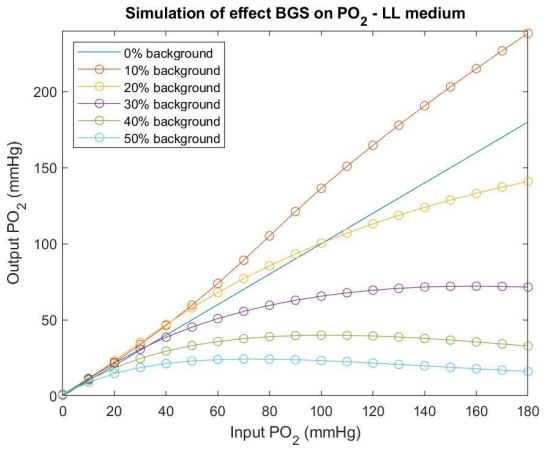

(b) Lab laser - rectangular fit

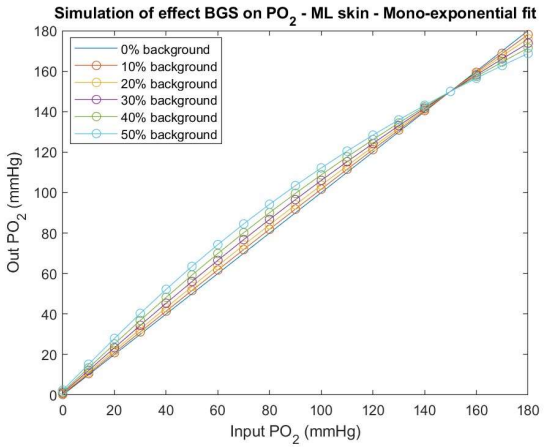

(c) Main laser - mono-exponential fit

Figure 14: Simulation of possible effect of BGS with different BGS inputs: (a) COMET skin (no ALA) measurements and (b) lab laser medium measurements; showing output PO_2s against input PO_2s, for multiple ratios of the PO_2-mono-exponent input and BGS

The simulation contains merely one mono-exponent as input value, whereas the in vivo situation consists of a distribution of lifetimes. We choose to use one input since the simulation should provide a first insight on the possible effect of BGS on the measured mitoPO_2, and that is achieved with this approach.

Overall the simulations indicate that BGS could have a large disturbing effect, especially when the BGS lifetime differs extensively and the contribution of BGS to the measured DF signal is large.

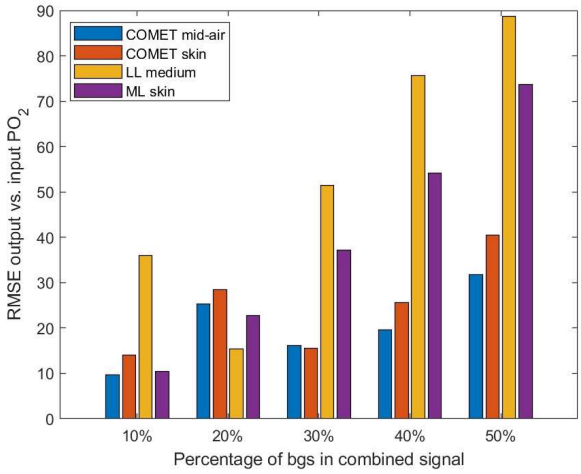

Figure 15: Results of the simulation of the effect of BGS on the PO_2 calculations - using the mono-exponential fit - with use of BGS from mid-air measurements made with the COMET.

It strikes that the BGS is a large contributor within the COMET measurements; even with long ALA application times the BGS may have an I_0 of (more than) half the DF I_0. The same subjects measured with the ML show much better ratios. Therefore, the BGS of the COMET appears more problematic than the ML. A contributing factor could be the different and longer emission fiber, which showed to be causing significant BGS see paragraph 3.1.1.

Compare signal intensity of BGS to DF

COMET and main laser BGS-ratios for skin measurements

The in vivo signal intensity ratios are obtained via the in vivo experiment. We included four subjects. The inclusions stopped as a result of adverse effects as a result of the ALA patches.

The ratios of BGS compared to the used DF signal for the COMET, shown in Figure 16, present a rather stable maximum intensity amplitude for BGS and, with fluctuating I_0 for the DF signal, result in different contributions of BGS to the useful DF signal.

Similar results are shown for the ML. The result of each subject is displayed in Table 6 and for visualization the bar-plot of subject four is displayed in Figure 17. The colored values in the Table visualize that an overall increased BGS contribution to the 670 nm signals; which is confirmed in the graphs of 670 nm in Figure 17b as well as for the other subjects as shown in Appendix B.3.Moreover, the BGS-ratio differ intersubjectly; e.g., subject 3 has generally a higher ratio than subject 2. With a fairly stable I_0 for the BGS of each subject - around $1*10^4$ a.u. for the COMET and 0.1 a.u. for 630 nm signal in the ML - this is considered to be the result of PpIX concentration.

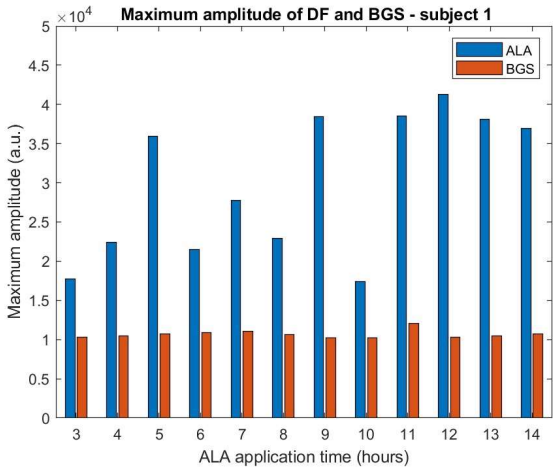

(a) Subject 1

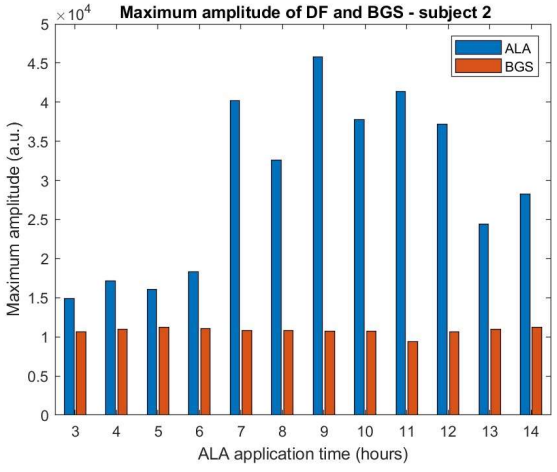

(b) Subject 2

Figure 16: Comparison of maximum intensity amplitude of DF signal with BGS signal, using the COMET, for (a) subject 1 and (b) subject 2.

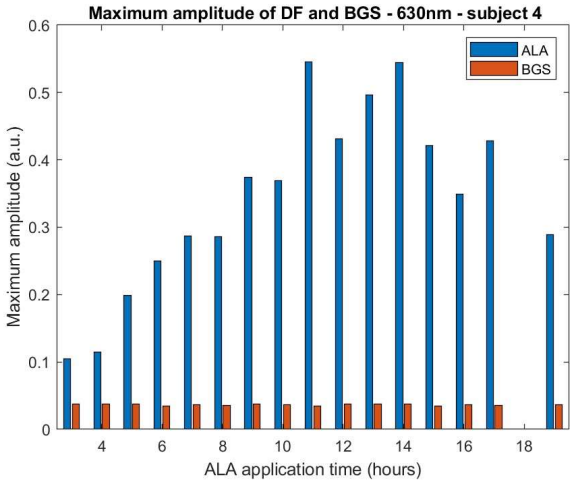

(a) 630 nm

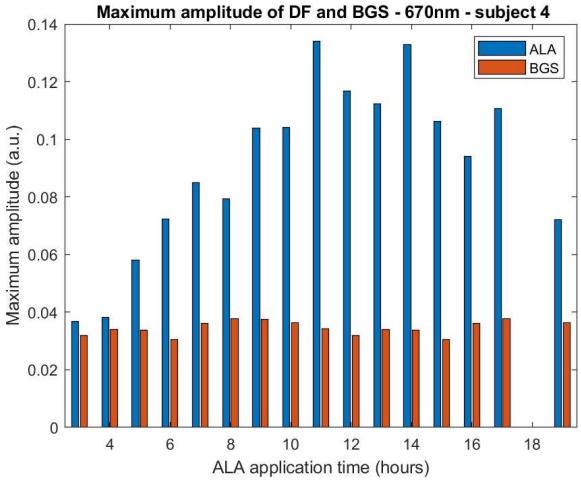

(b) 670 nm

Figure 17: Comparison of maximum intensity amplitude of DF signal with BGS signal, using the main laser set up, for subject 4 with (a) 630 nm signal and (b) 670 nm signal.

2

Table 6: Ratio of background signal compared to DF signal of four subject, for both 630nm and 670nm signal; displayed for all ALA application time of the in vivo experiment.

ALA application time [hours]	3	4	5	6	7	8	9	10	11	12	13	14	15	16	17	19
Sub 1 - 630nm	0.22	0.12	0.18	0.09	0.11	0.09	0.12	0.15	0.06	0.06	0.08	0.15	0.15	0.09	0.18	0.28
Sub 2 - 630nm	0.22	0.16	0.09	0.06	0.05	0.07	0.05	0.10	0.05	0.06	0.07	0.05	0.08	0.12	0.04	0.11
Sub 3 - 630nm	0.65	0.52	0.41	0.51	0.28	0.17	0.31	0.23	0.07	0.11	0.11	0.11	0.14	0.08	0.13	0.13
Sub 4 - 630nm	0.38	0.34	0.20	0.15	0.11	0.13	0.11	0.11	0.07	0.09	0.08	0.07	0.09	0.11	0.09	0.13
Sub 1 - 670nm	0.30	0.22	0.32	0.17	0.22	0.14	0.18	0.26	0.11	0.10	0.14	0.27	0.25	0.14	0.27	0.38
Sub 2 - 670nm	0.43	0.39	0.39	0.30	0.17	0.22	0.15	0.12	0.15	0.18	0.22	0.16	0.26	0.38	0.15	0.33
Sub 3 - 670nm	0.67	0.69	0.65	0.89	0.49	0.32	0.43	0.46	0.21	0.22	0.18	0.23	0.33	0.16	0.29	0.27
Sub 4 - 670nm	0.88	0.89	0.59	0.43	0.37	0.48	0.37	0.36	0.27	0.28	0.31	0.26	0.30	0.39	0.35	0.51

It strikes that the BGS is a large contributor within the COMET measurements; even with long ALA application times the BGS may have an I_0 of (more than) half the DF I_0. The same subjects measured with the ML show much better ratios. Therefore, the BGS of the COMET appears more problematic than the ML. A contributing factor could be the different and longer emission fiber, which showed to be causing significant BGS see paragraph 3.1.1.

When the BGS is a large contributor to the received signal, this is most problematic if the difference in lifetime is large, because the larger the lifetime difference, the more the determined lifetime and therefore mitoPO_2, differs from the true mitoPO_2, as shown in the simulations. The lifetime of the BGS are for the COMET 68.8μs (50.4μs - 85.2μs) for subject 1 and 63.6μs (53.9μs - 70.0μs) for subject 2; and for the ML for subject 1 10.6μs (9.7 - 11.1μs), subject 2 11.3 (8.8 - 12.4μs) subject 3 on average 12.5μs (9.7 - 13.0μs), for subject 4 11.7 (8.1 - 14.3). This corresponds to a mitoPO_2 value of approximately 17 mmHg for the COMET BGS and 108 mmHg for the ML BGS. Accordingly, the BGS of the COMET decreases most common mitoPO_2's; as these range from 40 - 70 mmHg which corresponds with lifetimes of 29 - 17μs [22, 57], but overestimates low mitoPO_2's; which can be critical values within clinical setting. In contrast, the BGS of the ML would result in overestimation of the mitoPO_2's.

Therefore, sufficient fluorescent porphyrins are essential in order to obtain a satisfactory signal to BGS ratio, therefore improving the accuracy of the determined mitoPO_2 values.

When measuring in vivo, the measurements are prone to fluctuations based on bodily differences. The measurement location may for example affect the result via skin lesions or birth marks. Although the subjects are instructed to avoid discrepancies in the skin, the different patch locations can influence the results. Moreover, it is unknown what the effect of the currently incorporated BGS correction of the COMET system might be.

In clinical setting the ALA application time is essential for obtainment of a satisfactory BGS to DF signal ratio. The ideal ALA application time is, however, difficult to determine due to the intersubject differences. Based on the obtained results, it appears suitable to apply ALA for minimally eight hours and no longer than nineteen hours, before starting the measurement.

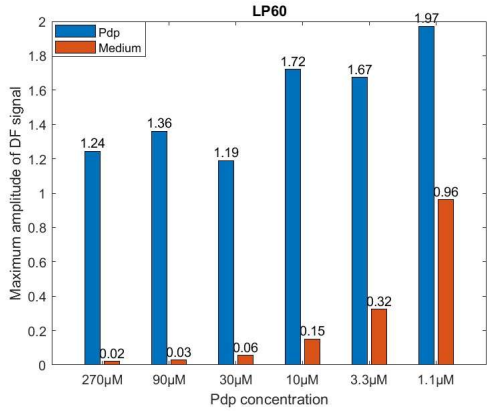

(a) LP60

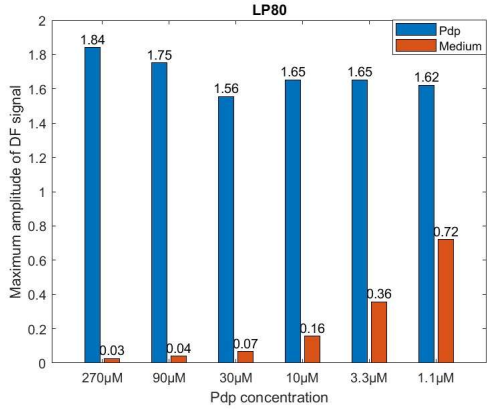

(b) LP80

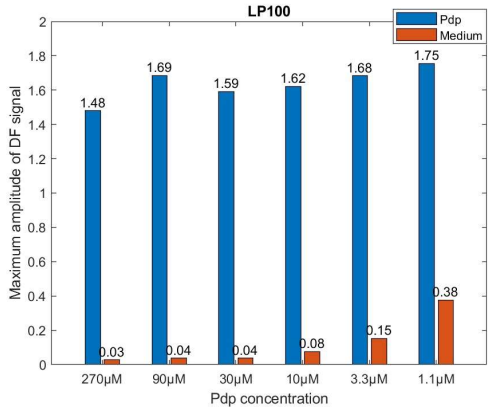

(c) LP100

Figure 18: Ratios of delayed fluorescence (DF) signal from palladium porphyrin samples with decreasing concentrations, compared to background signal from wells filled with medium. Represented for measurements with laser power (LP) (a) 60, (b) 80 and (c) 100.

Lab laser BGS-ratios for PdP and PtF_4 beads measurements

As shown in Figure 18, decreasing PdP concentrations result in an increasing contribution of BGS to the total DF signal; with a maximum ratio of 48.7% for 1.1μM PdP measured with LP60. When increasing the PdP concentration, the effect the BGS contribution decreases rapidly. This corresponds our hypothesis that an increased concentration improves the BGS-ratio. When regarding the different LP settings, it shows that with a higher LP the DF-BGS-ratio decreases. Therefore, increasing the LP during experiments might be beneficial for the DF-BGS-ratio. Note, the effect of excitation light intensity is not assessed for the COMET nor the ML. The COMET regulates its own excitation light intensity. Within the ML the excitation intensity can be regulated using neutral density filters for example. However, in the SQP experiments this let to either insufficient light or detector saturation. within the in vivo experiment practical (time) restrictions prevented examining the effect of LP.

The results of the PtF_4 beads experiment show similar results as PdP, as visible in Figure 19. In contrast to the PdP experiments, the LP appears to have hardly any influence on the BGS-ratios. The smaller differences in BGS-ratios as well ass lack of (clear) LP effect, is assumed to be the result of the smaller PtF_4 beads concentration difference.

Based on these results, in order to reduce the effect of BGS, we advice to use at least 3.3 μM PdP and consider increasing the LP - instead of the commonly used 60 - therefore decreasing the PMT, for better results. In regard of the PtF_4 beads, all concentrations and LP setting seem to produce appropriate BGS-ratios, and could therefore be tuned to specific cellular experiments.

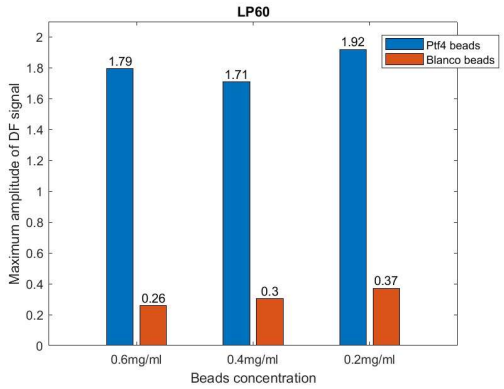

(a) LP60

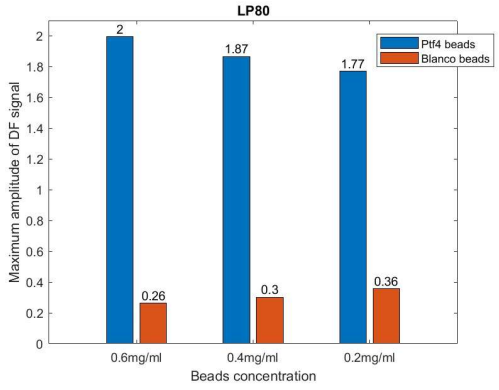

(b) LP80

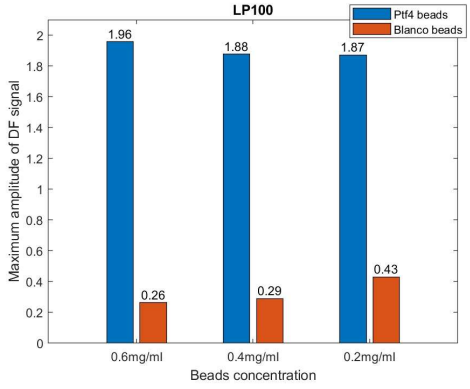

(c) LP100

Figure 19: Ratios of delayed fluorescence (DF) signal from platinum tetrafluoride beads samples with decreasing concentrations, compared to background signal from wells filled with medium. Represented for measurements with laser power (LP) (a) 60, (b) 80 and (c) 100.

3.2 Self-quenching phenomenon results

3.2.1 Experiment 1 and 2 - DMF solution

The results of SQP experiment 1 and 2 - i.e. testing the repeatability of results found in literature regarding SQP experiments, and measurements with multiple DMF samples with increasing PpIX concentrations - did not give the expected results. With two hours of bubbling N_2 gas through the samples and stirring the samples every eight minutes the PO_2 of the samples was not significantly reduced. Therefore, the N_2 gas bubbling and stirring was continued. However, with over four hours of bubbling, the samples did not sufficiently decrease in PO_2. This contrasts our expectations. The samples of Croizat et al. had a similar DMF volume and showed a stable, long lifetime after 10 minutes of N_2 gas bubbling and stirring simultaneously. Unfortunately, our samples have a large head space, requiring more N_2 gas. Furthermore, our stirring method might be suboptimal. Our set up lacked the possibility to combine: continuous stirring, N_2 gas bubbling, heat control and air tight sealing cuvettes without head space, which can be placed in the measurement holder. Accordingly, we advice to change the measurement setup with a different holder and heat control; preferably using cuvettes with a smaller head space. With air tight sealed cuvettes, it may be possible to separate the warming process of the samples from the reducing oxygen levels; i.e., first perform the N_2 gas bubbling with continuous stirring, followed by bringing the sample to the desired temperature and subsequently performing the measurements. Some additional tips for executing these measurements based on the process of this research are found in Appendix A.3.

Despite the high oxygen concentration, the samples were measured and are evaluated in the next section. Do note that this is merely supplementary and solid conclusions can not be drawn. Lastly, the experimental setup gave room for bubbling eight samples simultaneously, therefore sample 2.3μM to 150μM are examined.

The curves of the samples are shown in Figure 20 and show minimal to no signal for the lowest three samples. We consider this to be the result of the low PpIX concentration combined with the high PO_2. The other samples show some more signal. The lifetime of these concentrations are 25μM = 34μs, 50μM = 64μs, 75μM = 23μs, 75μM = 32μs, 100μM = 10μs, 150μM = 18μs. Therefore, the sample are not close to a PO_2 of 0 mmHg.

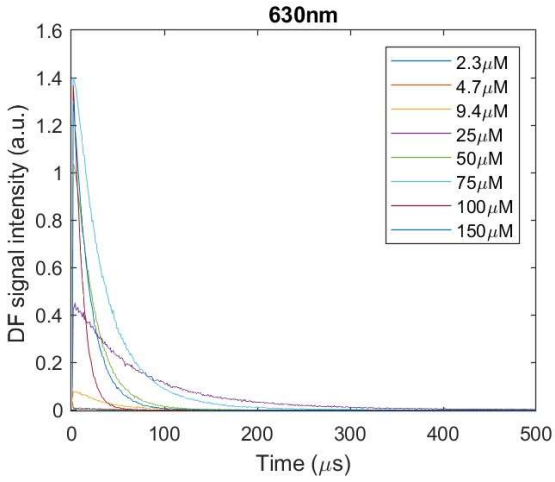

(a) 630 nm

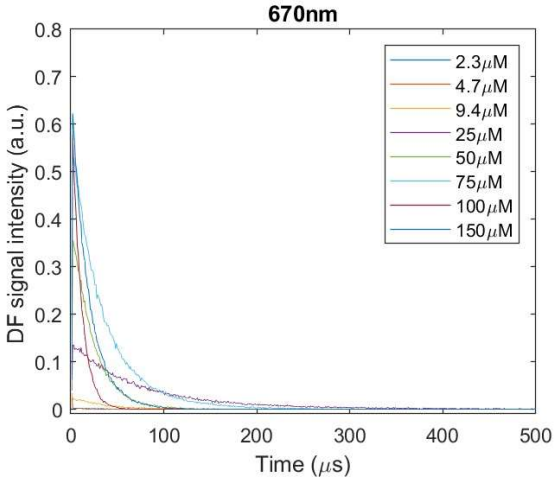

(b) 670 nm

Figure 20: Curves of DMF samples with increasing PpIX concentrations, for (a) 630 nm and (b) 670 nm.

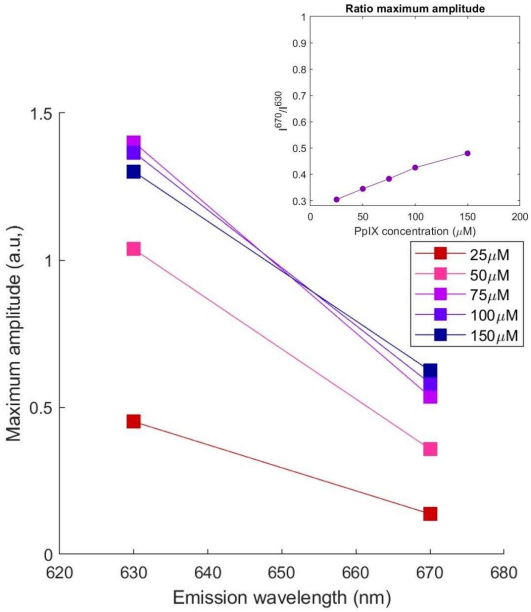

Figure 21: The maximum intensity amplitude for the 630 nm and 670 nm signal, with on top the ratio of these I_0's, for the DMF samples with increasing PpIX concentration.

When evaluating the maximum intensity amplitudes of the 630 nm and 670 nm signal, we do observe a ratio increase, see Figure 21. The increasing ratio corresponds with literature where similar samples did have a close to zero oxygen level, see Appendix A.2, but our results show a higher ratio, indicating more 670 nm.

Thus, even though no PO_2 of 0mmHg is achieved, an increase in PpIX concentration result in more 670 nm signal. With the varying PO_2 values of the samples as well as lacking proper knowledge of the characteristics of lifetime of the 670 nm signal compared to the 630 nm signal, no general conclusions can be drawn. When regarding the lifetime of the 670 nm signal (τ_{670}) at zero oxygen levels of SQP experiment three, it decreases with increasing PpIx concentration like the 630 nm lifetime (τ_{630}) does. However, the inconsistent differences between τ_{670} and τ_{630} ensures no firm conclusion can be drawn. See Appendix D Figure 47 for these lifetime results.

3.2.2 Experiment 3 - physiological solution

The averaged and filtered curves of the samples from the physiological experiment are presented in Figure 22.
As a result of increased amplification - using the amplifier in the hardware - the results remain noisy after averaging multiple measurements; therefore an Savitsky-Golay filtering - chosen for its ability to also keep the beginning and ending of a signal intact - is applied [58]. Based on keeping most prominent increases in the signal and removing noise, we use an order of 2 and range of 25 frames. This reduced most of the noise, but with still some noise bothering the signal, the maximum intensity amplitude is calculated as the mean value of peak intensity value and the twenty closest values.

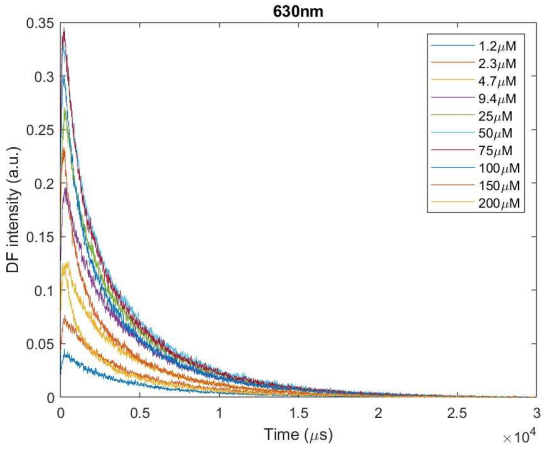

(a) 630 nm curves

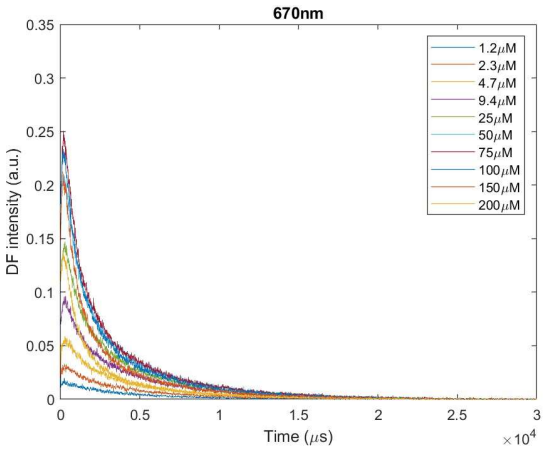

(b) 670 nm curves

Figure 22: Curves of each sample form the physiological SOK experiment

When plotted, these maximum intensity values produce Figure 23. As the ratio on top shows, the I_0^{670} values increase more than the I_0^{630} value with increasing PpIX concentration. Furthermore, the maximum amplitude of the 630 nm signal increases simultaneously with the PpIX concentration, until the 150μM. The 150μM has a lower I_0^{630} value than 25, 50, 75 and 100μM; the 200μM sample has as similar maximum intensity value as the 4.7μM sample. Similar results are found for the intensity integral of each sample, shown in Appendix C.1.
Besides changing maximum amplitudes and integral intensities, the different PpIX concentrations also have different τ_0's, as visible in Figure 24. The lifetime at zero oxygen decreases with increasing PpIX concentration. The inverse τ_0 corresponds rather well with the ratio of the intensity integral (Appendix C.1 Figure 44).

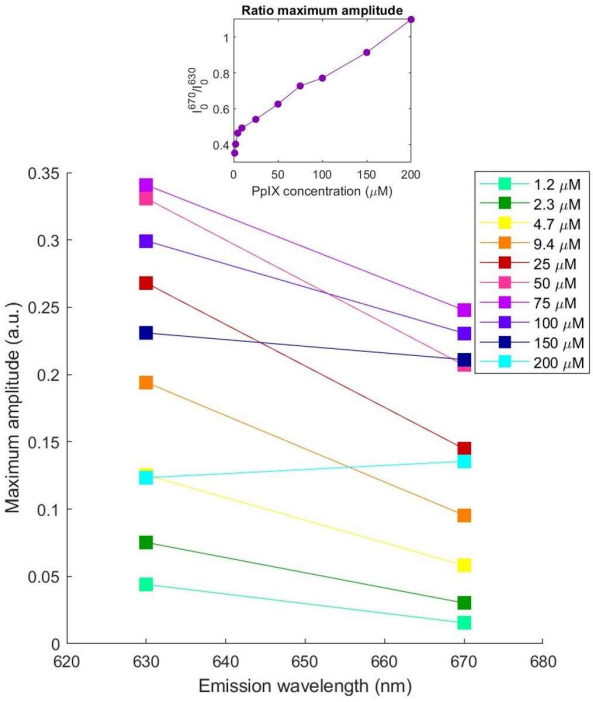

Figure 23: The maximum intensity amplitude for the 630 nm and 670 nm signal, with on top the ratio of these I_0's, for the physiological samples with increasing PpIX concentration

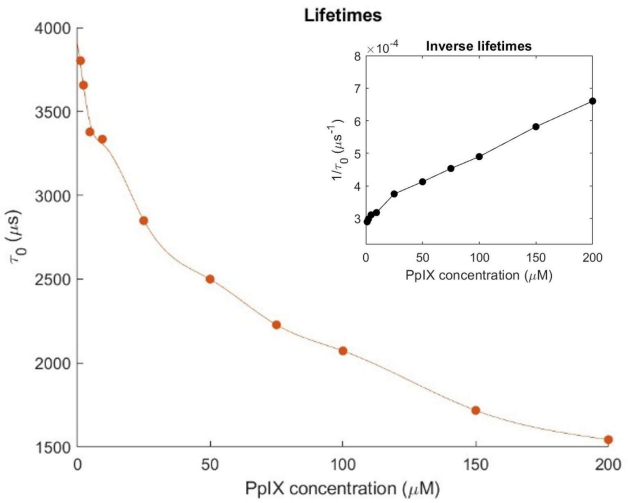

Figure 24: Lifetime per PpIX concentration

Regarding these results, most crucial is the inconsistent τ_0 for different PpIX concentrations, starting already at concentrations of 1.2 μM and 2.3 μM and persisting with increasing PpIX concentration. This lifetime appears to be correlated with the amount of 630 nm and 670 nm light. If the integral intensity ratio indeed corresponds well with the inverse tau, this could provide a possibility to include SQP occurrence into the (COMET) in vivo measurement; by incorporating measurement of both emission lengths and use the calculated E^{670}/E^{630} for which τ_0 value to use in determining the mitoPO_2. The curves of the integral intensity ratio and the inverse tau deviate lightly (see Appendix C.1 Figure 44), which could perhaps be improved when incorporating a BGS correction mechanism.
When evaluating the increasing maximum signal intensity results, we first consider that more PpIX molecules within the higher concentrated samples, provide more opportunity for excitation to the T1 state - with sufficient laser excitation intensity - and therefore possibly increasing the DF intensity. This could explain the increased maximum amplitudes of 630 nm as well as 670 nm within the higher PpIX concentration range compared to the lower range. Secondly, an increased number of T1 state PpIX molecules is a basis for the formation of excimers, according to the SQP-theory. This could explain why the I_0^{670} increases more than the I_0^{630}. According to these two considerations, the maximum amplitudes of the 150μM and 200μM sample should surpass the lower PpIX concentrations; which is, however, not the case. We speculate that the lower I_0^{630} and I_0^{670} of these two samples is the result of the concentrations and the experimental set up. The high concentration of the samples enhances the opaqueness, which may light to penetrate less. Furthermore, the excitation and emission fiber in a 90° angle. This combined could result in less received light. Note that the intensity integral, shown in Appendix C.1 Figure 45a, has similar results as the maximum amplitude. We consider comparison of the maximum intensity amplitude more valid, since this excludes the effect the lifetimes of the signal could have. Moreover, using maximum intensity amplitude provides better comparison possibilities with in vivo measurements, since the exact PO_2 in vivo is difficult to establish.

Our findings contrast the assumption of the PpIX-TSLT that τ_0 is independent of the PpIX concentration. Mik et al. show a τ_0 of approximately 1200 μs (pH 7.0-8.0) and a rather stable lifetime for a PpIX concentration range of 0.1 to 10 μM for samples containing 2% BSA, at 37°C and 1% oxygen as well as with 3% oxygen [19]. It strikes that our results show a decreasing τ_0 in this lower PpIX concentration range. A possible explanation could be that our results are affected by BGS of our system. As shown in the BGS experiments of this research, low fluorescent substance concentrations - i.e., PpIX - produce less DF signal, therefore a higher BGS to DF ratio resulting in more influence of BGS on the measurement. When increasing the PpIX concentration in the SQP experiments, the effect of BGS decreases gradually. This could explain the unexpected steep increase in maximum amplitude ratio of Figure 23.
For the higher PpIX concentration ranges, Croizat et al. found a similar decrease in lifetime at zero oxygen as we did in our samples, in samples with PpIX in DMF [4]; shown in Appendix A.2 Figure 30. They also show similar results for the increase of 670 nm signal with increasing PpIX concentration. Note, they use DF integral intensity to compare the PpIX concentrations. Our results differ in regard of the intensity ratio, where our ratio is higher than theirs. Our research differs in regard of physiology of our samples; they dissolved PpIX in DMF, while we use more physiological solutions containing PBS with 2% BSA. Sulkowski et al. found that binding of PpIX with humans serum albumin enlarges the absorbance spectrum, including 515nm. Furthermore, the presence of HSA results in an increase of PpIX fluorescence (with excitation wavelength of 280nm and 295nm) [59]. While delayed fluorescence is a different process than PF, this could perhaps be a contributor to the increased ratio.

Furthermore, our lifetimes are approximately a factor three to ten larger than those found in literature [4, 19]. We speculate this could be the result of better PO_2 reduction and accurate measurement hardware with high sample rates. In comparison to Croizat et al., the addition of BSA could alter the lifetime. However, Mik et al. did use BSA as well.

A limitation in regard to our setup is the guarantee of the sample's temperature. The temperature of the sample changes supposedly when moving it from the hot water bath to the hot holder. However, by minimizing the time of moving and with approximately the same measurement timing for each sample, we assume the effect of temperature differences to by minimal.

During this experiment, the signal required increasing the signal gain from a control voltage of 0.41V to 0.8V of the PMT, to obtain a visible lifetime signal [60]. Whether this is the result of the samples of change in hardware setup is unknown. However, since all samples of this experiment are measured with the same setup and the exact values of maximum amplitudes are merely compared within this research, we consider this increased amplification to have no effect on the obtained conclusions. Note that the PMT is slightly better equipped to obtain 630 nm signal than 670 nm. However, with the small difference as well as comparing ratios of each measurement, we consider the effect to hardly affect the results.

Since ascorbate may reduce the the pH significantly. Accordingly, we evaluated the pH, which remained stable around 7.3; presumably because of the buffering capacities of Trizma base and PBS in the samples. Although the optimum pH for ascorbate to function is 5.5, within less than 1 minute the PO_2 level reduced to approximately 0 mmHg.

To conclude regarding our hypothesis; when more physiological samples with increasing PpIX dissolved in PBS with 2% BSA, we do observe an increased 670 nm signal in comparison to 630 nm DF signal, suggesting presence of the self-quenching phenomenon. The addition of BSA does however not seem to decrease the self-quenching phenomenon when regarding the 670nm/630nm-ratio of either the maximum amplitude or the intensity integral.

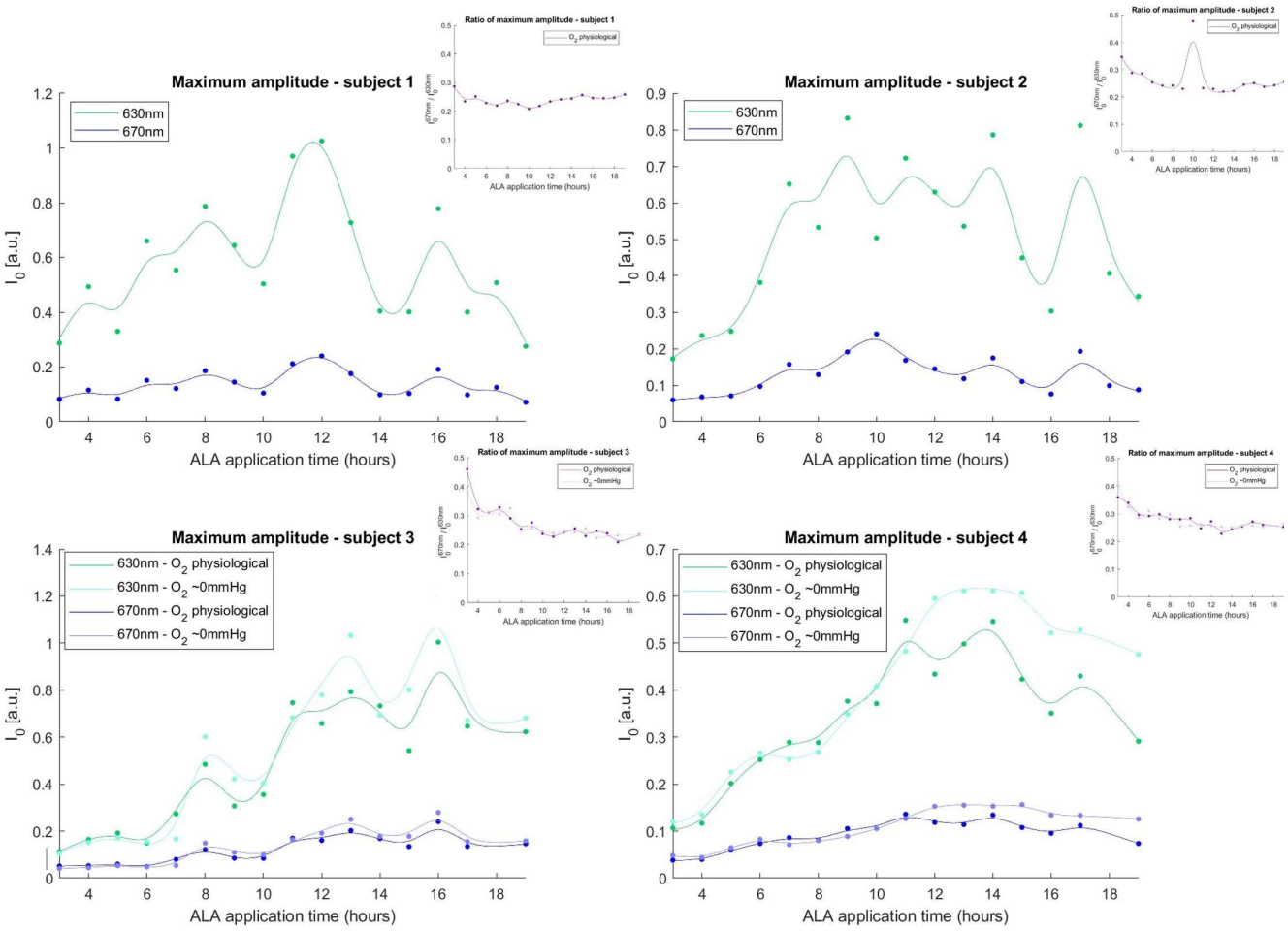

Figure 25: The maximum intensity amplitude of the four subjects for the 630nm and 670nm signal; the corresponding ratio is found in the top right corner of each graph. Note, these ratios are found in larger Appendix D.

3.2.3 Experiment 4 - in vivo experiment

This section start with the results regarding the effect of ALA application time on the DF, covering the signal intensity of 630 nm and 670 nm and comparing it to the lifetime. Therefore, answering ALA-sq3. Followed by what happens to the DF signal intensity after removal of a patch, i.e. ALA-sq2.

The in vivo experiment is performed for four healthy female subjects, ranging between 21 to 24 years old, and all subjects have skin type I on the Fitzpatrick scale except subject four, who has type III. Subject three and four are measured with the extended protocol; i.e., including measurements with mitoPO$_2$ brought towards ±0mmHg.

Delayed fluorescence behavior for varying ALA application times

With increasing ALA application time the maximum intensity amplitude of both the 630 nm signal and 670 nm signal increase, as shown in Figure 25. The exact increase varies per subject. The I_0 decreased after 18 and 19 hours of ALA application for all subjects, compared to shorter application times; especially two out of four subjects show a prominent decaying I_0 after 12 to 14 hours of application. Although the maximum intensity amplitudes increase, the I_0^{670}/I_0^{630}-ratio remains seemingly stable with application time, as can be seen in the top right corner of each graph in Figure 25. No difference is observed between physiological mitoPO$_2$ and the mitoPO$_2$ ±0mmHg. The ratios tend to decrease slightly with increasing ALA application time. Moreover, the ratios of physiological mitoPO$_2$ and

±0mmHg are highly comparable. Note, the I_0-ratios are shown enlarged in Figure 48 in Appendix D.

Although the change in I_0-ratios is limited, it seems to moderately anticorrelate to the fluctuating lifetime; as is shown in Figure 26 for subject 3. This goes for both the physiological mitoPO$_2$ as well as the mitoPO$_2$ ±0mmHg. Despite our considerations mentioned above for using maximum intensity amplitude rather than intensity integral values, the anticorrelation is more clear when comparing tau to the E-ratio, see Figure 27. These anticorrelations show for each subject, as the figure in Appendix D display.

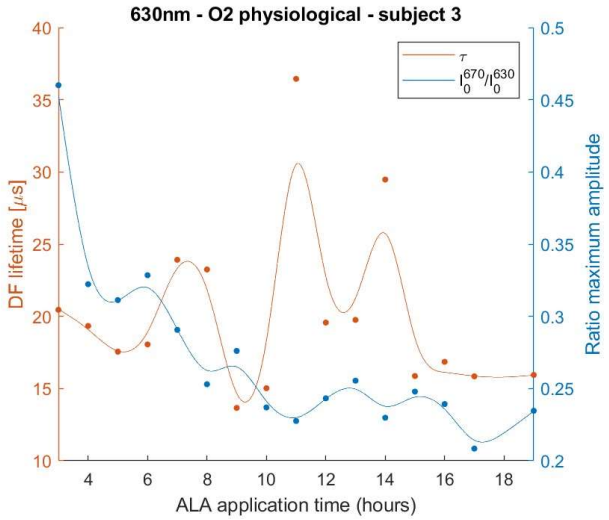

(a) mitoPO$_2$ physiological

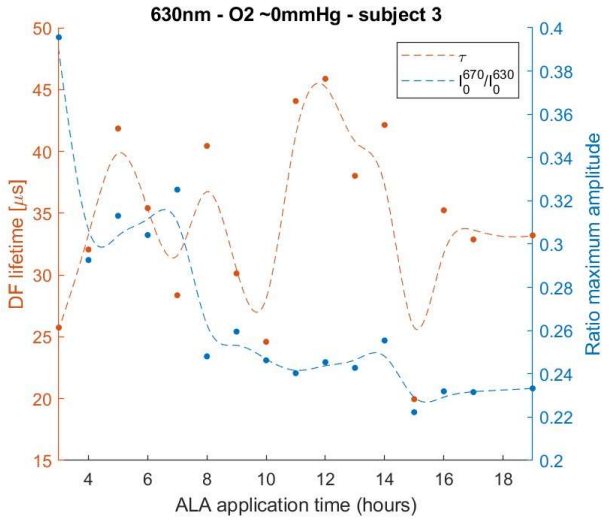

(b) mitoPO$_2$ ±0mmHg

Figure 26: The lifetime and maximum intensity amplitude of subject 3 plotted over ALA application time, for (a) mitoPO$_2$ at physiological level, i.e. no intervention, and (b) mitoPO$_2$ reduced to a minimum.

The observed maximum intensity amplitude follows our hypothesis stating that an increased application time results in more PpIX, therefore producing more DF signal. The decay of maximum amplitude values after many hours of application time, establishes the idea that ALA is absorbed and transferred to PpIX for at least 12 hours, therefore increasing the amount of DF signal. Intersubject differences exist for the required application time for the peak intensity. Next, a start of decreasing I_0 could indicate the stop of transformation of ALA to PpIX and start of both synthesis of Heme as well as transfer of PpIX to other tissue. With most I_0-ratios between 0.2 and 0.4, the in vivo concentrations seem most likely to be in below 2.3μM when compared to the physiological samples of the SQP experiments.

Our findings confirm that no change in the signal ratios occur at physiological O_2 levels; possible affirming that O_2 is a strong quencher and significantly stronger than P-type DF. With a reduction of O_2, similar ratios are observed, which suggests no difference occurs in regard to possible SQP in correlation to the mitoPO$_2$ at these oxygen levels. However, it is important to note that the lifetimes of the reduced mitoPO$_2$ measurements suggest the oxygen pressure is not close to 0 mmHg. The lifetimes are somewhat increased, but remains largely under 185μs, which resembles a mitoPO$_2$ of 5 mmHg and is used as appropriate minimum [22]. Higher mitoPO$_2$ values can be caused by insufficient pressure on the probe. However, a larger contribution may come from the small circular ML probe (±0.5 cm diameter) in comparison to the COMET sensor head (20x70 mm [10]), which decreases the pressured volume significantly. With a smaller pressurised volume, oxygen-carrying erytrocytes can more easily infiltrate the measurement side, therefore affecting the mitoPO$_2$. Thus, the hypothesis concerning the possibility of more P-type DF as a result of this increased amount of PpIX, therefore excimers formation producing 670 nm, with increasing ALA application time, appears false at these mitoPO$_2$ values. Whether this does occur at close to zero mmHg values of mitoPO$_2$ remains unanswered. The lack of increased ratios with the small decrease of mitoPO$_2$ values, might suggest a large decrease of oxygen pressure is required before SQP may occur in vivo. However, this is largely speculation and should be

properly evaluated. Additionally to the I_0-ratios, the E-ratios of the normalized 630 nm and 670 nm signals - see Figure 53 in Appendix D - do not show a increased ratio with the reduced mitoPO$_2$, but an overall lower result. With the I_0-ratios more stable, these results suggest the lifetime of the 670 nm signal reduces with the pressured measurement volume.
The more suiting anitcorrelation of the lifetimes with the E-ratio, suggest the lifetime of the and 670 nm signal affect the anticorrelation.

When evaluating the lifetimes at physiological mitoPO$_2$ levels, the intersubject differences suggest no general effect of the longer ALA-application time. The fluctuations could therefore be proscribed to the expected differences based on changes during the day -i.e., measurement timing - and measurement location. However, it strikes that the small changes in ratios, especially the intensity integral ratios, anticorrelate with these lifetime fluctuations. This could suggest that the ratio of 630 nm and 670 nm DF signal (negatively) affects the lifetime; or, vice versa, that the mitoPO$_2$ affects the DF signal ratio.

Our results regarding increase of PpIX with longer ALA application time, correspond to the results of Fauteck et al.[36]. They show that after 2 hours of ALA application, the fluorescence intensity keeps increasing even after patch removal as a result of a saturation of the heme synthesize path combined with an ALA deposit on the skin. Furthermore, when ALA is applied for 5 hours, this increase is stronger and results in more fluorescence. Our results show an addition of DF signal increase up until 9-16 hours of ALA application.

Our results regarding the anticorrelation of tau and the 670 nm 630 nm ratios, corresponds with the finding of Croizat et al. [4]; their results are shown in Appendix A.2. They suggest SQP to be the cause of the anticorrellation, based on the consideratin that they measured in vivo with a local zero oxygen level. However, their calculated lifetimes suggest mitoPO$_2$ was far from 0mmHg. Subsequently, fundamental prove of SQP occurence in vivo remains to be found.

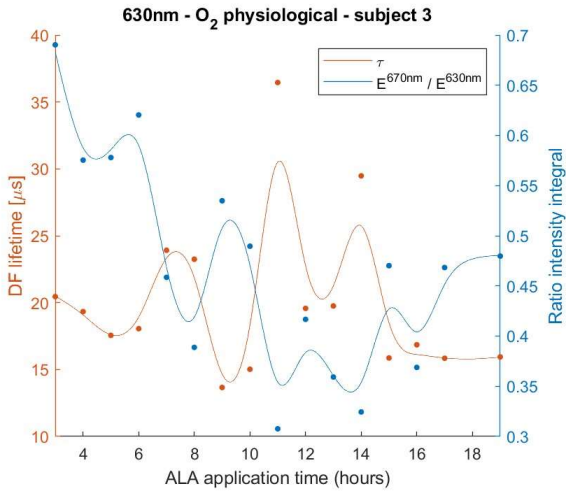

(a) mitoPO$_2$ physiological

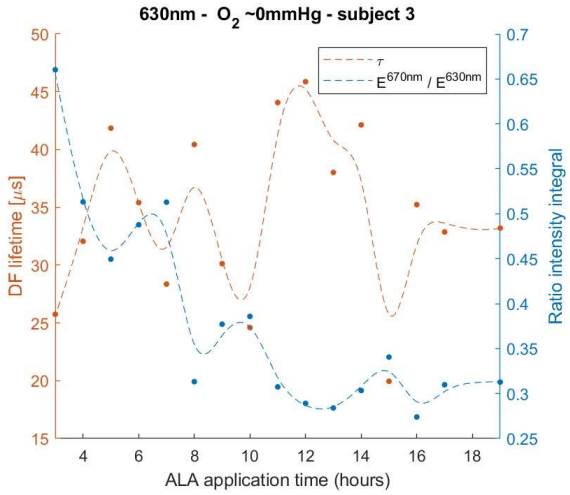

(b) mitoPO$_2$ ±0mmHg

Figure 27: Lifetime and the ratio of the intensity integral of subject 3 plotted over ALA application time, for (a) mitoPO$_2$ at physiological level, i.e. no intervention, and (b) mitoPO$_2$ reduced to a minimum.

The great number of ALA application time measurements provide insight into the characteristics and interaction of the ALA patch. Unfortunately the possible effect of intrasubject changes during the day as well as location presumably affect the results. However, we combined two to three measurement places for each application time to reduce this effect. Furthermore, when combining the measurements of the four subjects, a general increase and decrease is observed.

More insight could be gained regarding the occurrence of SQP when measuring at level of zero mitoPO$_2$. Therefore

we suggest to increase the pressured tissue around the measurement probe to obtain a ±0mmHg mitoPO$_2$ measurement area. A followup study could concern assessing two patches with different application time - e.g., 5 and 12 hours therefore aiming at a higher and lower in vivo PpIX concentration - which are measured with increasing excitation light intensity. If the PpIX concentration reaches level where SQP occurs, the DF intensity should increase quadratically, as compared to a linear increase for the lower PpIX concentrations [21]. Furthermore, these four subject provide merely a first perspective on the occurring processes. More subject should be included before general conclusions can be drawn.

In regard of clinical relevance, this research provides the knowledge that in some patients the DF intensity start to decline. This can affect the quality of the measurement due to a decreased signal to signal to noise ratio; including the BGS. In current clinical studies during surgery, the ALA patches are applied the night before the surgery, therefore having an extensive application time. Possibly the measurement quality could be improved by ensuring the measurements start not later than 18 hours after application. Moreover, if the measurement location indeed significantly affect the mitoPO$_2$ value, one should predominantly regard mitoPO$_2$ trends rather than individual values in clinical setting.

Delayed fluorescence behavior after ALA patch removal

As Figure 28 shows for three out of four subjects, a decrease in maximum intensity amplitudes starts after the removal of Patch one; with after 8 hours of removal having approximately half of the maximum intensity amplitude as the first measurement after removal for some subjects. In contrast, the I$_0$ tends to increase for subject three. Especially subject 1, 2 and 3 show considerable fluctuations within the maximum amplitude.

When evaluating the results of patch 1 in regard of the results of the maximum amplitudes of the different ALA application times, as shown in Figure 25, the increasing value of subject three seems appropriate in the sense that the peak intensity amplitude is reached after 13 to 16 hours. Therefore, after 11 hour of ALA application their might still be ALA deposit on the skin and room for extended synthesis of PpIX from ALA. [36]

When regarding the decreasing I$_0$ trends, the remaining after several hours ranges between 0.25-0.5 which, in comparison to the I$_0$ of the BGS from paragraph 3.1.2 of approximately 0.1, could either be sufficient signal or result in a concerning component of BGS.

Similar to the results of the measurements of the multiple ALA application times - in the previous paragraph - the fluctuations of the signal intensity of Patch 1 result in varying lifetimes; which anticorrelate with the intensity integral ratio (see Appendix D). Note that the fluctuations in mitoPO$_2$ do not correlate with a general increase of I_0^{630} and I_0^{670}, as can be seen in in Appendix D Figure 57 and 58.

In conclusion, the progress after ALA patch removal differs per subject and presumably of ALA application time. Whether sufficient signal remains after several hours of measurement, depends on the amount of signal at the start - in comparison the the BGS -, and whether more PpIX synthesis is possible or the peak intensity is already reached followed by decline of amount of signal.

The results of the ALA patches are assessed by Fauteck et al., showing a increase of fluorescence after removal of patches; both for 2 and 5 hours of application. This corresponds to the results of our subject three. Fauteck et al.'s results show that 5 hours of application results in more increase than 2 hours. [36] This validates that longer application time results in more PpIX and that if the peak concentration is not yet reached, the increase continuous after removal for several hours.

The decreasing trend is to our knowledge not shown before. Merely after 24 hours, the fluorescent signal intensity is indeed decreased [36]. The decay characteristics are important for clinical application of the PpIX-TSLT when longer measurement periods are required, such as on the OR.

Our research is a small pilot study and requires more subjects before general conclusions can be drawn.

The gained knowledge regarding these ALA characteristics are important for clinical application in regard of application time and measurement duration. In current clinical studies, the application time differs massively. Moreover, the measurements on the OR may take several hours. Accordingly, a decrease in signal quality is common during these procedures. This could therefore be the result of reducing PpIX concentration.

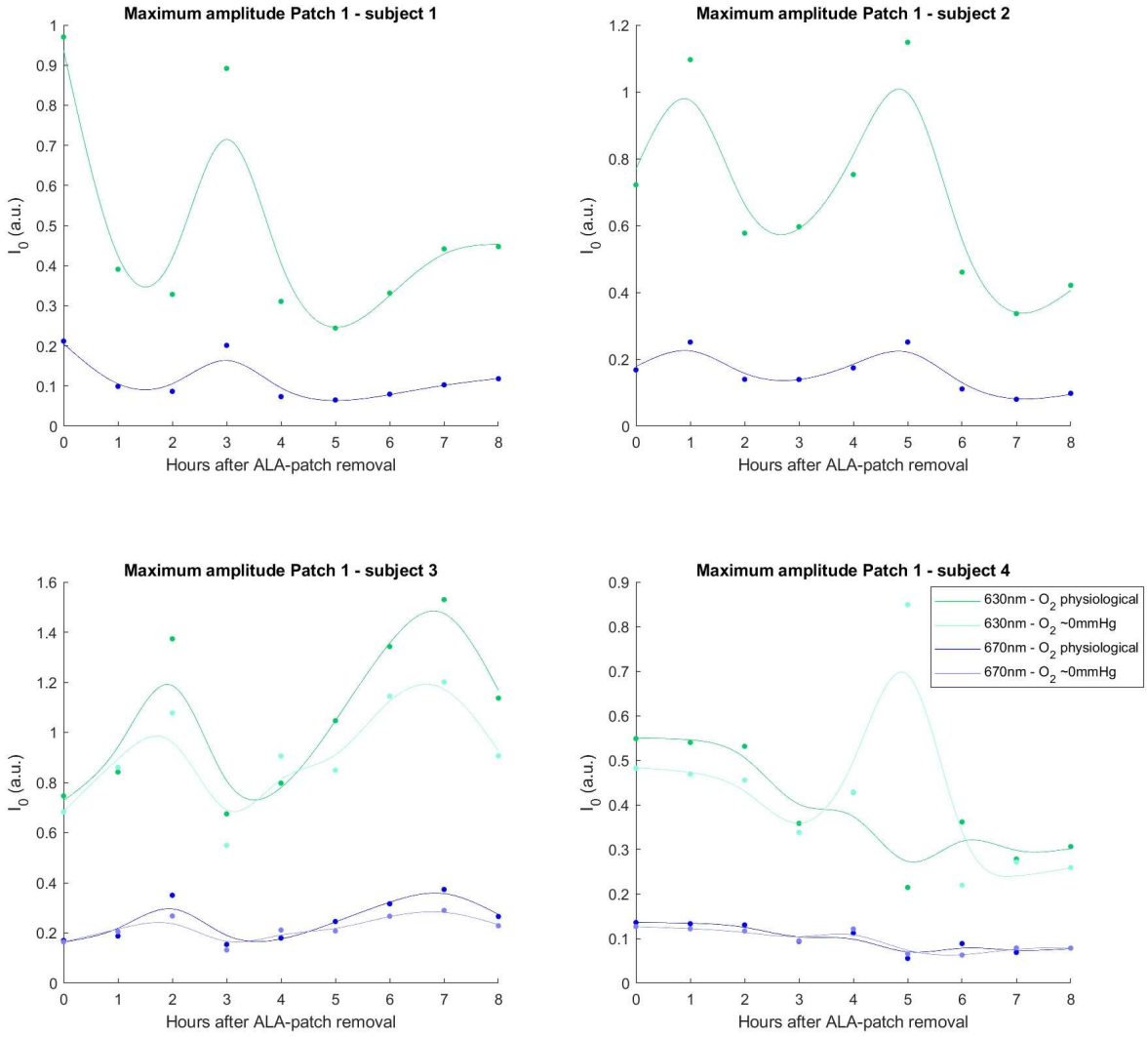

Figure 28: The maximum intensity amplitudes of patch 1, applied for 11 hours, and measured consecutively for nine hours after removal; for the four subjects.

3.3 Practical implications

The ultimate goal of this research is improvement of the PpIX-TSLT technique for accurate oxygen measurement in clinical setting and therefore improving patient care.

Our results already improved the application of the PpIX-TSLT in the LL. The cell experiment mentioned in the introduction, showing wrong mitoPO$_2$ measured values for the applied PO$_2$ of 8%, 5% and 9%, was repeated with the protocol changes of increased concentration of PtF$_4$ beads as well as increased LP, which led to a successful result of accurate mitoPO$_2$ measurements (see Appendix A.1 Figure 29).

The COMET is currently a research device, and therefore not a clinically applicable tool. However, when clinical application of the COMET proves feasible and of added value to the patient care, the BGS lifetimes and there implications are of great importance. Within current clinical trials, a mitoPO$_2$ <20mmHg is considered critically low. If this would in the future be a cut-off value for clinical interference, a BGS with a lifetime around the value of could cause a conceivable disturbance. Subsequently, reduction of the effect of BGS is essential. Steps towards that goal consist of reduction of the BGS as a start. Accordingly, measurement setups without the long emission fiber and diffusor are preferred. Exploring alternatives with for example a laser diode and using 405 nm instead of 515 nm - which is more absorbed by PpIX - could perhaps reduce the required excitation intensity, therefore reducing the necessity of the diffusor for user safety. Moreover, the current COMET system incorporates a BGS correction using the curve of an aluminium measurement. The results of this research show a discrepancy between the BGS of aluminium compared to skin BGS measurements. This, in combination with the negligible intrasubject BGS difference, suggest an average skin BGS measurement should replace the aluminium curve for the BGS correction method. Alternatively, an individual BGS correction could be used via a calibration method before every patient or subject measurement. However, this is time consuming and rather impractical. Therefore, including an average BGS skin correction seems best.

Besides BGS reduction, one can aim at DF signal intensity improvement with increasing fluorescent substances; e.g., increasing the concentration within laboratory experiments and ensuring sufficient PpIX accumulation within patient (by measuring within 8 to 18 hours after ALA application, based on our results).

With increased mitoPO$_2$ measurement accuracy the value of the COMET as research tool would also increase, besides make it more applicable in patient care, because it could provide the possibility to regard mitoPO$_2$ values instead of merely trends.

In regard of the occurrence of SQP, we showed that in physiological samples the same increase in 670 nm DF signal and increasing 670nm/630nm-ratio ensues increased PpIX concentrations. The hypothesizes that binding to the protein albumin decreases the mobility leading to less collisions and therefore less SQP, appears false. However, our results show the longest lifetime in absence of oxygen when compared to literature [4, 19, 26, 38, 56]. Possibly such limited quenching by oxygen occurs, providing the time for the excited PpIX molecules to collide, form excimers and produce 670nm light; i.e., SQP. Whether SQP occurs within higher PO$_2$ values should be assessed as well as the occurrence of SQP in vivo. Accordingly, SQP requires further research before practical implications are in place.

4 Conclusion

The results of this research indicate the importance of appropriate BGS correction in order to accurately determine mitoPO$_2$ values. The BGS curves differ between laser setups, resulting in predominantly overestimation of mitoPO$_2$ values when measuring with the ML, and generally underestimation when using the COMET considering normoxia average mitoPO$_2$'s of 40-70 mmHg and overestimation within critically low mitoPO$_2$'s. The extent of BGS presence is most prominent in the COMET, and to a lesser extent in the ML and the LL. Within the COMET the BGS is especially affected by the emission fiber length as well as an integrated diffusor. The BGS is minimally affected by skin pigmentation or in vivo mitoPO$_2$ levels. The effect of BGS can be reduced by decreasing the ratio of BGS to DF signal, by increasing the fluorescent substance - e.g., PpIX, PdP, PtF$_4$ beads - and possibly by increasing the laser excitation intensity.

Moreover, although a longer ALA application time results in increased DF intensity, intersubject differences exist regarding the optimal timing. This results in a general advice of measuring between eight to nineteen hours after ALA patch application.

The results of this research support the idea of SQP

within higher PpIX concentration, because of the increased DF intensity ratio of 670 nm signal compared to 630 nm signal with increasing PpIX concentrations and the affected τ_0. Presence of SQP in vivo remains to be established.

5 Recommendations

The ratio of BGS to DF signal imposes improvement of this ratio with optimization of the DF signal intensity, decreasing the BGS and/or correction for the BGS, as discussed in the practical implications. To summarize:

For the LL optimizing - i.e., increasing - the DF signal intensity seems the better solution by increasing the amount of porphyrin and possibly increasing the excitation light intensity. The rigid LL setup makes decreasing BGS difficult. Additionally, one could consider increasing the applied LP as this may decrease the effect of BGS.

The COMET requires more subject inclusions for the in vivo experiment to assess the increasing and decreasing trend of the DF signal intensity after certain ALA application times; in order to get more well-grounded advised measurement window. Our results suggest measurement between 8 to 18 hours after application is appropriate to obtain sufficient DF signal originating from PpIX compared to the BGS. In regard of decreasing the BGS, removal of the long fiber would be ideal. Possibly using excitation light of 405 nm instead of 515 nm could result in decrease in intensity since 405 nm is much better absorbed by PpIX, therefore possibly providing the possibility to remove the diffusor.

When correcting for the BGS in a system, a suitable BGS correction to each laser setup and measurement situation is advised. For the COMET this would most probably mean a BGS skin measurement, instead of aluminium. For the LL a BGS medium measurement could do. Incorporating a calibration BGS measurement before every measurement would be even more thorough, but might not be practical and worth the time due to similarities in BGS; e.g., little intersubject difference in BGS.

In regard of the occurrence of SQP, we showed that an increasing PpIX concentrations in physiological samples results in an increasing 670 nm DF signal intensity. This supports the idea of SQP occurrence within the physiological samples at zero oxygen level and shows there is more to the PpIX-TSLT than currently known. Next, the influence of the SQP on the (mito)PO_2 calculation accuracy should be determined. At zero oxygen level the SQP is present, but does it still occur at higher PO_2 concentrations; i.e., is SQP strong enough to persist with oxygen present as quencher? Moreover, does SQP indeed alter the (mito)PO_2 calculation? Using a setup where one can control the oxygen level of the samples, may provide this insight.

Furthermore, the anticorrelation of the lifetime and DF signal intensity of 670nm compared to 630nm suggest their might be in vivo SQP occurence. However, whether SQP occurs in vivo should be examined thoroughly. This could be assessed via either measuring with a local mitoPO_2 level 0 mmHg in the measurement volume; or examining the effect of increased excitation intensity. The latter could be performed via application of two ALA patches, one for 5 hours and the other 12 - resulting in different PpIX concentrations - and measuring with increasing excitation intensity. If SQP occurs, a quadratic increase of DF intensity should be observed; in contrast to a linear DF intensity increase with merely E-type DF. [21]

References

[1] Egbert G. Mik. Measuring mitochondrial oxygen tension: From basic principles to application in humans. *Anesthesia and Analgesia*, 117(4):834–846, 10 2013.

[2] Giancarlo Solaini, Alessandra Baracca, Giorgio Lenaz, and Gianluca Sgarbi. Hypoxia and mitochondrial oxidative metabolism, 6 2010.

[3] Patty J. Lee and Augustine M.K. Choi. Pathways of cell signaling in hyperoxia. *Free Radical Biology and Medicine*, 35(4):341–350, 8 2003.

[4] Gauthier Croizat. An optical method to quantify intracellular oxygen in human skin: Protoporphyrin IX delayed fluorescence. Technical report, Ecole polytechnique federale de Lausanne - School of life sciences, Lausanne, 2018.

[5] Roger Springett and Harold M. Swartz. Measurements of oxygen in vivo: Overview and perspectives on methods to measure oxygen within cells and tissues. *Antioxidants and Redox Signaling*, 9(8):1295–1301, 8 2007.

[6] Nagan Varadaraj Nagalakshmi, Ravi Madhusudhana, Nikhila Rajendra, and Abhishek Kanakuppe Manjunaht. Hemoglobin and Oxygen Transport. *Karnataka anaeshesia Journal1*, 2(1):1–6, 1 2016.

[7] Aude Carreau, Bouchra El Hafny-Rahbi, Agata Matejuk, Catherine Grillon, and Claudine Kieda. Why is the partial oxygen pressure of human tissues a crucial parameter? Small molecules and hypoxia. *Journal of Cellular and Molecular Medicine*, 15(6):1239–1253, 6 2011.

[8] Walter F. Boron and Emile L. Boulpaep. *Medical Physiology: a cellular and molecular approach.* Saunders Elsevier, Philedelphia, second edition edition, 2012.

[9] Harold M. Swartz and Jeff F. Dunn. Measurements of Oxygen in Tissues: Overview and Perspectives on Methods. In *Advances in Experimental Medicine and Biology*, volume 530, pages 1–12. Kluwer Academic/Plenum Publishers, 1 2003.

[10] Rinse Ubbink, Mark A.Wefers Bettink, Rineke Janse, Floor A. Harms, Tanja Johannes, F. Michael Münker, and Egbert G. Mik. A monitor for Cellular Oxygen METabolism (COMET): monitoring tissue oxygenation at the mitochondrial level. *Journal of Clinical Monitoring and Computing*, 31(6):1143–1150, 12 2017.

[11] Anthony Holley, William Lukin, Jennifer Paratz, Tracey Hawkins, Robert Boots, and Jeffrey Lipman. Review article: Part two: Goal-directed resuscitation - Which goals? Perfusion targets. *Emergency Medicine Australasia*, 24(2):127–135, 4 2012.

[12] C. M. Alexander, L. E. Teller, and J. B. Gross. Pulse Oximetry: Perception, Pitch, Psychoacoustics, and Pedagogy. *Anesthesia and Analgesia*, 68(3):368–376, 2 1989.

[13] Maria Angela Franceschini, David A. Boas, Anna Zourabian, Solomon G. Diamond, Shalini Nadgir, David W. Lin, John B. Mooreand, and Sergio Fantini. Near-infrared spiroximetry: Noninvasive measurements of venous saturation in piglets and human subjects. *Journal of Applied Physiology*, 92(1):372–384, 2002.

[14] David A. Benaron, Ilian H. Parachikov, Shai Friedland, Roy Soetikno, John Brock-Utne, Peter J.A. Van Der Starre, Camran Nezhat, Martha K. Terris, Peter G. Maxim, Jeffrey J.L. Carson, Mahmood K. Razavi, Hayes B. Gladstone, Edgar F. Fincher, Christopher P. Hsu, F. Landon Clark, Wai Fung Cheong, Joshua L. Duckworth, and David K. Stevenson. Continuous, noninvasive, and localized microvascular tissue oximetry using visible light spectroscopy. *Anesthesiology*, 100(6):1469–1475, 6 2004.

[15] Floor A. Harms, Sander I.A. Bodmer, Nicolaas J.H. Raat, and Egbert G. Mik. Cutaneous mitochondrial respirometry: non-invasive monitoring of mitochondrial function. *Journal of Clinical Monitoring and Computing*, 29(4):509–519, 11 2015.

[16] Egbert G. Mik, Gianmarco M. Balestra, and Floor A. Harms. Monitoring mitochondrial PO2: the next step, 6 2020.

[17] David F.S. Rolfe and Guy C. Brown. Cellular energy utilization and molecular origin of standard metabolic rate in mammals. *Physiological Reviews*, 77(3):731–758, 1997.

[18] Can Ince and Egbert G. Mik. Microcirculatory and mitochondrial hypoxia in sepsis, shock, and resuscitation, 1 2016.

[19] Egbert G. Mik, Jan Stap, Michiel Sinaasappel, Johan F. Beek, Jacob A. Aten, Ton G. van Leeuwen, and Can Ince. Mitochondrial PO2 measured by delayed fluorescence of endogenous protoporphyrin IX. *Nature Methods*, 3(11):939–945, 11 2006.

[20] Floor Harms, Robert Jan Stolker, and Egbert Mik. Cutaneous Respirometry as Novel Technique to Monitor Mitochondrial Function: A Feasibility Study in Healthy Volunteers. *PLOS ONE*, 11(7):e0159544, 7 2016.

[21] Gauthier Croizat, Aurélien Gregor, Jaroslava Joniova, Emmanuel Gerelli, and Georges Wagnières. Identification of excimer delayed fluorescence by Protoporphyrin IX: A novel access to local chromophore concentration? *Journal of Photochemistry and Photobiology B: Biology*, 229:112408, 4 2022.

[22] R. Ubbink, M. A. Wefers Bettink, W. van Weteringen, and E. G. Mik. Mitochondrial oxygen monitoring with COMET: verification of calibration in man and comparison with vascular occlusion tests in healthy volunteers. *Journal of Clinical Monitoring and Computing*, pages 1–10, 10 2020.

[23] R. Poulson. The enzymic conversion of protoporphyrinogen IX to protoporphyrin IX in mammalian mitochondria. *Journal of Biological Chemistry*, 251(12):3730–3733, 6 1976.

[24] Sander I. A. Bodmer, Gianmarco M. Balestra, Floor A. Harms, Tanja Johannes, Nicolaas J. H. Raat, Robert J. Stolker, and Egbert G. Mik. Microvascular and mitochondrial PO ₂ simultaneously measured by oxygen-dependent delayed luminescence. *Journal of Biophotonics*, 5(2):140–151, 2 2012.

[25] Haydée Fukuda, Adriana Casas, and Alcira Batlle. Aminolevulinic acid: From its unique biological function to its star role in photodynamic therapy, 2005.

[26] Egbert G. Mik, Tanja Johannes, Coert J. Zuurbier, Andre Heinen, Judith H.P.M. Houben-Weerts, Gianmarco M. Balestra, Jan Stap, Johan F. Beek, and Can Ince. In vivo mitochondrial oxygen tension measured by a delayed fluorescence lifetime technique. *Biophysical Journal*, 95(8):3977–3990, 10 2008.

[27] Egbert G. Mik, Can Ince, Otto Eerbeek, Andre Heinen, Jan Stap, Berend Hooibrink, Cees A. Schumacher, Gianmarco M. Balestra, Tanja Johannes, Johan F. Beek, Ab F. Nieuwenhuis, Pepijn van Horssen, Jos A. Spaan, and Coert J. Zuurbier. Mitochondrial oxygen tension within the heart. *Journal of Molecular and Cellular Cardiology*, 46(6):943–951, 6 2009.

[28] C. A. Parker, C. G. Hatchard, and Thelma A. Joyce. P-type delayed fluorescence from ionic species and aromatic hydrocarbons. *Journal of Molecular Spectroscopy*, 14(1-4):311–319, 1 1964.

[29] Ivo S. Vinklárek, Marek Scholz, Roman Dědic, and Jan Hála. Singlet oxygen feedback delayed fluorescence of protoporphyrin IX in organic solutions. *Photochemical and Photobiological Sciences*, 16(4):507–518, 2017.

[30] Egbert G. Mik, Cornelis Donkersloot, Nicolaas J. H. Raat, and Can Ince. Excitation Pulse Deconvolution in Luminescence Lifetime Analysis for Oxygen Measurements In Vivo. *Photochemistry and Photobiology*, 76(1):12–21, 8 2002.

[31] C. A. Parker and C. G. Hatchard. Delayed fluorescence of pyrene in ethanol. *Transactions of the Faraday Society*, 59:284–295, 1963.

[32] C. A. Parker. Delayed fluorescence from naphthalene solutions. *Spectrochimica Acta*, 19(6):989–994, 1963.

[33] Theresa M. Busch. Local physiological changes during photodynamic therapy. *Lasers in Surgery and Medicine*, 38(5):494–499, 6 2006.

[34] Marek Scholz, Roman Dědic, and Jan Hála. Microscopic time-resolved imaging of singlet oxygen by delayed fluorescence in living cells. *Photochemical and Photobiological Sciences*, 16(11):1643–1653, 11 2017.

[35] C. A. Parker and Thelma A. Joyce. Delayed fluorescence and some properties of the chlorophyll triplets. *Photochemistry and Photobiology*, 6(6):395–406, 6 1967.

[36] Jan Dirk Fauteck, Günther Ackermann, Manfred Birkel, Marion Breuer, Anne C.E. Moor, Andrea Ebeling, and Christoph Ortland. Fluorescence characteristics and pharmacokinetic properties of a novel self-adhesive 5-ALA patch for photodynamic therapy of actinic keratoses. *Archives of Dermatological Research*, 300(2):53–60, 2 2008.

[37] Frank Bubberman. NiMMOT: Noninvasive measurement of mitochondrial oxygen tension (mitoPO2) compared to continuous hemoglobin-monitoring during major surgery. Technical report, Erasmus Medical Centre, Rotterdam, 2017.

[38] Floor A. Harms, Wilhelmina J. Voorbeijtel, Sander I.A. Bodmer, Nicolaas J.H. Raat, and Egbert G. Mik. Cutaneous respirometry by dynamic measurement of mitochondrial oxygen tension for monitoring mitochondrial function in vivo. *Mitochondrion*, 13(5):507–514, 9 2013.

[39] Philipp Baumbach, Charles Neu, Steffen Derlien, Michael Bauer, Maria Nisser, Anja Buder, and Sina M. Coldewey. A pilot study of exercise-induced changes in mitochondrial oxygen metabolism measured by a cellular oxygen metabolism monitor (PICOMET). *Biochimica et Biophysica Acta - Molecular Basis of Disease*, 1865(4):749–758, 4 2019.

[40] Mark A. Wefers Bettink, Floor A. Harms, Nathalie Dollee, Patricia A.C. Specht, Nicolaas J.H. Raat, G.C. Schoonderwoerd, and Egbert G. Mik. Non-invasive versus ex vivo measurement of mitochondrial function in an endotoxemia model in rat: Toward monitoring of mitochondrial therapy. *Mitochondrion*, 50:149–157, 1 2020.

[41] Marcus P.J. van Diemen, Cécile L. Berends, Naila Akram, Joep Wezel, Wouter M. Teeuwisse, Bert G. Mik, Hermien E. Kan, Andrew Webb, Jan Willem M. Beenakker, and Geert Jan Groeneveld. Validation of a pharmacological model for mitochondrial dysfunction in healthy subjects using simvastatin: A randomized placebo-controlled proof-of-pharmacology study. *European Journal of Pharmacology*, 815:290–297, 11 2017.

[42] Charles Neu, Philipp Baumbach, Alina K. Plooij, Kornel Skitek, Juliane Götze, Christian von Loeffelholz, Christiane Schmidt-Winter, and Sina M. Coldewey. Non-invasive Assessment of Mitochondrial Oxygen Metabolism in the Critically Ill Patient Using the Protoporphyrin IX-Triplet State Lifetime Technique—A Feasibility Study. *Frontiers in Immunology*, 11:757, 5 2020.

[43] Louisa J.D. van Dijk, Rinse Ubbink, Luke G. Terlouw, Desirée van Noord, Egbert G. Mik, and Marco J. Bruno. Oxygen-dependent delayed fluorescence of protoporphyrin IX measured in the stomach and duodenum during upper gastrointestinal endoscopy. *Journal of Biophotonics*, 12(10):201900025, 10 2019.

[44] Frederick J. Pearce, Christine Waasdorp, Howard Hufnagel, David Burris, Joseph DeFeo, Peter Soballe, and William R. Drucker. Subcutaneous PO2 as an index of the physiological limits for hemodilution in the rat. *Journal of applied physiology (Bethesda, Md. : 1985)*, 99(3):814–821, 9 2005.

[45] Luuk H.L. Römers, Charlotte Bakker, Nathalie Dollée, Sanne E. Hoeks, Alexandre Lima, Nicolaas J.H. Raat, Tanja Johannes, Robert J. Stolker, and Egbert G. Mik. Cutaneous Mitochondrial P o 2, but Not Tissue Oxygen Saturation, Is an Early Indicator of the Physiologic Limit of Hemodilution in the Pig. *Anesthesiology*, 125(1):124–132, 7 2016.

[46] Joscha Hoche, Hans Christian Schmitt, Alexander Humeniuk, Ingo Fischer, Roland Mitrić, and Merle I.S. Röhr. The mechanism of excimer formation: an experimental and theoretical study on the pyrene dimer. *Physical Chemistry Chemical Physics*, 19(36):25002–25015, 9 2017.

[47] Xiang Ma and He Tian. Photochemistry and Photophysics. Concepts, Research, Applications. By Vincenzo Balzani, Paola Ceroni and Alberto Juris. *Angewandte Chemie International Edition*, 53(34):8817–8817, 8 2014.

[48] J. B. Birks, G. F. Moore, and I. H. Munro. Delayed excimer fluorescence. *Spectrochimica Acta*, 22(2):323–331, 2 1966.

[49] Tanja Johannes, Egbert G. Mik, and Can Ince. Dual-wavelength phosphorimetry for determination of cortical and subcortical microvascular oxygenation in rat kidney. *Journal of Applied Physiology*, 100(4):1301–1310, 4 2006.

[50] Aleksander S Golub, Aleksander S Popel, Lei Zheng, and Roland N Pittman. Analysis of Phosphorescence in Heterogeneous Systems Using Distributions of Quencher Concentration. *Biophysical Journal*, 73:452–465, 1997.

[51] Jonathan S. Dysart and Michael S. Patterson. Photobleaching kinetics, photoproduct formation, and dose estimation during ALA induced PpIX PDT of MLL cells under well oxygenated and hypoxic conditions. *Photochemical & Photobiological Sciences 2006 5:1*, 5(1):73–81, 1 2006.

[52] Leu Wei Lo, Cameron J. Koch, and David F. Wilson. Calibration of oxygen-dependent quenching of the phosphorescence of Pd-meso-tetra (4-carboxyphenyl) porphine: A phosphor with general application for measuring oxygen concentration in biological systems. *Analytical Biochemistry*, 236(1):153–160, 4 1996.

[53] Protoporphyrin IX (free acid) - ALX-430-041 - Enzo Life Sciences.

[54] H. Verweu and J. van Steveninck. MODEL STUDIES ON PHOTODYNAMIC CROSS-LINKING. *Photochemistry and Photobiology*, 35(2):265–267, 1982.

[55] Arnone Nithichanon, Inthira Tussakhon, Waraporn Samer, Chidchamai Kewcharoenwong, Manabu Ato, Gregory J. Bancroft, and Ganjana Lertmemongkolchai. Immune responses in beta-thalassaemia: heme oxygenase 1 reduces cytokine production and bactericidal activity of human leucocytes. *Scientific Reports*, 10(1), 12 2020.

[56] Floor A. Harms, Sander I. A. Bodmer, Nicolaas J. H. Raat, Robert J. Stolker, and Egbert G. Mik. Validation of the protoporphyrin IX–triplet state lifetime technique for mitochondrial oxygen measurements in the skin. *Optics Letters*, 37(13):2625, 7 2012.

[57] Thomas P. Keeley and Giovanni E. Mann. Defining physiological normoxia for improved translation of cell physiology to animal models and humans. *Physiological Reviews*, 99(1):161–234, 1 2019.

[58] Theodor D. Popescu. Introduction to signal processing. *Control Engineering Practice*, 4(12):1771–1772, 12 1996.

[59] Leszek Sułkowski, Bartosz Pawełczak, Mariola Chudzik, Małgorzata Maci,˛ A˙ Zek-Jurczyk, Josef Jampilek, and Atanas G Atanasov. Characteristics of the Protoporphyrin IX Binding Sites on Human Serum Albumin Using Molecular Docking. *Molecules 2016, Vol. 21, Page 1519*, 21(11):1519, 11 2016.

[60] Hamamatsu. Specifications Metal Package PMT with Gate Function Photosensor Modules H11526 Series Product Variations.

Appendices

A Examples from literature and previous studies

For easy comparison to our results, this paragraph contains some results from other studies.

A.1 Examples PpIX-TSLT unexplained results

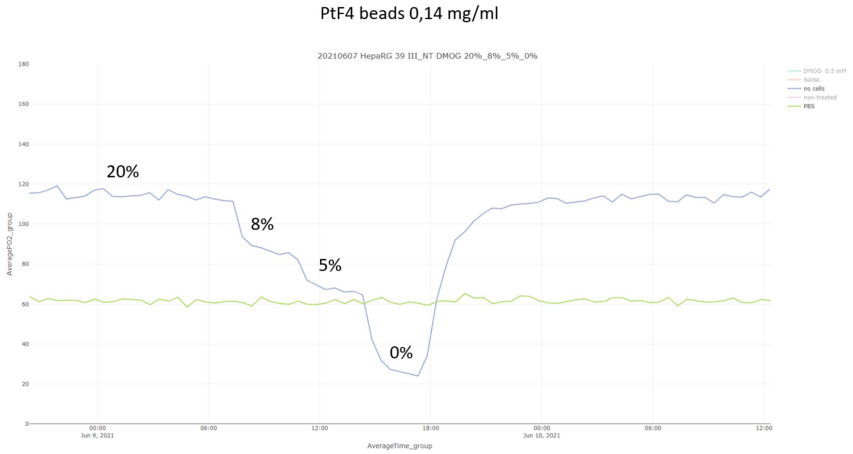

(a) Minimal difference in received signal and determined PO_2 level when adjusting applied oxygen level to 8%, 5% or 0% oxygen within cell measurements from in house experiments.

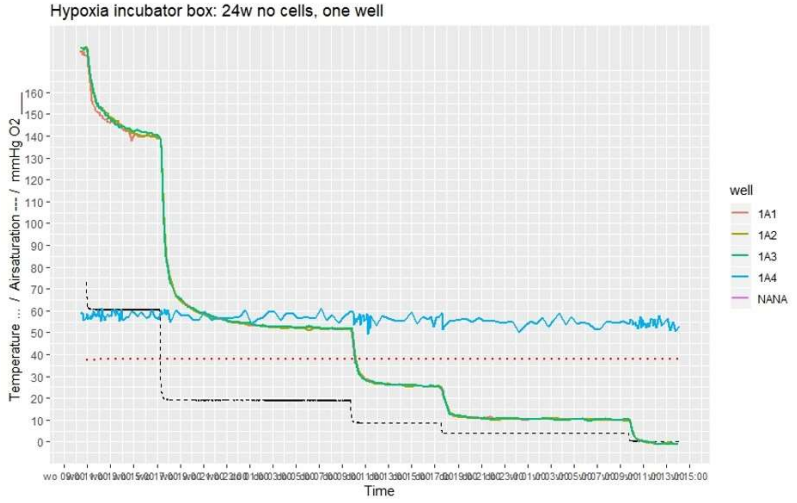

(b) Clear difference in received signal and determined PO_2 level when adjusting applied oxygen level of 8%, 5% or 0% oxygen within cell measurements from in house experiments.

Figure 29: Results of in house experiments regarding mitoPO_2 level measurements within cells combined with platinum tetrafluoride beads, when applying different PO_2 levels, showing measured mitoPO_2 values.

Figure 29 shows the results of cell experiment with the LL; with in (a) unsuccessful measurements with no decrease of measured O_2 to 0mmHg when 0% was given to the sample. The measurement was done with a beads concentration of 0.14 mg/ml. In (b) successful measurements are shown after protocol adjustment: increasing PtF_4 beads concentration to 0.4mg/ml and increasing LP from 60 to 100.

A.2 Example results from literature

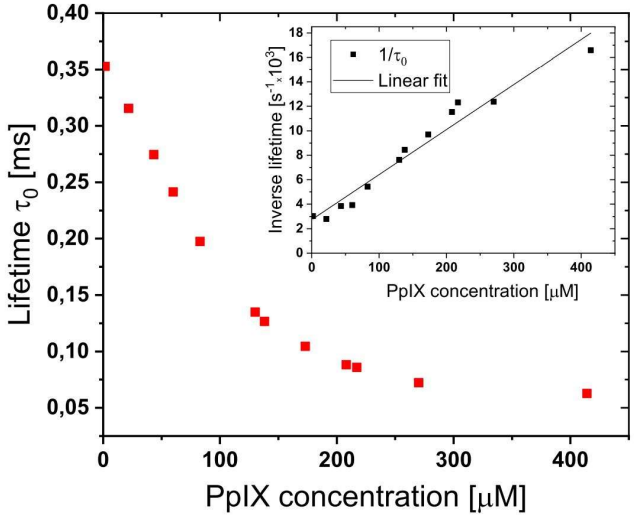

Figure 30: Results of Croizat et al. [4] showing a decreasing τ_0 with increasing PpIX concentration; measured in samples with PpIX dissolved in dimethylformamide at zero oxygen level.

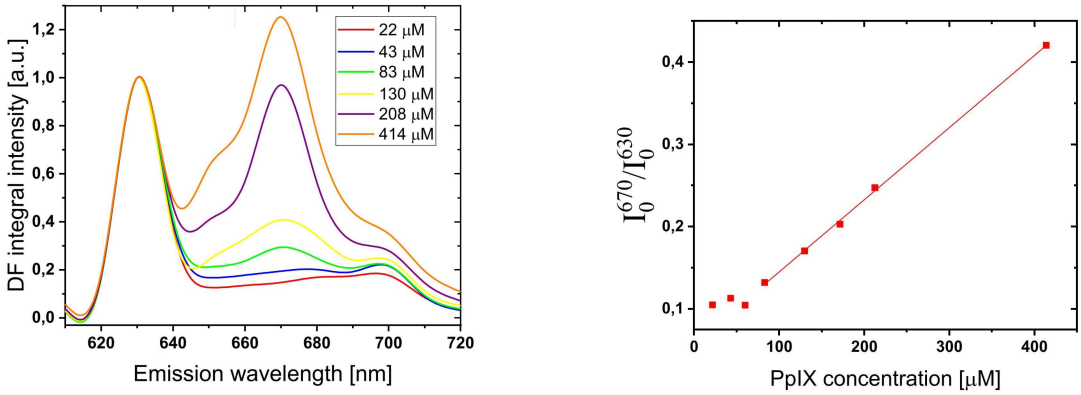

(a) DF intensity integral results of Croizat et al. [21] for multiple PpIX concentration over the 600 to 720nm spectrum.

(b) Results of Croizat et al. [4] showing a increasing ratio of maximum intensity amplitudes

Figure 31: Results of Croizat et al. [21, 4].

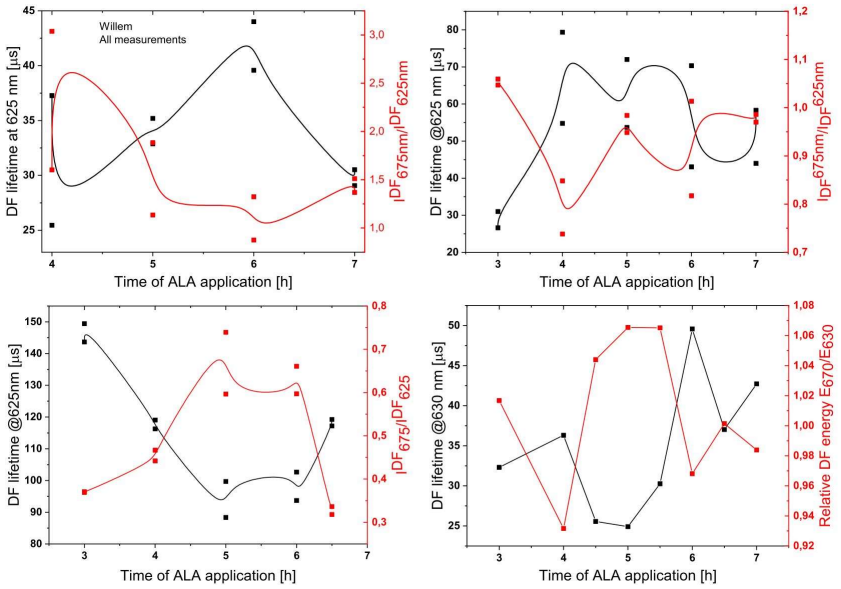

Figure 32: Results of Croizat et al. [4] showing anticorrelation of lifetime and DF intensity signals decreasing

A.3 Tips for assessment methods

In attempted to reduce the PO_2 in samples containing 2% BSA, bubbling with N_2 gas produces massive foam at the top of the sample. With our system, it was impossible to find a minimum for bubbling with N_2 and preventing massive foam formation. The bubbles left the sample via the air needle - i.e., the needle ensuring air can flow out of the sample when adding N_2 - therefore disrupting the sample. In conclusion, bubbling N_2 is not an appropriate method to remove oxygen from samples with BSA.

For dissolving PpIX, DMF works best. Using Dimethyl Sulfoxide (DMSO) works to some extent but results in more opaque samples. Ethanol badly dissolves the PpIX. For the physiological samples the describes method of Lo et al. [52] - i.e., using Trizma, DMF and then aqueous solutions like PBS - appears essential.

Combining DMF with dithionite (Sodium dithionite, Sigma, to reduce the oxygen level results in a chemical reaction producing a wamr and thick substance. Don't combine these two substances.

Meauring samples at air PO_2 levels results in no signal as a result of the fast lifetime and the gating period of the PMT. The 'air satured' samples of for example Mik et al. [19] are probably locally reduced in PO_2 due to the very fast pulsed laser pulse repitition. This results in oxygen consumption.

B Background signal

This section contains some (extra) results regarding the BGS study.

B.1 BGS - Lab laser experiments

B.1.1 Palladium porphyrin experiments

Table 7: Lifetimes of the wells with decreasing pdp concentration; presented for each laser power (LP) measurement.

Lifetime per pdp concentration (μM)	**270**	**90**	**30**	**10**	**3.3**	**1.1**
LP60	133	120	108	105	102	138
LP80	139	123	109	102	101	114
LP100	141	122	110	101	99	116

Table 8: Lifetimes of the BGS from empty wells, ranked per pdp concentration, therefore, corresponding to the accessory PMT setting.

Lifetime of BGS from empty well, ranked per pdp concentration (μM)	**270**	**90**	**30**	**10**	**3.3**	**1.1**
LP60	164	194	194	227	232	219
LP80	192	196	215	223	231	227
LP100	147	213	195	208	222	211

Table 9: Lifetimes of the BGS from wells filled with PBS, ranked per pdp concentration, therefore, corresponding to the accessory PMT setting.

Lifetimes of BGS from PBS, ranked per pdp concentrations (μM)	**270**	**90**	**30**	**10**	**3.3**	**1.1**
LP60	229	198	199	227	229	220
LP80	183	210	208	226	225	222
LP100	193	190	215	211	219	217

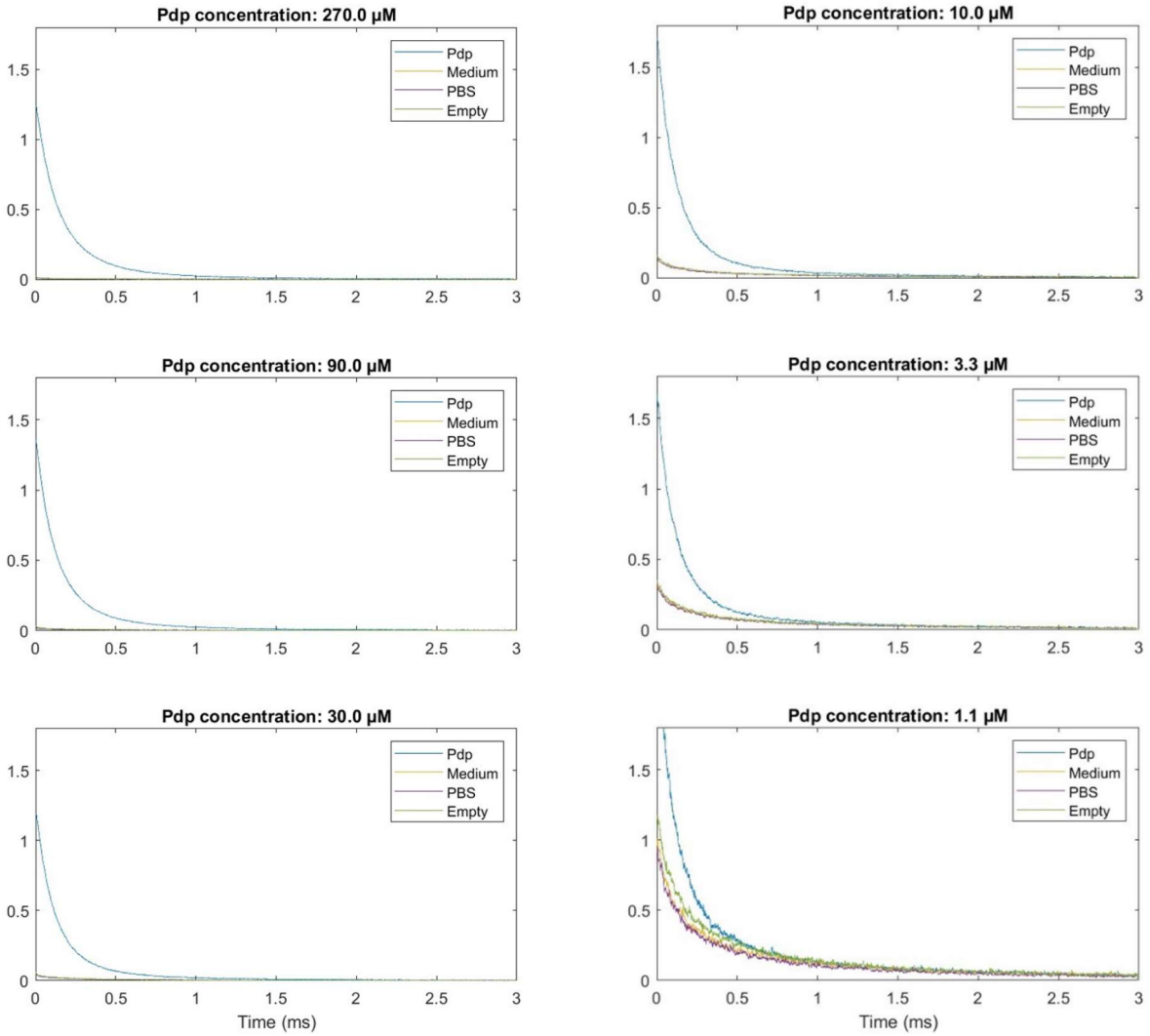

Figure 33: Curves of palladium porphyrin measurements - with laser power 60 - with multiple concentrations, simultaneously measured with well filled with medium, PBS and empty wells.

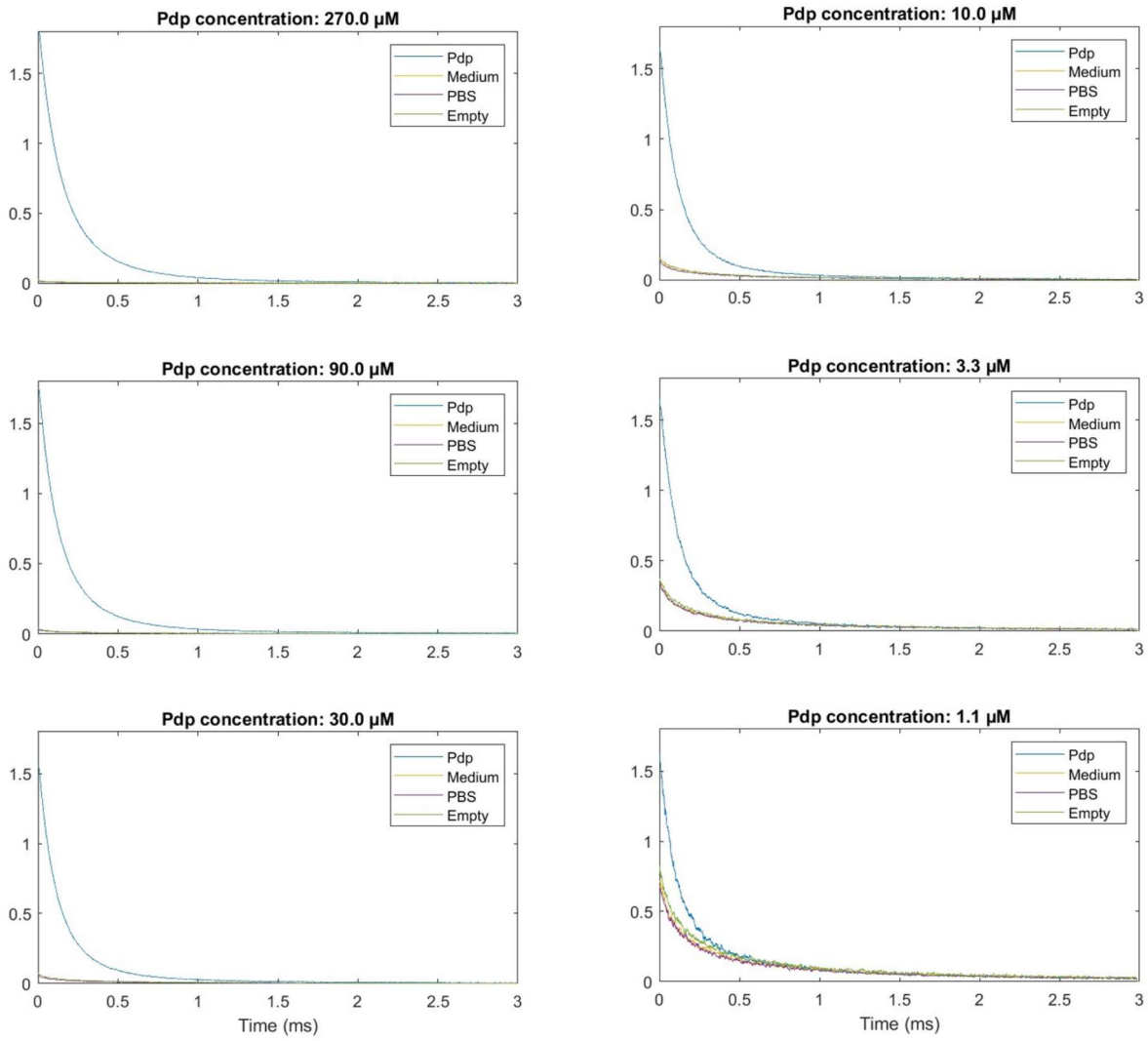

Figure 34: Curves of palladium porphyrin measurements - with laser power 80 - with multiple concentrations, simultaneously measured with well filled with medium, PBS and empty wells.

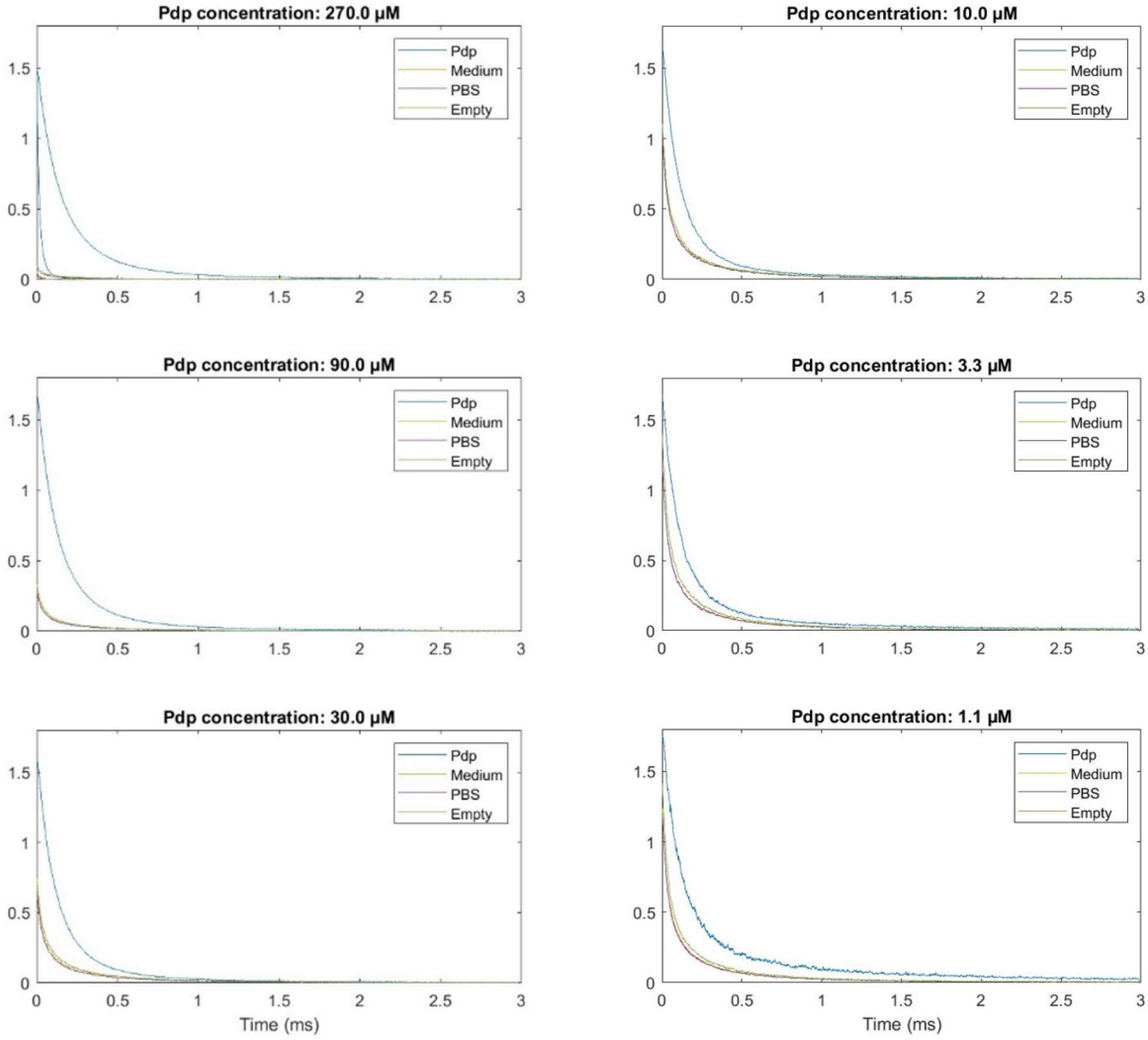

Figure 35: Curves of palladium porphyrin measurements - with laser power 100 - with multiple concentrations, simultaneously measured with well filled with medium, PBS and empty wells.

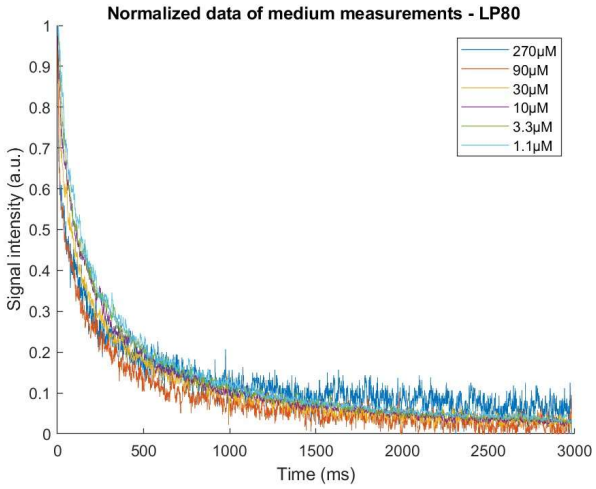

Figure 36: Curves of BGS from wells filled with medium, mesaured - with laser power (LP) 80 - simultaneously with wells increasing palladium porphyrin concentrations.

The PMT setting merely effects the ratio of the BGS compared to the DF. The curve, i.e. a certain lifetime, is not altered as much by the increased amplification strength.

B.1.2 Platinum tetrafluoride beads experiments

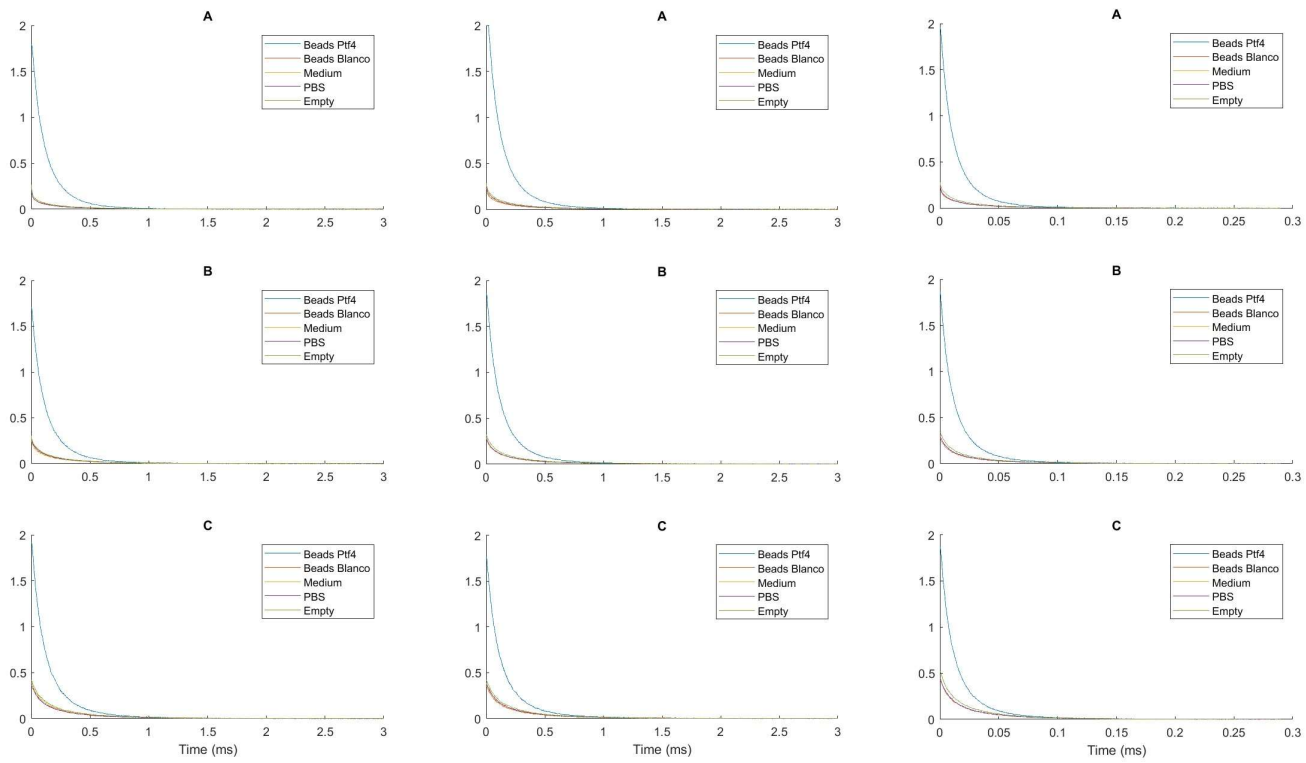

(a) Curves of platinum tetrafluoride beads measurements - with laser power 60 - with concentration (A) 0.6, (B) 0.4 and (C) 0.2mg/ml, which are simultaneously measured with wells filled with medium, PBS and empty wells.

(b) Curves of platinum tetrafluoride beads measurements - with laser power 80 - with concentration (A) 0.6, (B) 0.4 and (C) 0.2mg/ml, which are simultaneously measured with wells filled with medium, PBS and empty wells.

(c) Curves of platinum tetrafluoride beads measurements - with laser power 100 - with concentration (A) 0.6, (B) 0.4 and (C) 0.2mg/ml, which are simultaneously measured with wells filled with medium, PBS and empty wells.

Table 10: Lifetimes of the wells platinum tetrafluoride (PtF4) beads for multiple concentrations; presented for each laser power (LP) measurement.

Lifetime of PtF4 beads for different concentration (mg/ml)	**0.6**	**0.4**	**0.2**
LP60	104	104	105
LP80	114	104	105
LP100	102	102	105

Table 11: Lifetimes of the empty wells for decreasing platinum tetrafluoride (PtF4) beads concentration; presented for each laser power (LP) measurement.

Lifetime of BGS from empty well, ranked per beads concentration (mg/ml)	**0.6**	**0.4**	**0.2**
LP60	91	125	143
LP80	120	132	145
LP100	125	133	146

Table 12: Lifetimes of the wells with medium for decreasing platinum tetrafluoride (PtF4) beads concentration; presented for each laser power (LP) measurement.

Lifetime of BGS from medium, ranked per beads concentration (mg/ml)	**0.6**	**0.4**	**0.2**
LP60	93	113	137
LP80	110	122	139
LP100	125	133	146

Table 13: Lifetimes of the wells with phosphate buffered saline (PBS) for decreasing platinum tetrafluoride beads concentration; presented for each laser power (LP) measurement.

Lifetime of BGS from PBS, ranked per beads concentration (mg/ml)	**0.6**	**0.4**	**0.2**
LP60	104	104	105
LP80	114	104	105
LP100	102	102	104

B.2 Extra BGS simulation results

The mono-exponential fit does not appear to be an appropriate fit, as the result of the simulation show. The PO_2 deviates strongly from the input PO_2, as can be seen in Figure 39a and 39b. The lower PO_2 values correspond, due to the similarity of the BGS curve and the input mono-exponent, see Figure 40a. However, the more the BGS curve differs from the mono-exponent, the larger the miscalculated PO_2 is; an example is shown in Figure 40b.

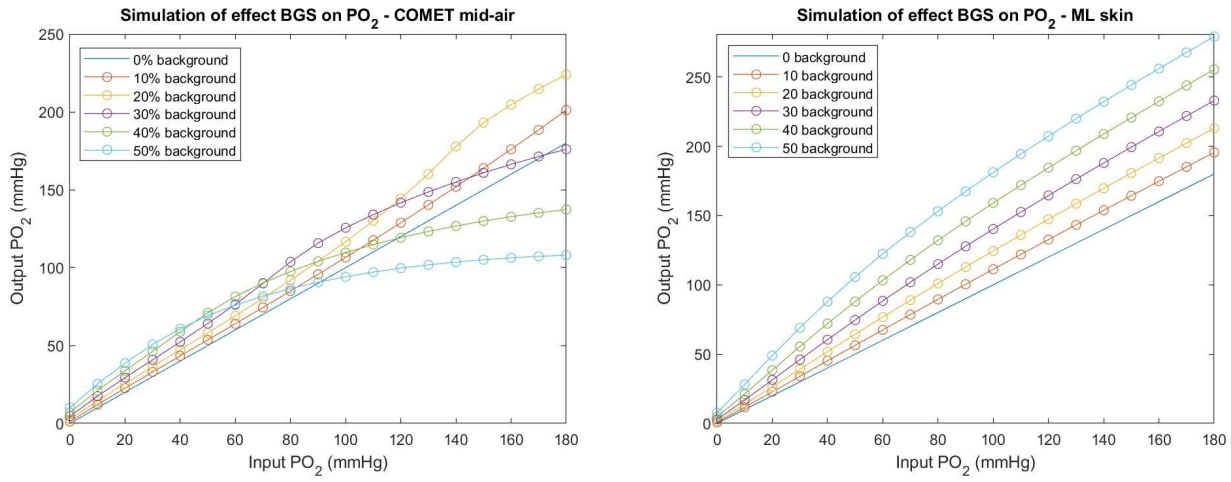

(a) COMET mid-air (b) Main laser skin

Figure 38: Simulation with the rectangular fit of possible effect of BGS with different BGS inputs: (a) COMET mid-air measurements, (b) main laser skin (no ALA) measurements; showing output PO_2 against input PO_2, for multiple ratios of the PO_2-mono-exponent input and BGS

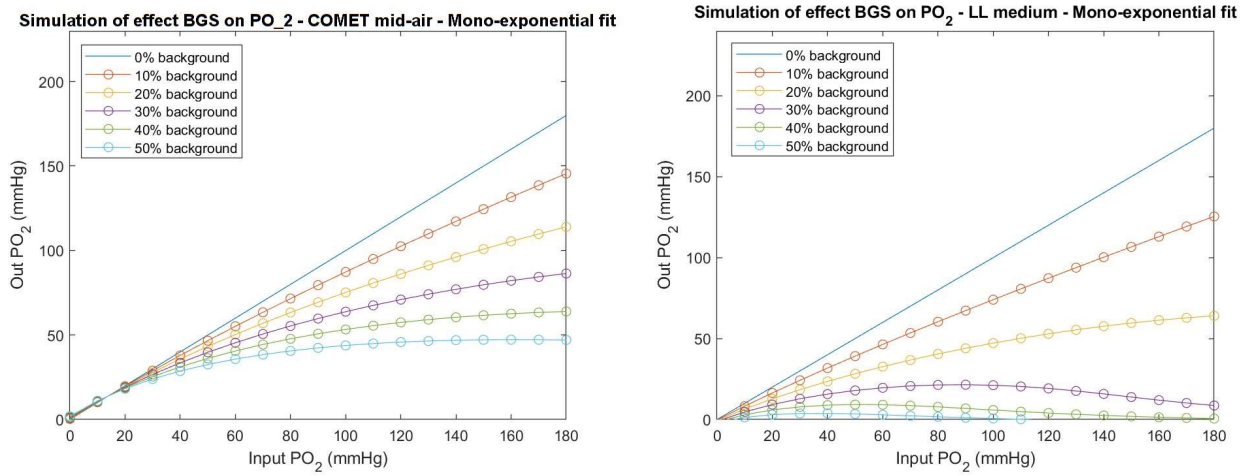

(a) COMET mid-air (b) Lab laser

Figure 39: Simulation with a mono-exponential fit of possible effect of BGS with different BGS inputs: (a) the COMET mid-air measurements and (b) the lab laser medium measurement; showing output PO_2 against input PO_2, for multiple ratios of the PO_2-mono-exponent input and BGS

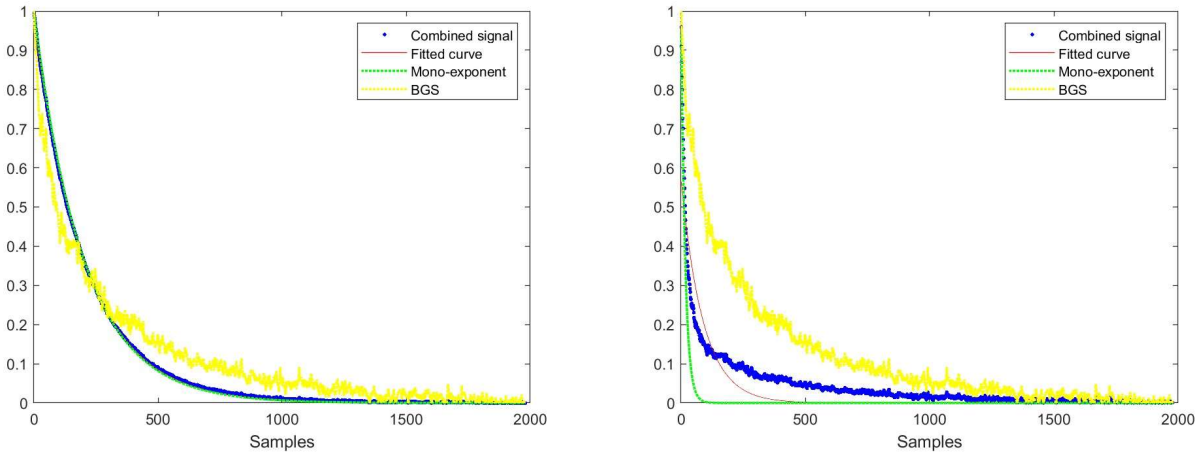

(a) 0 mmHg (b) 150 mmHg

Figure 40: Example of simulation using the mono-exponential curve of (a) 0mmHg and (b) 150mmHg, combined with the BGS from the LL medium, and the fitted curve - using the mono-exponential fit - on this combined signal with 30% BGS.

B.3 Extra results of BGS-ratios

Figure 41 to 43 show the results of the in vivo experiment for subject 1, 2 and 3 regarding the DF intensity ratio compared to the corresponding BGS.

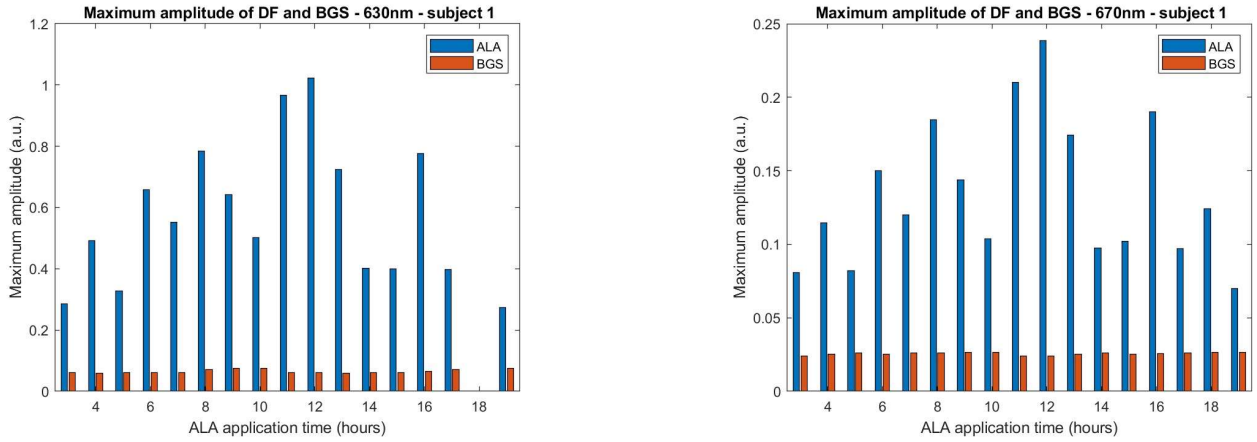

(a) 630nm (b) 670nm

Figure 41: Comparison of maximum intensity amplitude of DF signal with BGS signal, using the main laser set up, for subject 1 with (a) 630nm signal and (b) 670nm signal.

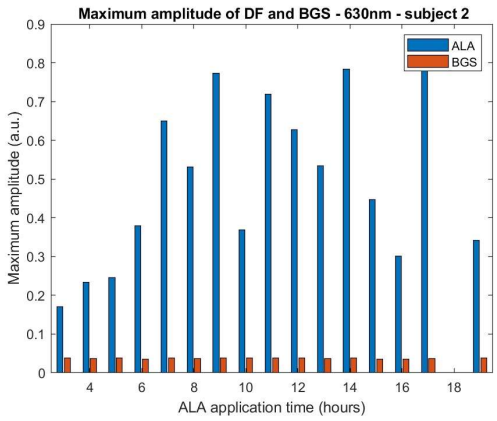

(a) 630nm

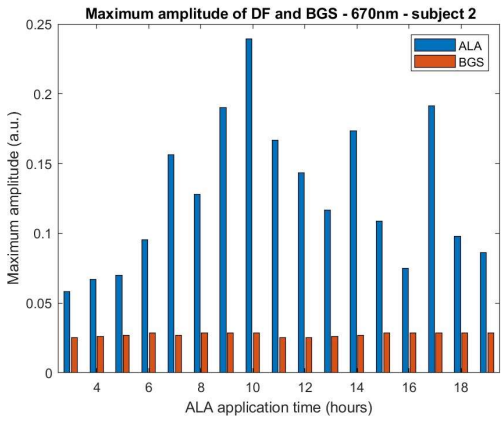

(b) 670nm

Figure 42: Comparison of maximum intensity amplitude of DF signal with BGS signal, using the main laser set up, for subject 2 with (a) 630nm signal and (b) 670nm signal.

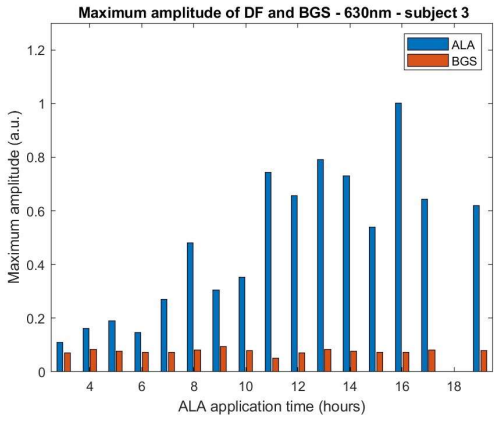

(a) 630nm

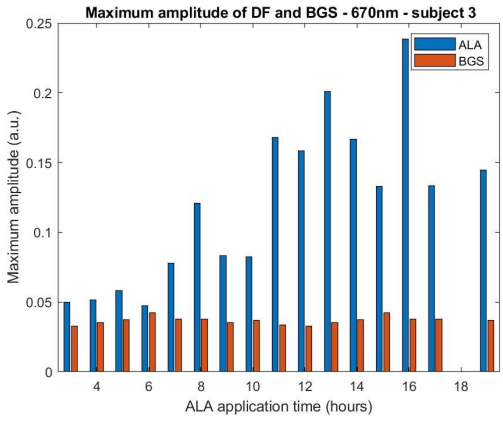

(b) 670nm

Figure 43: Comparison of maximum intensity amplitude of DF signal with BGS signal, using the main laser set up, for subject 3 with (a) 630nm signal and (b) 670nm signal.

C Self-quenching phenomenon

C.1 Extra results of the SQP physiological experiment

Several additional results of the physiological experiment; i.e., the samples containing mainly PBS with 2% BSA as solvent. The figures show the intensity integral values, plotted signal curves and the lifetime of both the 630 nm as well as the 670 nm signal.

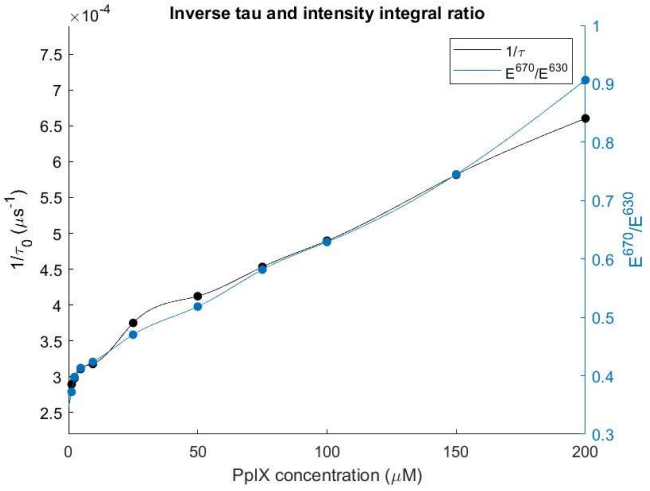

Figure 44: Compare inverse tau with intensity integral ratio for increasing PpIX concentrations of SQP experiment 3 (physiological samples).

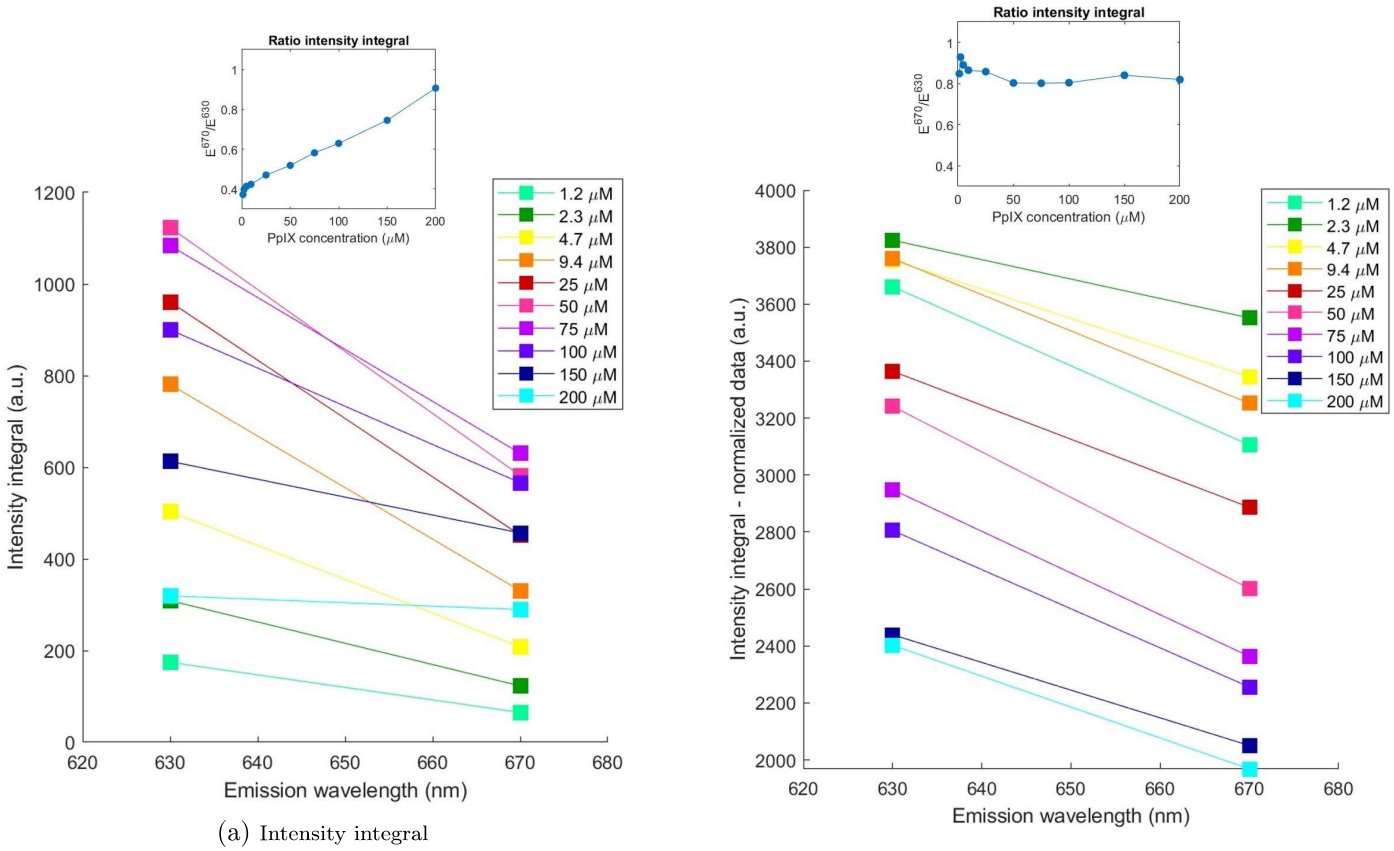

(a) Intensity integral

(b) Normalized intensity integral

Figure 45: For each sample of the physiological experiment the (a) intensity integral for 630nm and 670nm, and in (b) the normalized intensity integral for 630nm and 670nm,

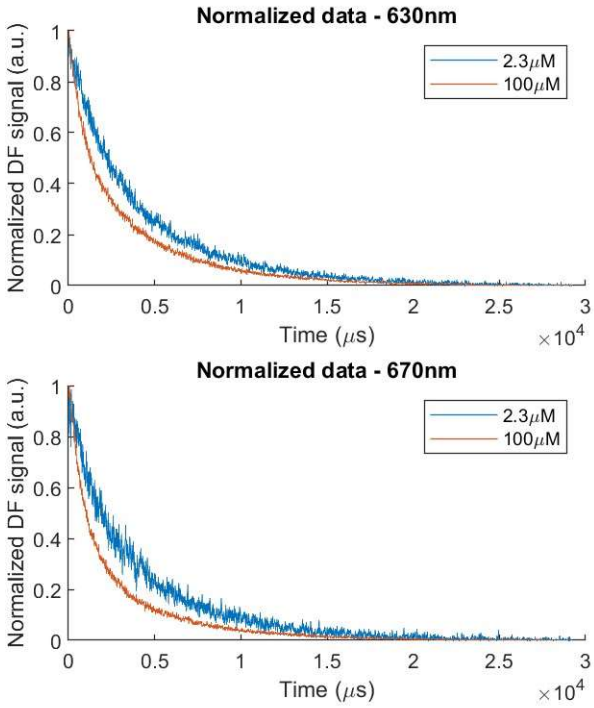

Figure 46: Compare normalized data curves of physiological samples - i.e., samples with mainly PBS with 2% BSA as solvent - with 2.3μM and 10μM

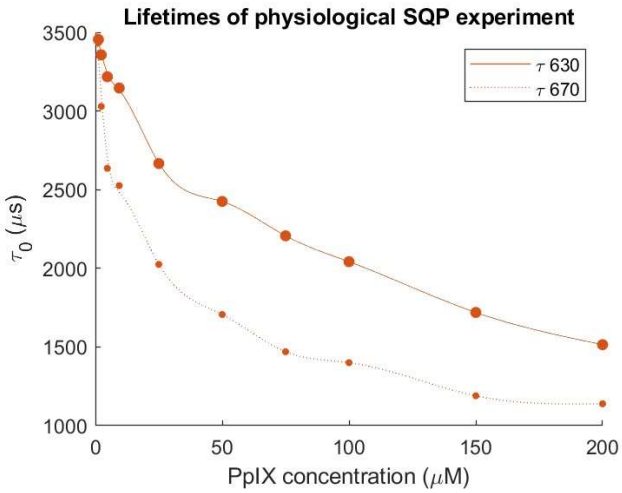

Figure 47: Compare normalized data curves of physiological samples - i.e., samples with mainly PBS with 2% BSA as solvent - with 2.3μM and 10μM

D Extra results of the in vivo experiment

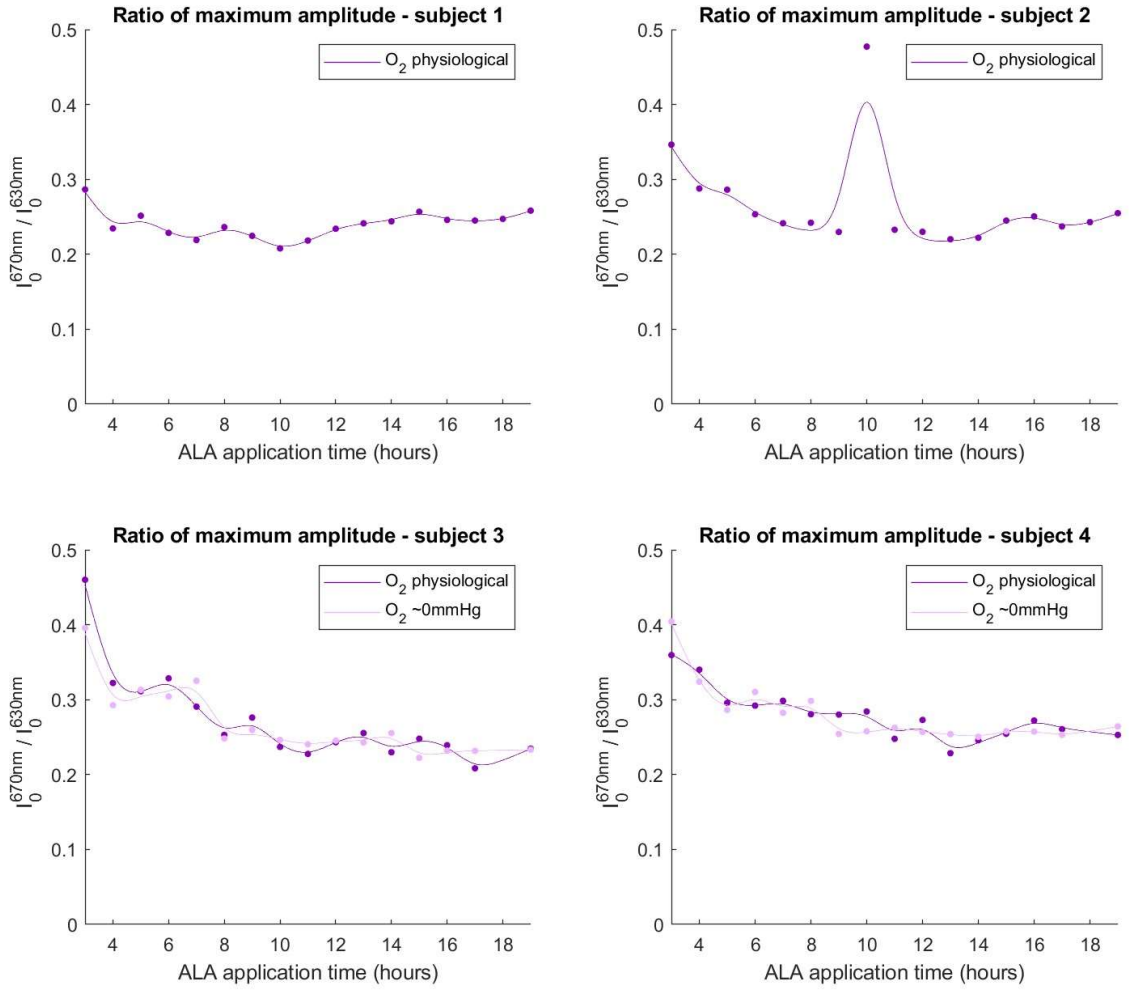

Figure 48: The ratio of the maximum intensity amplitude of 670nm devided by 630nm, for four subjects

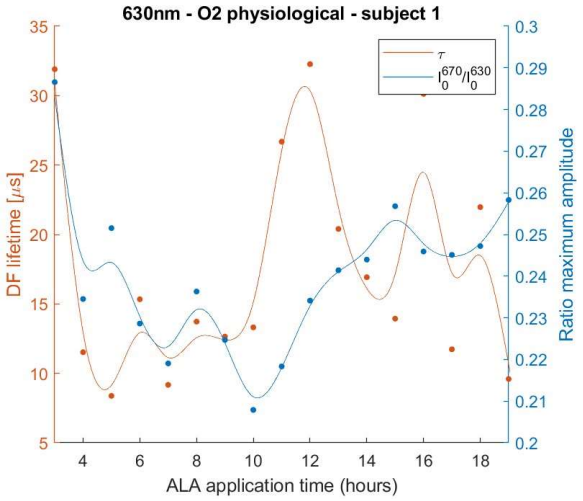

(a) Subject 1 - mitoPO$_2$ physiological

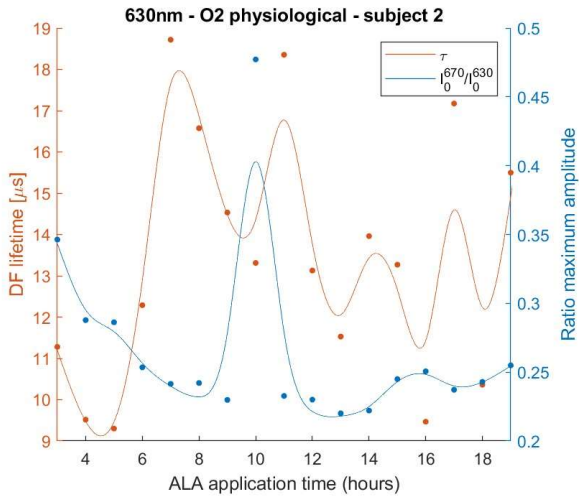

(b) Subject 2 - mitoPO$_2$ physiological

Figure 49: The lifetime and maximum intensity amplitude of subject (a) 1 and (b) 2 plotted over ALA application time, with the mitoPO$_2$ at physiological level, i.e. no intervention.

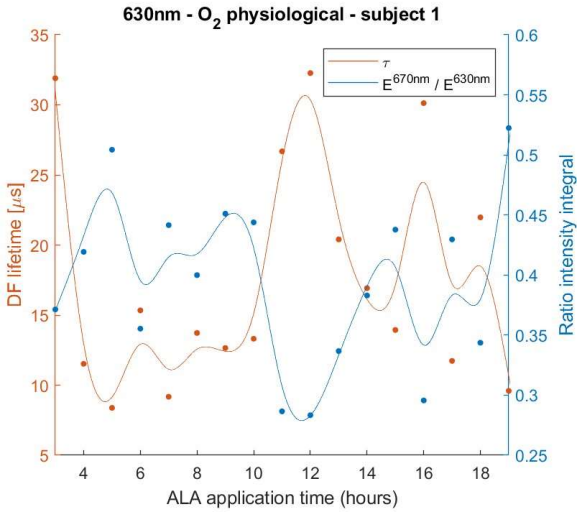

(a) Subject 1 - mitoPO$_2$ physiological

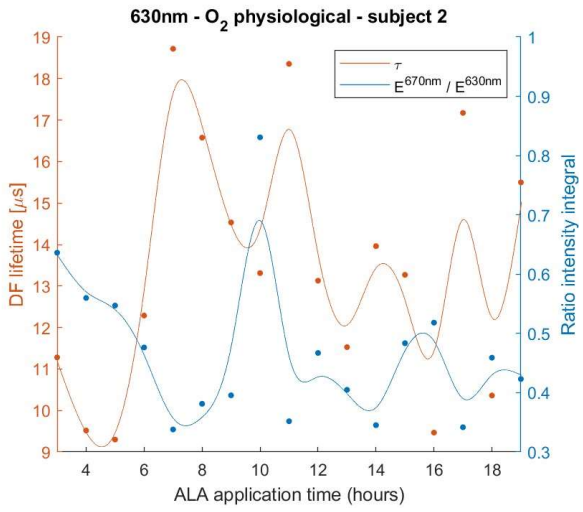

(b) Subject 2 - mitoPO$_2$ physiological

Figure 50: The lifetime and intensity integral of subject (a) 1 and (b) 2 plotted over ALA application time, with the mitoPO$_2$ at physiological level, i.e. no intervention.

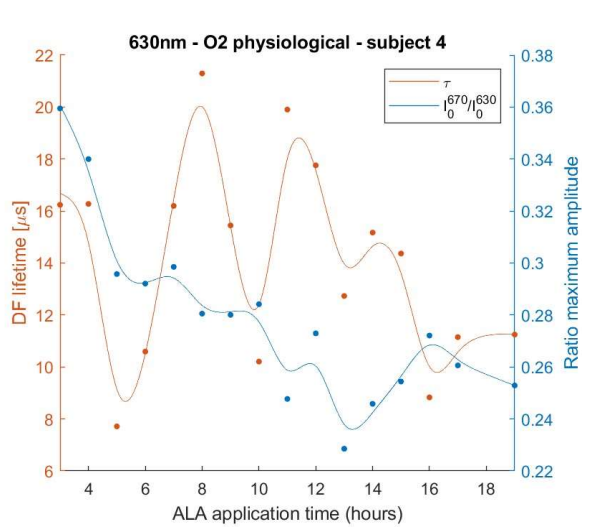

(a) mitoPO$_2$ physiological

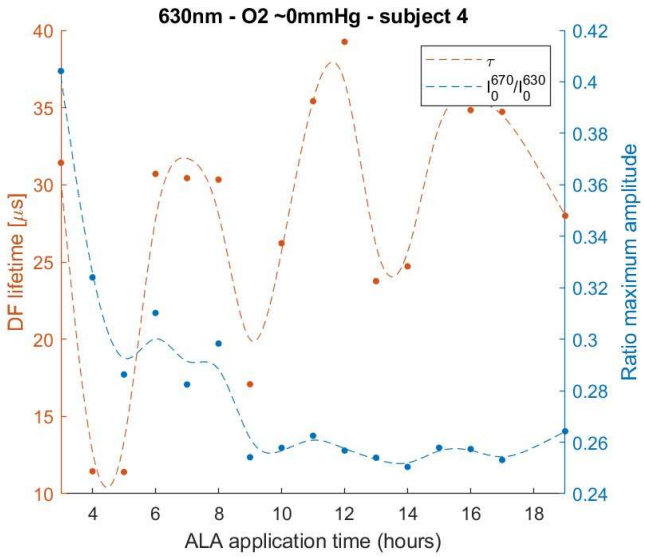

(b) mitoPO$_2$ 0mmHg

Figure 51: The lifetime and maximum intensity amplitude of subject 3 plotted over ALA application time, for (a) mitoPO$_2$ at physiological level, i.e. no intervention, and (b) mitoPO$_2$ reduced to a minimum.

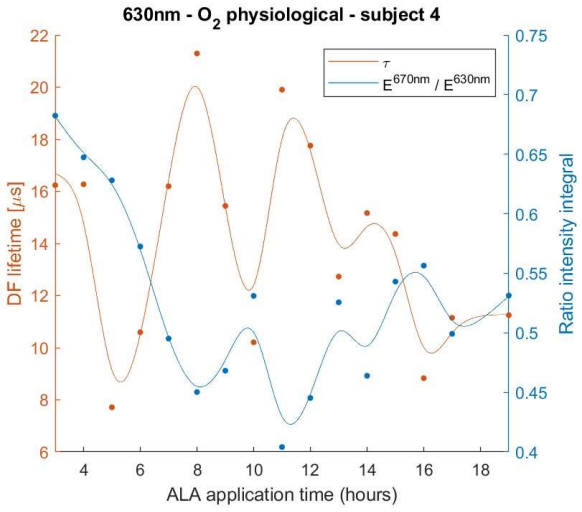

(a) mitoPO$_2$ physiological

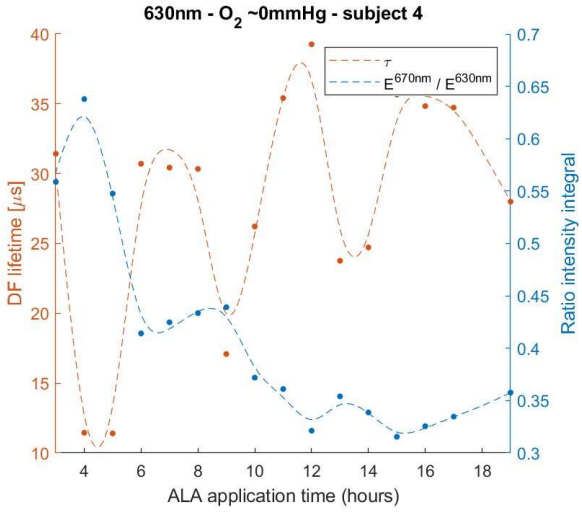

(b) mitoPO$_2$ 0mmHg

Figure 52: Lifetime and the ratio of the intensity integral of subject 3 plotted over ALA application time, for (a) mitoPO$_2$ at physiological level, i.e. no intervention, and (b) mitoPO$_2$ reduced to a minimum.

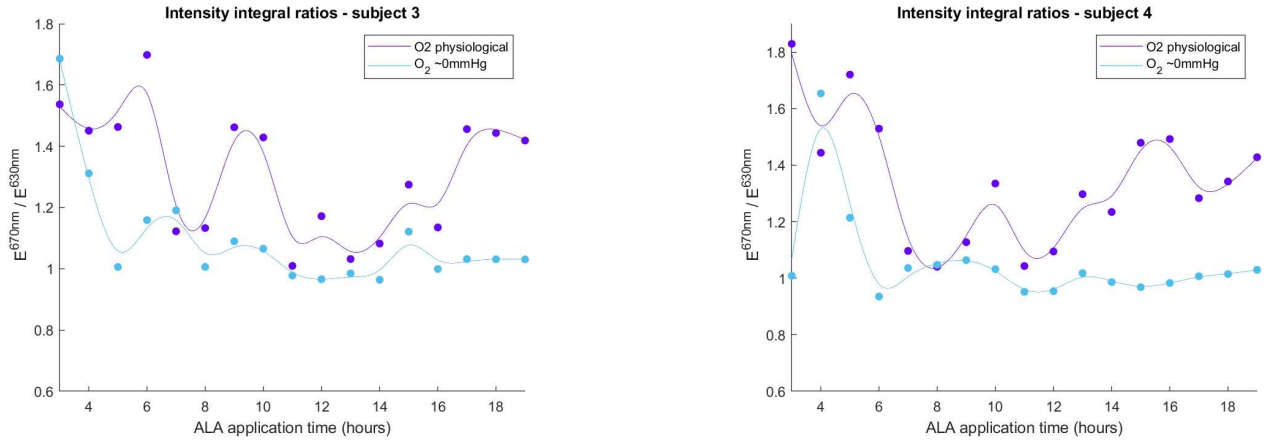

(a) Subject 3 (b) Subject 4

Figure 53: The intensity integral of normalized data, for increasing ALA application time for physiological mitoPO$_2$ as well as reduced mitoPO$_2$ to 0mmHg, for (a) subject 3 and (b) subject 4.

D.1 Patch 1

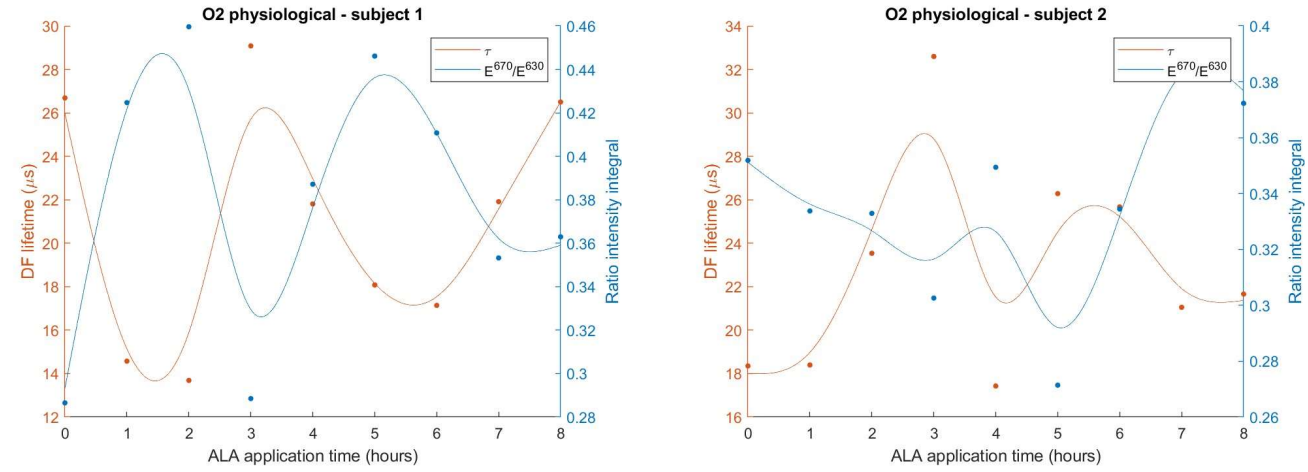

(a) Subject ‘1 (b) Subject 2

Figure 54: Lifetime compared to the ratio of the maximum intensity amplitude for the measurements of patch 1 for (a) subject 1 and (b) 2.

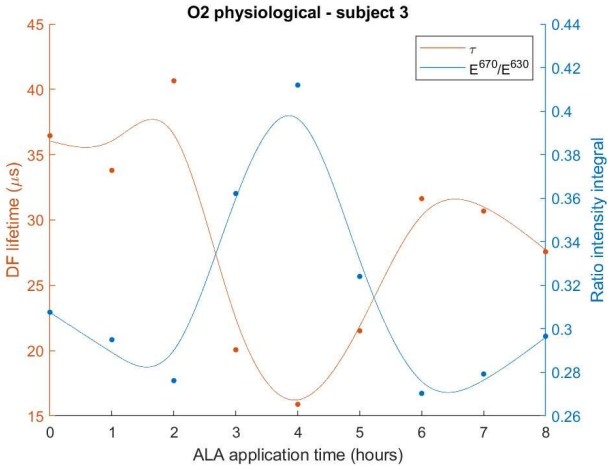

(a) Subject 3 - PO_2 physiological

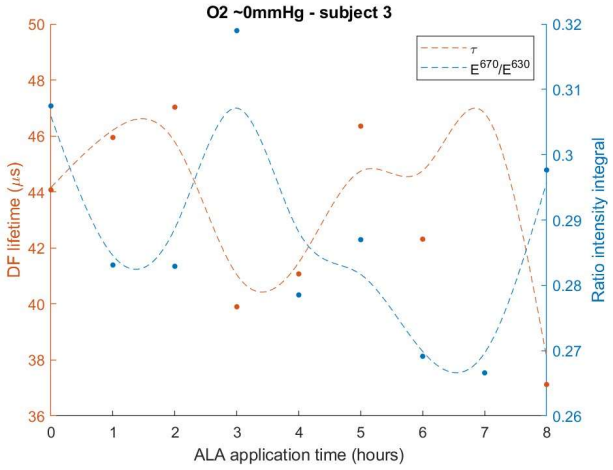

(b) Subject 3 - O_2 0mmHg

Figure 55: Lifetime compared to the ratio of maximum intensity amplitude for the measurements of patch 1 for subject 3 with measurements with (a) physiological PO_2 and (b) 0mmHg.

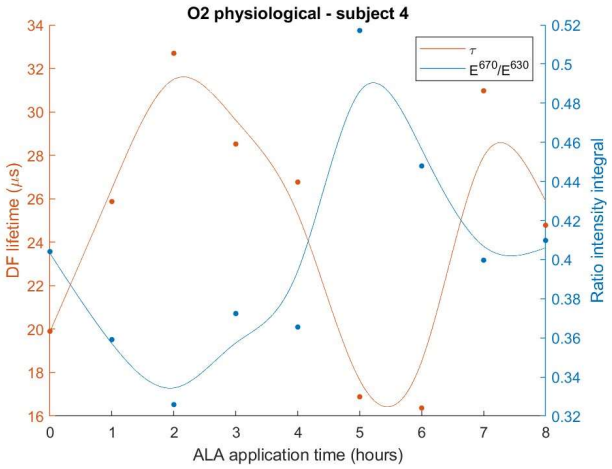

(a) Subject 4 - PO_2 physiological

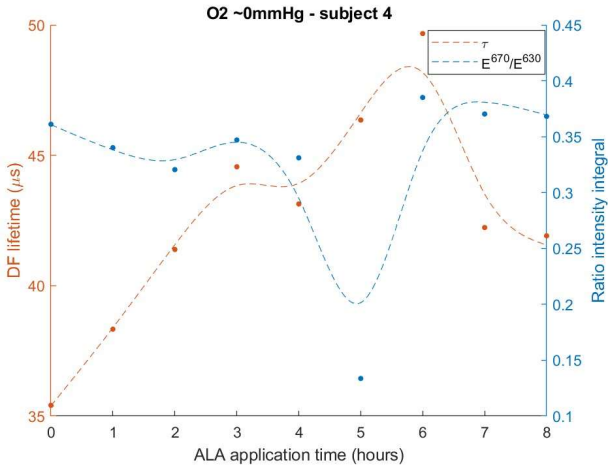

(b) Subject 4 - O_2 0mmHg

Figure 56: Lifetime compared to the ratio of maximum intensity amplitude for the measurements of patch 1 for subject 4 with measurements with (a) physiological PO_2 and (b) 0mmHg.

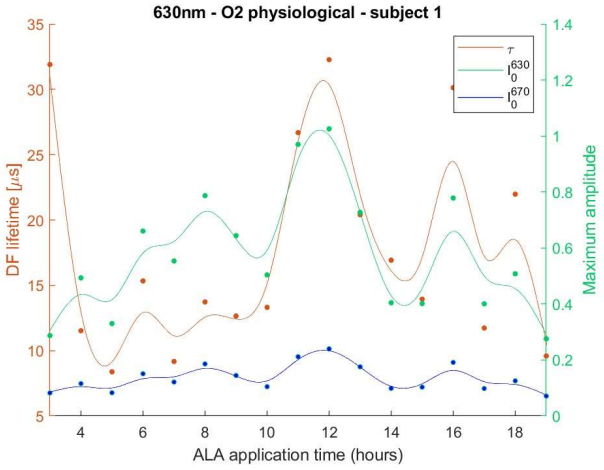

(a) Subject 1

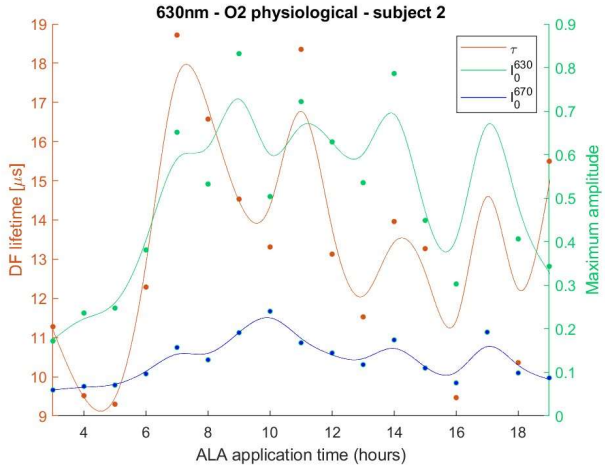

(b) Subject 2

Figure 57: Lifetime compared to the maximum intensity amplitude for the measurements of patch 1 for (a) subject 1 and (b) subject 2.

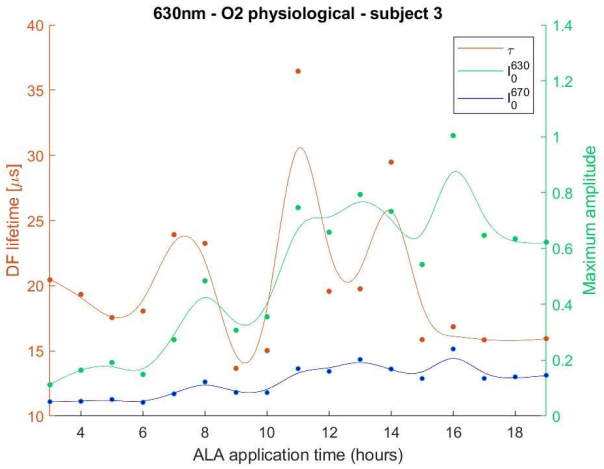

(a) Subject 3

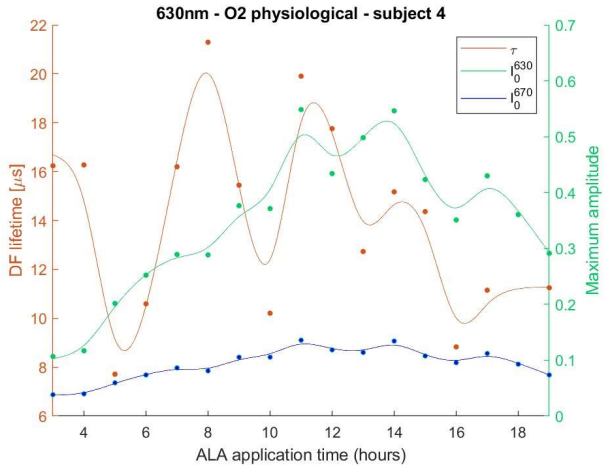

(b) Subject 4

Figure 58: Lifetime compared to the maximum intensity amplitude for the measurements of patch 1 for (a) subject 3 and (b) subject 4;mitoPO$_2$ at physiological level.